
Background and Derivation of ANS-5.4 Standard Fission Product Release Model

Compiled by:
Southern Science Applications, Inc.

American Nuclear Society
Working Group 5.4

U.S. Nuclear Regulatory
Commission

NOTICE

This report was prepared as an account of work sponsored by an agency of the United States Government. Neither the United States Government nor any agency thereof, or any of their employees, makes any warranty, expressed or implied, or assumes any legal liability or responsibility for any third party's use, or the results of such use, of any information, apparatus product or process disclosed in this report, or represents that its use by such third party would not infringe privately owned rights.

Available from

GPO Sales Program
Division of Technical Information and Document Control
U. S. Nuclear Regulatory Commission
Washington, D. C. 20555

Printed copy price: \$6.50

and

National Technical Information Service
Springfield, Virginia 22161

Background and Derivation of ANS-5.4 Standard Fission Product Release Model

Manuscript Completed: July 1981
Date Published: January 1982

Compiled by:
Southern Science Applications, Inc.
Dunedin, FL 33528

American Nuclear Society
Working Group 5.4
LaGrange Park, IL 60525

Division of Systems Integration
Office of Nuclear Reactor Regulation
U.S. Nuclear Regulatory Commission
Washington, D.C. 20555

Availability of Reference Materials Cited in NRC Publications

Most documents cited in NRC publications will be available from one of the following sources:

1. The NRC Public Document Room, 1717 H Street., N.W.
Washington, DC 20555
2. The NRC/GPO Sales Program, U.S. Nuclear Regulatory Commission,
Washington, DC 20555
3. The National Technical Information Service, Springfield, VA 22161

Although the listing that follows represents the majority of documents cited in NRC publications, it is not intended to be exhaustive.

Referenced documents available for inspection and copying for a fee from the NRC Public Document Room include NRC correspondence and internal NRC memoranda; NRC Office of Inspection and Enforcement bulletins, circulars, information notices, inspection and investigation notices; Licensee Event Reports; vendor reports and correspondence; Commission papers; and applicant and licensee documents and correspondence.

The following documents in the NUREG series are available for purchase from the NRC/GPO Sales Program: *formal NRC staff and contractor reports, NRC-sponsored conference proceedings, and NRC booklets and brochures.* Also available are Regulatory Guides, NRC regulations in the *Code of Federal Regulations*, and *Nuclear Regulatory Commission Issuances*.

Documents available from the National Technical Information Service include NUREG series reports and technical reports prepared by other federal agencies and reports prepared by the Atomic Energy Commission, forerunner agency to the Nuclear Regulatory Commission.

Documents available from public and special technical libraries include all open literature items, such as books, journal and periodical articles, transactions, and codes and standards. *Federal Register* notices, federal and state legislation, and congressional reports can usually be obtained from these libraries.

Documents such as theses, dissertations, foreign reports and translations, and non-NRC conference proceedings are available for purchase from the organization sponsoring the publication cited.

Single copies of NRC draft reports are available free upon written request to the Division of Technical Information and Document Control, U.S. Nuclear Regulatory Commission, Washington, DC 20555.

BACKGROUND AND DERIVATION OF ANS - 5.4 STANDARD FISSION PRODUCT RELEASE MODEL

ANS 5.4 Membership

S. E. Turner, Chairman	Southern Science Applications, Inc.
C. E. Beyer	Battelle Pacific Northwest Laboratory
B. J. Buescher	EG&G Idaho, Inc.
D. A. Himes	Hanford Engineering Development Laborator
R. J. Klotz	Combustion Engineering, Inc.
W. J. Leech	Westinghouse Electric Corporation
R. A. Lorenz	Oak Ridge National Laboratory
R. O. Meyer	U.S. Nuclear Regulatory Commission
L. D. Noble	General Electric Company
M. J. F. Notley	Atomic Energy of Canada, Ltd.
C. S. Rim	Korea Atomic Energy Research Institute
R. L. Ritzman	Science Applications Incorporated

July 1981

Compiled by
Southern Science Applications, Inc.
P. O. Box 10
Dunedin, Florida 33528

TABLE OF CONTENTS

	Page
I. INTRODUCTION (R. O. Meyer, U.S. Nuclear Regulatory Commission)	1
II. HIGH TEMPERATURE FISSION PRODUCT RELEASE	7
A. Mathematical Formulation for High Temperature Release	7
A-1 General Mathematics of the Booth Model (L. D. Noble, General Electric Company)	8
A-2 Time Varying	13
A-2.a Time Dependent Diffusion Parameters (L. D. Noble, General Electric Company)	13
A-2.b Mathematical Formulation for Time-Varying Power Histories (C. S. Rim, Korea Atomic Energy Research Institute)	19
B. High Temperature Data Base (C. E. Beyer, Hanford Engineering Development Laboratory)	32
1. Low Burnup Data Base and Selection Criteria	32
2. High Burnup Data Base and Selection Criteria	36
C. Model Fitting	44
1. Diffusion Theory (ANS 5.4 Model) (C. S. Rim, Korea Atomic Energy Research Institute)	44
2. Comparison with Beyer-Hann/NRC Model (R. O. Meyer, U.S. Nuclear Regulatory Commission)	53
D. Reducing Application Errors (L. D. Noble, General Electric Company).	56

TABLE OF CONTENTS (Continued)

	Page
E. Release of Iodine, Cesium, and Tellurium (R. L. Ritzman, Science Applications Incorporated)	60
1. General	60
2. Data Sources	62
3. Analysis of the Data Sources	70
4. Discussion of Results and Recommendations	76
F. Effect of Precursors on Release of Fission Product Gases (M. J. F. Notley, Atomic Energy of Canada, Ltd.)	79
F.1 Release by Diffusion	79
F.2 Release by Knock Out and Recoil	80
F.3 Consequences of the Release of a Precursor.	80
III. LOW TEMPERATURE FISSION PRODUCT RELEASE (R. A. Lorenz, Oak Ridge National Laboratory)	83
A. Mathematics of the Knockout Model	83
B. Low Temperature Data Base	86
1. Stable Fission Gas Release	86
2. Radioactive Fission Gas Release at Production-Decay Equilibrium	93
C. Model Fitting - Low Temperature Release	95

- APPENDIX A
- APPENDIX B
- APPENDIX C
- APPENDIX D
- APPENDIX E
- APPENDIX F

FOREWORD

This report summarizes work performed by the ANS 5.4 Working Group on Fuel-Plenum Fission Gas Inventory and is a compilation of individual contributions by members of the Working Group. The report was compiled to document the basis for the ANSI/ANS Standard on "Method for Calculating the Fractional Release of Volatile Fission Products from Oxide Fuels," ANSI/ANS 5.4-1981. The information contained in this report is important to an understanding of the Standard, and has been reviewed and approved by the Working Group.

Views expressed in this report are solely those of the individual contributors. Neither the members of the Working Group, their respective employers, the American Nuclear Society, nor the United States Government makes any warranty, expressed or implied, or assumes any legal liability or responsibility for the accuracy, completeness, or usefulness of any information presented herein.

I. Introduction (R. O. Meyer, U.S. Nuclear Regulatory Commission)

ANS Working Group 5.4 was established in 1974 to examine fission product releases from UO_2 fuel. The scope of ANS-5.4 was narrowly defined to include the following:

1. Review available experimental data on release of volatile fission products from UO_2 and mixed-oxide fuel.
2. Survey existing analytical models currently being applied to light-water reactors.
3. Develop a standard analytical model for volatile fission product release to the fuel rod void space. Place emphasis on obtaining a model for radioactive fission product releases to be used in assessing radiological consequences of postulated accidents.

The standard as developed applies to steady-state conditions. When used with isotopic yields, this method will give the so-called "gap activity," which is the inventory of volatile fission products that could be available for release from the fuel rod if the cladding were breached. This gap inventory of radioactive fission products can be used in accident analyses not involving large abrupt temperature changes.

The volatile and gaseous fission products of primary significance are krypton, xenon, iodine, cesium, and tellurium. These gaseous and volatile fission products can be divided into two categories: (1) short-lived radioactive isotopes (half-life less than one year) and (2) long-lived radioactive isotopes

(half-life greater than one year) and stable species. This division is convenient since the most important release mechanism involves thermally activated migration processes that proceed slowly such that the short-lived isotopes decay appreciably before they are released from the pellet. Consequently, release calculations for short-lived isotopes must include their decay rate, whereas, for long-lived and stable isotopes, decay does not have to be considered.

Most experimental measurements of released fission gas were preceded by a cooldown period of approximately a year, during which time all of the short-lived radioactive species disappeared. As a result, insufficient data exist to directly determine a release correlation for short-lived isotopes. While gas-release correlations based on stable-isotope data are useful for fuel-performance calculations, they are usually not capable of predicting the radioactive releases. However, it is possible to derive an analytical model that is based on mechanistic or phenomenological principles that will predict releases as a function of half-life and can be calibrated with stable-gas-release data. This is the approach taken by ANS-5.4.

The Working Group has chosen what is believed to be the simplest such phenomenological model, the Booth diffusion-type mode (1-5), and has fitted the model empirically to selected data, whose characteristics will be described later.

The Booth model describes diffusion of fission-product atoms in a sphere of fuel material. The governing equation is

$$\partial C/\partial t = B - \lambda C - \text{div } J, \quad (1)$$

where C is the isotope concentration (atoms/cm³), B is the production or birth rate (atoms/cm³-sec), λ is the decay constant (sec⁻¹), and J is the local mass flux (atoms/cm²-sec). This equation is fundamental and applies to isotopes of any chemical species with any half-life. The rate of concentration change in a region is equal to the rate of production minus the rate of decay minus the rate of loss by mass flow out of the region. Equation 1 implies nothing about the mechanism of mass flow. The apparent diffusion coefficient D is contained in the flux term, which is given by

$$J = -D \text{ grad } C. \quad (2)$$

This diffusion equation, like Eq. 1, contains no information about the diffusion mechanism and merely assumes that a net flow of matter occurs because of the existence of a concentration gradient and that the flux is proportional to that gradient. The production rate B and decay constant λ in Eq. 1 are known for most isotopes, but the diffusion coefficient D in Eq. 2 is unknown and must be determined from experimental data.

From a general knowledge of atomic migration (6), it is known that the diffusion coefficient of a species in a host material depends on the properties of that material and its interaction with the diffusing species. These interactions are primarily electronic in nature so that different atoms (elements) would have different diffusion coefficients. Because the valence and ionic properties of krypton and xenon are similar, their diffusion coefficients in UO_2 are similar. However, there is no reason to expect the noble gases to behave like iodine or other chemical species. Therefore, it must be presumed that different elements migrate and are released at different rates.

On the other hand, the diffusion behavior of a chemical species can be expected to be the same for all isotopes of that species. While, strictly speaking, there is a diffusion isotope effect that is dependent on isotopic mass (7), this effect is very small and has only been detected in a few precise experiments using isotopes with large mass differences. Small differences in diffusion behavior would be imperceptible in the context of fission gas release.

The Booth diffusion model is an over-simplification of the physical process. The effective diffusion parameters that are determined by empirically fitting the Booth model to gas release data are not the diffusion coefficients for atomic diffusion of inert gases and other chemical species in pure UO_2 . Atomic diffusion, gas bubble nucleation, bubble migration, bubble coalescence, interaction of bubbles with structures, and irradiation resolution are all involved in fission gas release. Some of these processes, like bubble migration, are relatively well understood. The microscopic parameters that govern these mechanisms are, in turn, dependent on the materials properties, such as diffusion coefficient, heats of vaporization, etc., which are independent of isotopic makeup. It, therefore, seems appropriate to assume that the overall release kinetics are the same for all isotopes of the same chemical species regardless of the complicated nature of the release mechanisms. Precursor effects may, however, cause a small apparent difference in release kinetics.

The Booth equations describe a smooth continuous release process and should not be applied to discontinuous releases or bursts (i.e., abrupt releases observed during sudden temperature changes). It is considered beyond the

state of the art to model burst releases in a quantitative manner. Nevertheless, gases released in bursts are included in the data and are, therefore, accounted for in the cumulative releases predicted by the empirical model.

Finally, temperature-independent mechanisms are expected to be important for gas releases at low temperatures. As with the temperature-dependent (high temperature) diffusion-type model, the release fraction for radioactive species will depend on the isotopic half-life. However, the low-temperature release mechanisms are thought to be controlled by knock-out and recoil and, therefore, all chemical species are treated alike.

References, Section I

1. A. H. Booth, Atomic Energy of Canada Report, CRDC-721 (1957).
2. A. H. Booth, Atomic Energy of Canada Report, DCI-17 (1957).
3. A. H. Booth, and G. T. Rymer, Atomic Energy of Canada Report, CRDC-720 (1958).
4. S. D. Beck, Battelle Columbus Report, BMI-1433 (1960).
5. B. Lustman, in J. Belle (ed.), "Uranium Dioxide: Properties and Nuclear Applications" (USAEC, Washington, 1961) p. 431.
6. P. G. Shewmon, "Diffusion in Solids" (McGraw-Hill, New York, 1963).
7. N. L. Peterson, Solid State Physics 22, 409 (1968).

II HIGH TEMPERATURE FISSION PRODUCT RELEASE

II. A. Mathematical Formulation for High Temperature Release

A general mathematical formulation of the Booth model for diffusion of radioactive species during constant power and temperature operation is described in Section 1. The formulation relies heavily on the work of Beck¹, and many expressions are taken directly from his work rather than being "re-derived".

In Section 2, the model is expanded upon to obtain the formulas for cases in which neither the power nor temperature need be assumed constant. The first portion (Section A.2.a) of the Section treats the generalized case of time (exposure) varying power and diffusion coefficients, with explicit solutions for two cases. One, where the power and diffusion coefficient are assumed to be step-wise continuous functions, and the other where the diffusion coefficient is assumed to vary exponentially with time (exposure) but the power remains constant. The second portion (Section A.2.b) uses a different approach to derive the solution for the step-wise continuous case, and it formats the equations into the form used in the standard. It can be shown, with some mathematical manipulation and noting the slightly different notation, that the release fraction F defined as the division of equation (31) by equation (33) in Section A.2.a is identical to equation 19 of Section A.2.b.

A-1 General Mathematics of the Booth Model (L. D. Noble)

NOMENCLATURE

C = Concentration of nuclei in the sphere (atoms/cm³)

D = Diffusion coefficient (cm²/sec)

B = Production rate (atoms/cm³-sec)

λ = Decay constant (sec⁻¹)

t = Time (sec)

r = Radial coordinate in the sphere (cm)

a = Radius of the sphere (cm)

R = Rate of release from unit volume of sphere (atoms/cm³-sec)

N = Accumulation of undecayed, released atoms from a unit volume of sphere (atoms/cm³)

D' = D/a² (sec⁻¹)

μ = $\lambda a^2/D$

τ = Dt/a²

Constant Diffusion Parameters

The release of volatile products from a UO_2 fuel matrix may, under certain assumptions, be represented as diffusion of an isotope to the surface of an equivalent sphere. Using the notation of Beck⁽¹⁾, the equation for the concentration in a sphere may be written as

$$\frac{\partial C}{\partial t} = \frac{1}{r^2} \frac{\partial}{\partial r} \left(r^2 D \frac{\partial C}{\partial r} \right) + B - \lambda C \quad (1)$$

The release rate $R(t)$ from the fuel matrix into the void regions surrounding the fuel, and the accumulation of the undecayed atoms in this void region, $N(t)$, are of particular interest.

The release rate per unit volume of fuel, $R(t)$, is defined as follows:

$$R(t) = \left. \frac{-3D}{a} \frac{\partial C}{\partial r} \right|_{r=a} \quad (2)$$

The accumulation in the void space is then related to the release rate by the following equation:

$$\frac{dN}{dt} = R - \lambda N \quad (3)$$

Since the total number of atoms present at any time is

$$\frac{B}{\lambda} [1 - e^{-\lambda t}] \quad (4)$$

the fraction, F , that is present in the void space is

$$F = \frac{N\lambda}{B(1 - e^{-\lambda t})} \quad (5)$$

For the case of stable isotopes, $\lambda=0$, and

$$F = \frac{N}{Bt} \quad (6)$$

As shown by Beck⁽¹⁾, the solution for R may be written either as

$$R = 3B \left(\frac{1}{\sqrt{\mu}} \coth \sqrt{\mu} - \frac{1}{\mu} \right) - 6B e^{-\mu\tau} \sum_{n=1}^{\infty} \frac{e^{-n^2 \pi^2 \tau}}{n^2 \pi^2 + \mu} \quad (7)$$

or as

$$R = 3B \left[\frac{1}{\sqrt{\mu}} \operatorname{erf}(\sqrt{\mu}\tau) - \frac{(1 - e^{-\mu\tau})}{\mu} \right] + E \quad (8)$$

where

$$E = \frac{3B}{\sqrt{\mu}} \sum_{n=1}^{\infty} \exp(-2n\sqrt{\mu}) \operatorname{erfc}\left(\frac{n}{\sqrt{\tau}} - \sqrt{\mu}\tau\right) - \exp(2n\sqrt{\mu}) \operatorname{erfc}\left(\frac{n}{\sqrt{\tau}} + \sqrt{\mu}\tau\right) \quad (9)$$

Either form of the expression for R is exact; however, equation 7 converges much faster for large values of either τ or $\mu\tau$ while equation 8 converges rapidly for small values of τ .

The relations for F may be written as

$$F = 3 \left[\frac{1}{\sqrt{\mu}} \coth \sqrt{\mu} - \frac{1}{\mu} \right] - \frac{6B}{(e^{\mu\tau} - 1)} \sum_{n=1}^{\infty} \frac{1 - e^{-n^2 \pi^2 \tau}}{n^2 \pi^2 (n^2 \pi^2 + \mu)} \quad (10)$$

or as

$$F = \frac{3}{(1 - e^{-\mu\tau})} \left[\frac{1}{\sqrt{\mu}} \left\{ \operatorname{erf} \sqrt{\mu}\tau - 2 \sqrt{\frac{\mu\tau}{\pi}} e^{-\mu\tau} \right\} - \frac{1 - (1 + \mu\tau)e^{-\mu\tau}}{\mu} \right] + E_1 \quad (11)$$

where

$$E_1 = \frac{E}{B(1 - e^{-\mu\tau})} - \frac{12}{(1 - e^{-\mu\tau})} \sum_{n=1}^{\infty} \left[\sqrt{\frac{\tau}{\pi}} e^{-\frac{(\mu\tau + n^2)\tau}{\tau}} - n e^{-\mu\tau} \operatorname{erfc}(n/\sqrt{\tau}) \right] \quad (12)$$

In the special case of a stable isotope, $\lambda=0$, and the relations for F, are as follows:

$$F = 1 - \frac{1}{15\tau} + \frac{6}{\tau} \sum_{n=1}^{\infty} \frac{e^{-n^2 \frac{2}{\tau}}}{n^4 \frac{4}{\pi}} \quad (13)$$

or

$$F = \frac{4}{\sqrt{\pi}} \sqrt{\tau} - \frac{3}{2}\tau + E_2 \quad (14)$$

where

$$E_2 = 4 \sum_{n=1}^{\infty} \left[2 \sqrt{\frac{\tau}{\pi}} \left(1 + \frac{n^2}{\tau}\right) e^{-n^2/\tau} - n(3 + 2n^2/\tau) \operatorname{erfc}\left(\frac{n}{\sqrt{\tau}}\right) \right] \quad (15)$$

The equations for E_1 and E_2 were not given explicitly by Beck⁽¹⁾, although he did suggest the method for obtaining them.

Beck⁽¹⁾ indicated that for values of $\tau \leq 0.1$ the approximate formulas obtained by deleting the terms E , E_1 and E_2 in equations 8, 11 and 14 are in error by less than 0.0001. In fact, if the asymptotic expansion for $\operatorname{erf}(x)$ given by Beck (equation 32 of reference 1), is utilized, it can be shown that for small τ and for $\mu\tau \ll 1/\tau$

$$E \approx \frac{3}{\pi} \exp\left(-\frac{1}{\tau} - \mu\tau\right) \frac{2\tau^{3/2}}{1 - \mu\tau^2} \quad (16)$$

for a value of $\tau = 0.1$, this expression gives a value of $\sim 5 \times 10^{-6}$. Similar use of the asymptotic expression for E_1 and E_2 shows that for $\tau \leq 0.1$, the approximate expressions for R and F obtained by neglecting E , E_1 , or E_2 are in error by $\leq 10^{-5}$. Conversely, for values of $\tau > 0.1$, the expressions in equations 10 and 13 converge quite rapidly and should be used for larger values of τ .

As was indicated by Beck⁽¹⁾, equations 10, 11, 13 and 14 are exact. However, when $\tau \leq 0.1$ the following simplified expressions have an error of $< 10^{-5}$.

For $\tau < 0.1$

$$F = \frac{3}{1 - \exp(-\mu\tau)} \left[\frac{1}{\sqrt{\mu}} \left\{ \operatorname{erf}(\sqrt{\mu\tau}) - 2\sqrt{\mu\tau/\pi} \exp(-\mu\tau) \right\} - \frac{1 - (1 + \mu\tau) \exp(-\mu\tau)}{\mu} \right] \quad (17)$$

or when $\lambda = 0$

$$F = 4\sqrt{\tau/\pi} - 3\tau/2. \quad (18)$$

For $\tau > 0.1$

$$F = 3 \left[\frac{1}{\sqrt{\mu}} \coth(\sqrt{\mu}) - \frac{1}{\mu} \right] - \frac{6\mu}{\exp(\mu\tau) - 1} \sum_{n=1}^{\infty} \frac{1 - \exp(-n^2\pi^2\tau)}{n^2\pi^2(n^2\pi^2 + \mu)} \quad (19)$$

or when $\lambda = 0$

$$F = 1 - \frac{1}{15\tau} + \frac{6}{\tau} \sum_{n=1}^{\infty} \frac{\exp(-n^2\pi^2\tau)}{n^4\pi^4} \quad (20)$$

For practical application, only three terms in the sum (Eq. 19 and 20) are required, since this gives an accuracy of better than 10^{-5} .

A-2 Time Varying

A-2.a Time Dependent Diffusion Parameters

The solution for the release and accumulation of volatile fission products is slightly different when the diffusion coefficient D is a function of time. However, the solution may be obtained by modifying the previous definition of τ as follows:

$$\tau(t) = \frac{1}{a^2} \int_0^t D(u) du \quad (21)$$

When D is constant this new definition corresponds to the previous one. For convenience, the following definitions are also introduced:

$$\begin{aligned} X &= r/a \\ G(t) &= B(t)a^2 e^{\lambda t}/D(t) \\ H(t, X) &= C(t, X)e^{\lambda t} \\ I(t) &= a^2 R(t)e^{\lambda t}/D(t) \\ J(t) &= N(t)e^{\lambda t} \end{aligned}$$

The differential equation for H is then obtained from the equation for C by multiplying equation (1) with $a^2 e^{\lambda t}/D$.

This equation is:

$$\frac{\partial H}{\partial \tau} = \frac{1}{X^2} \frac{\partial}{\partial X} \left(X^2 \frac{\partial H}{\partial X} \right) + G \quad (22)$$

Further, from equation 2

$$I(t) = -3 \left. \frac{\partial H}{\partial X} \right|_{X=1} \quad (23)$$

and from equation 3

$$-\frac{\partial}{\partial \tau} J(t) = I(t) \quad (24)$$

Using S as the transform variable, and using a bar over the symbol to denote the Laplace transform with respect to τ , the solution for the transform of I is:

$$\begin{aligned}\bar{I}(S) &= 3 \bar{G}(S) \left[\frac{\coth \sqrt{S}}{\sqrt{S}} - \frac{1}{S} \right] \\ &= 3 \bar{G}(S) \left[\frac{1 + 2 \sum_{n=1}^{\infty} e^{-n\sqrt{S}}}{\sqrt{S}} - \frac{1}{S} \right] \quad (25)\end{aligned}$$

where \bar{G} is the transform of G .

Further, the transform \bar{J} , of J , is:

$$\bar{J}(S) = \bar{I}(S)/S$$

The solution for $N(t)$ is obtained from the inverse of \bar{J} , and may be written as follows (where z is defined as $\tau(t) - \tau(u)$):

$$N(t) = 6 e^{-\lambda t} \int_0^t B(u) e^{\lambda u} du \sum_{n=1}^{\infty} \frac{1 - e^{-n^2 \pi^2 z}}{n^2 \pi^2} \quad (26)$$

or it may be written as

$$N(t) = 3 e^{-\lambda t} \int_0^t B(u) e^{\lambda u} du \left[2\sqrt{z}/\pi - z + E_3(z) \right] \quad (27)$$

where E_3 is defined as follows:

$$E_3(z) = 4 \sum_{n=1}^{\infty} \left\{ \frac{\sqrt{z}}{\pi} \exp(-n^2/z) - \operatorname{erfc} \left(n/\sqrt{z} \right) \right\}$$

The release fraction F is then determined by dividing the value for $N(t)$ by the total production up to time t ; where $t_k \leq t \leq t_{k+1}$

$$\int_0^t B(u) du = B_k (t - t_k) + \sum_{j=1}^{K-1} \left[B_j (t_{j+1} - t_j) \right] \quad (33)$$

The previously derived equations can also be used to develop explicit equations for a particular case in which the effective diffusion coefficient D' is assumed to increase exponentially with time. Only stable species are considered.

If $D' = D_0 \exp(\alpha\tau)$ where α is a constant, then from equation 21

$$\tau = D_0 \left[\exp(\alpha\tau - 1) \right] / \alpha. \text{ Using equation 26 with } \lambda=0 \text{ and a}$$

constant production rate B , the expression for the number of released atoms, N , can be written as follows for large values of time.

$$N = B \int_0^\tau \frac{dx}{D' - \alpha x} \left[1 - 6 \sum_{\eta=1}^{\infty} \frac{\exp(-\eta^2 \pi^2 x)}{\eta^2 \pi^2} \right] \quad (34)$$

Note that a transformation $x = \tau(t) - \tau(u)$, and the identity $\sum 1/\eta^2 = \pi^2/6$ has been used. Also note that $D' = D_0 + \alpha\tau$.

In a similar manner, neglecting the term E_3 in equation 27, the value of N for shorter times becomes

$$N = \frac{6B}{\sqrt{\pi}} \int_0^\tau \frac{\sqrt{x} dx}{D' - \alpha x} - \frac{3D_0 B}{\alpha} \int_0^\tau dy \left[e^{\alpha t} - e^{\alpha y} \right] \quad (35)$$

Using the relationship that the release fraction is N/Bt , the expressions for F may be written as follows for long times.

$$F = 1 - 6 \sum_{\eta=1}^{\infty} \frac{\exp(-\eta^2 \pi^2 D' / \alpha)}{\eta^2 \pi^2 \alpha t} \left[E_i(\eta^2 \pi^2 D' / \alpha) - E_i(\eta^2 \pi^2 D_0 / \alpha) \right] \quad (36)$$

A particular case of interest is one for stable isotopes ($\lambda=0$) in which the time dependence of both the source term and the diffusion coefficient may be represented by a succession of values which are constant within any time increment t_j to t_{j+1}

Specifically

$$B(t) = B_j \quad \text{when } t_j \leq t \leq t_{j+1} \quad (28)$$

and

$$D'(t) = D'_j \quad \text{when } t_j \leq t \leq t_{j+1} \quad (29)$$

with $t_1 = 0$

With these assumptions, and the notation that

$$\tau_j = \tau(t_j) = \sum_{i=1}^{j-1} D'_i (t_{i+1} - t_i) \quad (30)$$

the solution for $N(t)$ may be written as follows:

on the interval $t_k \leq t \leq t_{k+1}$

$$N(t) = B_k (t - t_k) + \sum_{j=1}^{K-1} B_j (t_{j+1} - t_j) - 6 \frac{B_k}{D'_k} \sum_{n=1}^{\infty} \left\{ \frac{1 - \exp \left[-n^2 \pi^2 (\tau - \tau_k) \right]}{n^4 \pi^4} \right\} \quad (31)$$

$$- 6 \sum_{j=1}^{K-1} \frac{B_j}{D'_j} \sum_{n=1}^{\infty} \frac{\exp \left[\frac{-n^2 \pi^2 (\tau - \tau_{j+1})}{n^4 \pi^4} \right]}{n^4 \pi^4} \left\{ 1 - \exp \left[-n^2 \pi^2 (\tau_{j+1} - \tau_j) \right] \right\}$$

or, for smaller values of time, where the term E_3 in equation 27 may be neglected.

$$N(t) = \frac{B_k}{D'_k} \left[\frac{4}{\sqrt{\pi}} (\tau - \tau_k)^{3/2} - \frac{3(\tau - \tau_k)^2}{2} \right]$$

$$+ \sum_{j=1}^{K-1} \frac{B_j}{D'_j} \left[\frac{4}{\sqrt{\pi}} \left\{ (\tau - \tau_j)^{3/2} - (\tau - \tau_{j+1})^{3/2} \right\} - \frac{3}{2} \left\{ (\tau - \tau_j)^2 - (\tau - \tau_{j+1})^2 \right\} \right] \quad (32)$$

where E_i is the exponential integral

$$E_i(x) = - \int_{-\infty}^x e^v / v$$

Or, for shorter times, the expression is:

$$F = \frac{12}{\alpha t} \sqrt{\frac{D_c}{\alpha \pi}} \left[\tanh^{-1} \sqrt{\alpha \tau / D'} - \sqrt{\alpha \tau / D'} \right] - \frac{3}{\alpha t} \left[D' t - \tau \right] \quad (37)$$

References

- 1) Beck, Stephen D., "The Diffusion of Radioactive Fission Products From Porous Fuel Elements", USAEC Report BMI - 1433, April 1960.

A-2b.

Mathematical Formulation for Time-Varying Power Histories

(C. S. Rim, Korea Atomic Energy Research Institute)*

The diffusion model presented in Section II-A1 is applicable when power and diffusion parameters remain constant with time. Fuel rods are often subject to time-varying power histories. Even when the power level remains constant, fuel temperatures change with time due to changes in gap conductance, radial power distribution within the pellet, etc. Diffusion parameters vary due to changes in fuel temperatures and are assumed to vary with burnup.

A mathematical formulation for stable fission gas release calculations is established in this section which will accommodate temperature and burnup dependent diffusion parameters as well as a variable power history. Model fitting to high temperature fission gas release data and application of this model to variable power and temperature cases are presented in the next section.

* Work performed at Westinghouse Electric Corporation, in collaboration with B. S. Preble.

N O M E N C L A T U R E

C	gas concentration (moles/cm ³)
D	diffusion coefficient (cm ² /sec)
P	production rate (moles/(sec cm ³))
t	time (sec)
r	radial location in sphere (cm)
a	equivalent radius of sphere (cm)
f	fractional release (moles/moles)
m	gas released (moles)

$$D' = D/a^2 \text{ (sec}^{-1}\text{)}$$

$$\tau = D't$$

1) Derivation of the basic equation

The diffusion equation for stable isotopes can be written as

$$\frac{\partial C}{\partial t} = \frac{D}{r} \frac{\partial^2 (rC)}{\partial r^2} + P \quad (1)$$

Let $u = rC$

$$\text{then } \frac{1}{r} \frac{\partial u}{\partial t} = D/r \frac{\partial^2 u}{\partial r^2} + P$$

$$\frac{\partial u}{\partial t} = D \frac{\partial^2 u}{\partial r^2} + Pr \quad (2)$$

$$\text{Let } u = w - \frac{Pr^3}{6D}$$

$$\frac{\partial u}{\partial t} = \frac{\partial w}{\partial t}; \quad D \frac{\partial^2 u}{\partial r^2} = D \left[\frac{\partial^2 w}{\partial r^2} - \frac{Pr}{D} \right] = D \frac{\partial^2 w}{\partial r^2} - Pr$$

Equation (2) then becomes,

$$\frac{\partial w}{\partial t} = D \frac{\partial^2 w}{\partial r^2} \quad (3)$$

$$\text{where } C = \frac{1}{r} u = \frac{w}{r} - \frac{Pr^2}{6D}$$

Boundary Conditions (B.C.);

$$1) \quad C = C_0(r) \text{ at } t = 0 \rightarrow w = r C_0(r) + \frac{Pr^3}{6D} = f(r) \text{ at } t = 0$$

$$2) \quad C = 0 \text{ at } r = a \rightarrow w = \frac{Pa^3}{6D} \text{ at } r = a$$

$$3) \quad C \text{ is finite at } r = 0 \rightarrow W = 0 \text{ at } r = 0$$

The general solution to eq. (3) with B.C. 1) to 3) is given by Carslaw and Jaeger^[1] (p. 104) as

$$W = (2/a) \sum_1^{\infty} e^{-Dn^2 \pi^2 t/a^2} \sin \frac{n\pi r}{a} \left\{ \int_0^a f(r') \sin \frac{n\pi r'}{a} dr' - \frac{nD\pi}{a} \int_0^t e^{Dn^2 \pi^2 \lambda/a^2} (-1)^n \frac{Pa^3}{6D} d\lambda \right\}$$

or

$$W = (2/a) \sum_1^{\infty} e^{-Dn^2 \pi^2 t/a^2} \sin \frac{n\pi r}{a} \left\{ \int_0^a r' C_0(r') \sin \frac{n\pi r'}{a} dr' + \int_0^a \frac{Pr'^3}{6D} \sin \frac{n\pi r'}{a} dr' + (-1)^n \frac{Pa^4}{6Dn\pi} (1 - e^{-Dn^2 \pi^2 t/a^2}) \right\} \quad (4)$$

The 2nd term in eq. (4) can be simplified

$$\begin{aligned} \int_0^a \frac{Pr'^3}{6D} \sin \frac{n\pi r'}{a} dr' &= \frac{P}{6D} \int_0^a r'^3 \sin \frac{n\pi r'}{a} dr' \\ &= \frac{P}{6D} \left[\frac{3(\frac{n\pi}{a})^2 r'^2 - 6}{(\frac{n\pi}{a})^4} \sin \left(\frac{n\pi r'}{a} \right) - \frac{(\frac{n\pi}{a})^2 r'^3 - 6r'}{(\frac{n\pi}{a})^3} \cos \left(\frac{n\pi r'}{a} \right) \right]_0^a \\ &= -(-1)^n \frac{Pa^4}{6Dn^3 \pi^3} (n^2 \pi^2 - 6) \end{aligned}$$

so that eq. (4) becomes :

$$\begin{aligned}
 W = & (2/a) \sum_{n=1}^{\infty} e^{-Dn^2 \pi^2 t/a^2} \sin\left(\frac{n\pi r}{a}\right) \int_0^a r' C_0(r') \sin\left(\frac{n\pi r'}{a}\right) dr' \\
 & + (-1)^n \frac{Pa^4}{Dn^3 \pi^3} \\
 & - (-1)^n \frac{Pa^4}{6Dn\pi} e^{-Dn^2 \pi^2 t/a^2} \quad (5)
 \end{aligned}$$

Expanding we then have

$$\begin{aligned}
 W = & (2/a) \sum_{n=1}^{\infty} e^{-Dn^2 \pi^2 t/a^2} \sin\left(\frac{n\pi r}{a}\right) \int_0^a r' C_0(r') \sin\left(\frac{n\pi r'}{a}\right) dr' \\
 & + \frac{2Pa^3}{D\pi^3} \sum_{n=1}^{\infty} \frac{(-1)^n}{n^3} e^{-Dn^2 \pi^2 t/a^2} \sin\left(\frac{n\pi r}{a}\right) \\
 & - (2/a) \frac{Pa^4}{6D\pi} \sum_{n=1}^{\infty} \frac{(-1)^n}{n} \sin\left(\frac{n\pi r}{a}\right) \quad (6)
 \end{aligned}$$

Equation (6) can be further simplified using a relationship from Ref. (2), P.470 ;

$$\begin{aligned}
 \sum_{n=1}^{\infty} \frac{(-1)^n}{n} \sin\left(\frac{n\pi r}{a}\right) &= \frac{-r\pi}{2a} \\
 W = & (2/a) \sum_{n=1}^{\infty} e^{-Dn^2 \pi^2 t/a^2} \sin\left(\frac{n\pi r}{a}\right) \int_0^a r' C_0(r') \sin\left(\frac{n\pi r'}{a}\right) dr' \\
 & + \frac{2Pa^3}{D\pi^3} \sum_{n=1}^{\infty} \frac{(-1)^n}{n^3} e^{-Dn^2 \pi^2 t/a^2} \sin\left(\frac{n\pi r}{a}\right) \\
 & + \frac{Pa^2 r}{6D} \quad (7)
 \end{aligned}$$

Since $C = \frac{w}{r} - \frac{Pr^2}{6D}$ and defining $D' = D/a^2$, we have

$$C = \frac{2}{ar} \sum_1^{\infty} e^{-n^2 \pi^2 D' t} \sin\left(\frac{n\pi r}{a}\right) \int_0^a r' C_0(r') \sin\left(\frac{n\pi r'}{a}\right) dr' + \frac{2Pa}{\pi^3 D' r} \sum_1^{\infty} \frac{(-1)^n}{n^3} e^{-n^2 \pi^2 D' t} \sin\left(\frac{n\pi r}{a}\right) + \frac{P}{6D'} (1 - (r/a)^2) \quad (8)$$

which forms the basis for the remaining solution.

2) Calculation of the 1st time step with P_1 , T_1 and D_1

Since there is no initial concentration

$$C_0 = 0$$

$$\therefore C_1 = \frac{2P_1 a}{\pi^3 D_1' r} \sum_1^{\infty} \frac{(-1)^n}{n^3} e^{-n^2 \pi^2 D_1' t} \sin\left(\frac{n\pi r}{a}\right) + \frac{P_1}{6D_1'} (1 - (r/a)^2) \quad (9)$$

Moles released during time step Δt_1

$$m_1 = - \int_0^{\Delta t_1} 4\pi a^2 D_1 \frac{\partial C_1}{\partial r} \Big|_{r=a} dt$$

$$m_1 = (4/3)\pi a^3 P_1 \Delta t_1 + \frac{8a^3 P_1}{\pi^3 D_1'} \sum_1^{\infty} \frac{1}{n^4} (e^{-n^2 \pi^2 D_1' \Delta t_1} - 1) \quad (10)$$

Fractional release at the end of 1st time step

$$f_1 = \frac{m_1}{\frac{4}{3} \pi a^3 P_1 \Delta t_1}$$

$$f_1 = 1 + \frac{6}{\pi^4 D_1^2 \Delta t_1} \sum_{n=1}^{\infty} \frac{1}{n^4} (e^{-n^2 \pi^2 D_1^2 \Delta t_1} - 1) \quad (11)$$

Since $\sum_{n=1}^{\infty} \frac{1}{n^4} = \frac{\pi^4}{90}$, equation (11) is the same expression

obtained by Booth⁽³⁾ for the constant power, constant temperature case :

$$f = 1 - \frac{6}{90 D_1^2 t} + \frac{6}{\pi^4 D_1^2 t} \sum_{n=1}^{\infty} \frac{1}{n^4} e^{-n^2 \pi^2 D_1^2 t}$$

3) 2nd Time Step (P_2, T_2, D_2')

$$C_2 = \frac{2}{a r} \sum_{n=1}^{\infty} e^{-n^2 \pi^2 D_2'^2 t} \sin\left(\frac{n\pi r}{a}\right) \int_0^a r' C_1(\Delta t_1, r') \sin\left(\frac{n\pi r'}{a}\right) dr' \\ + \frac{P_2}{6 D_2'^2} (1 - (r/a)^2)$$

$$+ \frac{2 P_2 a}{3 \pi D_2'^2 r} \sum_{n=1}^{\infty} \frac{(-1)^n}{n^3} e^{-n^2 \pi^2 D_2'^2 t} \sin\left(\frac{n\pi r}{a}\right) \quad (12)$$

but from eq. (9); considering C_1 at $\Delta t_1, r'$

$$\int_0^a r' C_1 (\Delta t_1, r') \sin \left(\frac{n\pi r'}{a} \right) dr' =$$

$$\begin{aligned} & \int_0^a \frac{P_1}{6D_1} (a^2 r' - r'^3) \sin \left(\frac{n\pi r'}{a} \right) dr' \\ & + \frac{2P_1 a^3}{3D_1} \sum_{n=1}^{\infty} \frac{(-1)^n}{n^3} \sin \left(\frac{n\pi r'}{a} \right) e^{-n^2 \pi^2 D_1 \Delta t_1} \sin \left(\frac{n\pi r'}{a} \right) dr' \\ & = \frac{P_1}{D_1} \left(\frac{a^2}{\pi^3} \right) \left(\frac{(-1)^n}{n^3} \right) (e^{-n^2 \pi^2 D_1 \Delta t_1} - 1) \end{aligned}$$

$$\begin{aligned} \therefore C_2 &= \frac{2P_1 a}{3D_1 r} \sum_{n=1}^{\infty} e^{-n^2 \pi^2 D_2 t} \sin \left(\frac{n\pi r}{a} \right) \frac{(-1)^n}{n^3} (e^{-n^2 \pi^2 D_1 \Delta t_1} - 1) \\ &+ \frac{P_2}{6D_2} (a^2 - r^2) \\ &+ \frac{2P_2 a}{3D_2 r} \sum_{n=1}^{\infty} \frac{(-1)^n}{n^3} \sin \left(\frac{n\pi r}{a} \right) e^{-n^2 \pi^2 D_2 t} \end{aligned} \quad (13)$$

Number of moles released during time step Δt_2

$$m_2 = - \int_0^{\Delta t_2} 4\pi a^2 D_2 \frac{\partial C_2}{\partial r} \Big|_{r=a} dt$$

$$\begin{aligned}
 m_2 &= (4/3)\pi a^3 P_2 - t_2 \\
 &+ \frac{8a^3}{\pi^3} \left\{ \frac{P_1}{D_1'} \sum_{n=1}^{\infty} \frac{1}{n^4} \left(e^{-n^2 \pi^2 (D_1' \Delta t_1 + D_2' \Delta t_2)} - e^{-n^2 \pi^2 D_2' \Delta t_2} \right) \right. \\
 &- \frac{P_1}{D_1'} \sum_{n=1}^{\infty} \frac{1}{n^4} \left(e^{-n^2 \pi^2 D_1' \Delta t_1} - 1 \right) \\
 &\left. + \frac{P_2}{D_2'} \sum_{n=1}^{\infty} \frac{1}{n^4} \left(e^{-n^2 \pi^2 D_2' \Delta t_2} - 1 \right) \right\} \quad (14)
 \end{aligned}$$

Cumulative fractional release at the end of step 2

$$f_2 = \frac{m_1 + m_2}{\frac{4}{3} \pi a^3 (P_1 \Delta t_1 + P_2 \Delta t_2)}$$

$$\begin{aligned}
 f_2 &= 1 + \frac{6}{\pi^4 (P_1 \Delta t_1 + P_2 \Delta t_2)} \left(\frac{P_1}{D_1'} \sum_{n=1}^{\infty} \frac{1}{n^4} \left[e^{-n^2 \pi^2 (D_1' \Delta t_1 + D_2' \Delta t_2)} \right. \right. \\
 &\quad \left. \left. - e^{-n^2 \pi^2 D_2' \Delta t_2} \right] \right. \\
 &\quad \left. + \frac{P_2}{D_2'} \sum_{n=1}^{\infty} \frac{1}{n^4} \left(e^{-n^2 \pi^2 D_2' \Delta t_2} - 1 \right) \right) \quad (15)
 \end{aligned}$$

4) 3rd Time Step

In a similar manner

$$C_3 = \left[\frac{2}{ar} \sum_{n=1}^{\infty} e^{-n^2 \pi^2 D_3' t} \sin\left(\frac{n\pi r}{a}\right) \int_0^a r' C_2(\Delta t_2, r') \sin\left(\frac{n\pi r'}{a}\right) dr' \right] \\ + \left[\frac{P_3}{6D_3'} (a^2 - r^2) \right] \\ + \left[\frac{2P_3 a^3}{3rD_3'} \sum_{n=1}^{\infty} \frac{(-1)^n}{n^3} \sin\left(\frac{n\pi r}{a}\right) e^{-n^2 \pi^2 D_3' t} \right]$$

for which

$$m_3 = \frac{4}{3} \pi a^3 P_3 \Delta t_3 \\ + \frac{8a^3}{3} \left[\frac{P_1}{D_1'} \sum_{n=1}^{\infty} \frac{1}{n^4} (e^{-n^2 \pi^2 D_1' \Delta t_1} - 1) e^{-n^2 \pi^2 D_2' \Delta t_2} (e^{-n^2 \pi^2 D_3' \Delta t_3} - 1) \right. \\ + \frac{P_2}{D_2'} \sum_{n=1}^{\infty} \frac{1}{n^4} (e^{-n^2 \pi^2 D_2' \Delta t_2} - 1) (e^{-n^2 \pi^2 D_3' \Delta t_3} - 1) \\ \left. + \frac{P_3}{D_3'} \sum_{n=1}^{\infty} \frac{1}{n^4} (e^{-n^2 \pi^2 D_3' \Delta t_3} - 1) \right] \quad (16)$$

and for which

$$f_3 = \frac{m_1 + m_2 + m_3}{\frac{4}{3} \pi a^3 (P_1 \Delta t_1 + P_2 \Delta t_2 + P_3 \Delta t_3)}$$

$$f_3 = 1 + \frac{6}{\pi^4 (P_1 \Delta t_1 + P_2 \Delta t_2 + P_3 \Delta t_3)} \cdot Z \quad (17)$$

where

$$\begin{aligned}
 Z = & \frac{P_1}{D_1'} \sum_{n=1}^{\infty} \frac{1}{n^4} \left[e^{-n^2 \pi^2 (D_1' \Delta t_1 + D_2' \Delta t_2 + D_3' \Delta t_3)} - e^{-n^2 \pi^2 (D_2' \Delta t_2 + D_3' \Delta t_3)} \right] \\
 & + \frac{P_2}{D_2'} \sum_{n=1}^{\infty} \frac{1}{n^4} \left[e^{-n^2 \pi^2 (D_2' \Delta t_2 + D_3' \Delta t_3)} - e^{-n^2 \pi^2 D_3' \Delta t_3} \right] \\
 & + \frac{P_3}{D_3'} \sum_{n=1}^{\infty} \frac{1}{n^4} \left[e^{-n^2 \pi^2 D_3' \Delta t_3} - 1 \right] \quad (18)
 \end{aligned}$$

5) General Case

In general, cumulative fractional release at the end of k^{th} time step can be calculated by

$$\begin{aligned}
 f_k = 1 + \frac{6}{\pi^4} \sum_{i=1}^k \frac{P_i \Delta t_i}{D_i'} & \left[\frac{P_1}{D_1'} \sum_{n=1}^{\infty} \frac{1}{n^4} \left(e^{-n^2 \pi^2 \sum_{i=1}^k D_i' \Delta t_i} - e^{-n^2 \pi^2 \sum_{i=2}^k D_i' \Delta t_i} \right) \right. \\
 & + \frac{P_2}{D_2'} \sum_{n=1}^{\infty} \frac{1}{n^4} \left(e^{-n^2 \pi^2 \sum_{i=2}^k D_i' \Delta t_i} - e^{-n^2 \pi^2 \sum_{i=3}^k D_i' \Delta t_i} \right) \\
 & \quad \vdots \\
 & \left. + \frac{P_k}{D_k'} \sum_{n=1}^{\infty} \frac{1}{n^4} \left(e^{-n^2 \pi^2 D_k' \Delta t_k} - 1 \right) \right] \quad (19)
 \end{aligned}$$

Defining $\tau_1 = \sum_{i=1}^k D_i' \Delta t_i, \tau_2 = \sum_{i=2}^k D_i' \Delta t_i, \dots, \tau_k = D_k' \Delta t_k$

and $g(\tau) = \frac{6}{\pi^4 \tau} \sum_{n=1}^{\infty} \frac{1}{n^4} (1 - e^{-n^2 \pi^2 \tau})$ (20)

Eq. (19) can be transformed to

$$f_k = 1 - \frac{1}{\sum_{i=1}^k P_i \Delta t_i} \left[\frac{P_1}{D_1'} (\tau_1 g(\tau_1) - \tau_2 g(\tau_2)) + \frac{P_2}{D_2'} (\tau_2 g(\tau_2) - \tau_3 g(\tau_3)) + \dots + \frac{P_k \Delta t_k}{D_k'} g(\tau_k) \right] \quad (21)$$

Using a relationship $\sum_{n=1}^{\infty} \frac{1}{n^4} = \frac{\pi^4}{90}$, Eq. (20) can be rewritten as :

$$g(\tau) = \frac{1}{15\tau} - \frac{6}{\tau} \sum_{n=1}^{\infty} \frac{e^{-n^2 \pi^2 \tau}}{n^4 \pi^4} \quad (22)$$

A comparison between Eq. (22) above and Eq. (13) of Section II-B1 shows that

$$g(\tau) = 1 - F \text{ (Eq. (13) of Section II-B1).}$$

Therefore, the function $g(\tau)$ in Eq. (21) can be determined using a finite number of terms (for an accuracy better than 10^{-5}) :

For $\tau \leq 0.1$, $g(\tau) = 1 - 4 \sqrt{\frac{\tau}{\pi}} + \frac{3}{2} \tau$ (23)

For $\tau > 0.1$, $g(\tau) = \frac{1}{15\tau} - \frac{6}{\tau} \sum_{n=1}^3 \frac{e^{-n^2 \pi^2 \tau}}{n^4 \pi^4}$ (24)

References:

1. H. S. Carslaw and J. C. Jaeger, Conduction of Heat in Solids, Oxford Press, London, 1959.
2. S. M. Selby (Ed.), Standard Mathematical Tables (17th Edition), The Cleveland Rubber Co., Cleveland, Ohio (1969).
3. A. H. Booth, Chalk River Report, CRCD-721 (1957).

B. HIGH TEMPERATURE DATA BASE (C. E. Beyer, HEDL)

Several sources of high-temperature oxide gas release data have been examined in order to cover the operating range of commercial reactors. The vast majority of in-reactor gas release data have been obtained from post-irradiation puncturing of fuel pins. This is done several days following irradiation after the radioactive gases have decayed off, leaving only the stable gases for measurement. There have been a few sweep-gas experiments which have measured in-situ release and thus, the radioactive species; however, the majority of these have been at low temperatures with small thermal gradients and low fission densities. This has necessitated the use of stable gas release data by the Working Group to define the diffusion coefficients for the radioactive species.

The High Temperature Data Base consists of two sources of data which are referred to here as the Low Burnup Data Base and the High Burnup Data Base.

1. Low Burnup Data Base and Selection Criteria

Early in the Working Group's inception, a data base was selected from an earlier analysis by Beyer and Hann⁽¹⁾ which yielded 45 well-characterized data sets for stable gas releases. The major limitation of these data was that burnups did not exceed 19,000 MWd/t, which led to the data being referred to as "the low burnup data base."

This data base substantially reduced the variance among in-reactor gas release data by establishing discriminative criteria for data selection and providing a systematic approach to data reduction. The criteria for data selection in this report were:

- Stoichiometric UO_2 ($O/M = 2.00 \pm 0.005$)
- Relatively constant rod powers over time.

$$\left(\frac{P_{max}}{P_{time\ avg.}} \leq 1.15 \right)$$

- Relatively flat axial rod power (temperature) profile

$$\left(\frac{\text{Axial Peak Power}}{\text{Axial Avg. Power}} \leq 1.15\right)$$

- Fuel temperatures measurable either from thermocouples or inferred from a microstructural change.

Several sources of data were considered in this analysis with only 7 sources⁽²⁻⁸⁾ and 45 data points able to meet all of the above criteria. These data have shown a relatively small amount of variance even though they have come from five different experimenter's with varying fuel rod designs.

Since the issuance of the Beyer-Hann report, the ANS 5.4 Committee has scrutinized these data very closely and found some minor inconsistencies among the data. Because of these inconsistencies, additional criteria for reduction of the data in Table 1 were established. These criteria are as follows:

- Burnup within the fuel is based on 200 MeV/fission.
- Heat generated within the fuel is based on 182 MeV/fission.
- Fission gas generated within the fuel is based on a yield of 26.9 cc/MWd for Xe and 4.1 cc/MWd for Kr production.
- Irradiation time is based on effective-full-power days.

The remaining methodology used for calculating the fuel temperature profiles is the same as described in Reference 1, which in brief consists of the:

- MAIN computer code
- Time-averaged rod powers
- Use of Lyon's, et al.,⁽⁹⁻¹⁰⁾ thermal conductivity equation for UO₂ along with the Maxwell-Eucken⁽¹¹⁻¹²⁾ relationship to account for effects of porosity.
- Use of flux depression subroutine from GAPCON-Thermal-1⁽¹³⁾ and a method proposed by Robertson.⁽¹⁴⁾

The reduced form (rod powers, fuel temperatures, burnups, irradiation time, etc.) of the 45 data points is presented in Table 1 of this report. The data

Table 1. Low Burnup Released Data and Reduced Temperatures

REFERENCE	SPECIMEN NO.	HEAT RATING (kW/FT)	FUEL TEMPERATURES (°C)		IRRADIATION TIME (10 ⁶ SEC)	BURNUP (MWD/MTM)	RELEASE FRACTIONS
			SURFACE	CENTERLINE			
DTECH ^o	ELP-4	12.3	597.	1771.	8.683	11348.	0.108
ECS-EEC 73-595 (BNES CONF. 1973)	ELP-5	13.5	490.	1717.	2.678	3870.	0.049
"	ELP-6	15.1	662.	2187. ^b	8.623	13713.	0.227
"	ELP-9	14.9	586.	2050. ^b	11.759	18804.	0.258
"	ELP-10	14.9	606.	2082. ^b	5.841	9348.	0.203
"	ELP-12	13.3	661.	1989. ^b	5.901	8424.	0.197
HPR-129 ^o	116-5	18.9	509.	2305.(2010. ^c)	7.482	4579.	0.275
"	117-1	19.8	549.	2276.(2000. ^c)	13.366	8713.	0.254
AECL-1676 ^o	DFE	35.0	416.	3724.	1.397	794.	0.388
"	DFH	28.9	402.	2780.	1.397	648.	0.311
"	DFD	29.1	474.	2904.	1.397	658.	0.317
"	DFB	23.9	462.	2466.	1.397	528.	0.169
"	DFA	17.4	402.	1728.	1.397	386.	0.046
AECL-2662 ^o	LFL	15.6	455.	1661.	9.336	2230.	0.057
"	LFF	15.5	560.	1901.	9.336	2230.	0.173
"	LFB	15.1	642.	2046. ^b	9.336	2230.	0.234
"	LFS	21.9	561.	2451. ^b	9.336	3120.	0.379
"	LPW	23.1	432.	2339. ^b	9.336	3290.	0.248
"	LFT	22.2	554.	2609. ^b	9.336	3290.	0.496
"	LPX	23.0	519.	2551. ^b	9.336	3290.	0.368
"	LFM	21.3	441.	2189. ^b	9.336	3030.	0.155
"	LFH	21.1	533.	2403. ^b	9.336	3030.	0.311
"	LFD	20.7	620.	2571. ^b	9.336	3030.	0.458
AECL-2230	CBN	17.1	455.	1820. ^b	7.30	2650.	0.123
"	CBO	17.3	463.	1956. ^b	7.30	2670.	0.149
"	CBP	16.8	458.	1812. ^b	7.30	2610.	0.141
"	CBR	17.4	497.	1950. ^b	7.30	2710.	0.157
"	CBT	16.6	496.	1888. ^b	7.30	2620.	0.153
"	CBV	17.5	470.	1941. ^b	7.30	2760.	0.165
"	CBY	16.55	518.	1957. ^b	7.30	2630.	0.168
"	CBX	17.1	525.	2020. ^b	7.30	2710.	0.188
CEA-R-3618	CYRANO-II	13.9	758.	2069.	1.588	1033.	0.150
ALSO CERAMIC NUCL. FUELS	CYRANO-VII	11.5	843.	1969.	3.544	1409.	0.130
CEA-R-3358	4110-AE1	18.1	612.	2296.	11.2	7051.	0.216
"	4110-AE2	17.6	570.	2175.	11.2	6860.	0.221
"	4110-BE1	15.1	548.	1876.	11.2	5738.	0.139
"	4110-BE2	17.8	485.	2047.	11.2	7215.	0.159
"	4112-AE1	19.5	420.	2126. ^b	5.80	3795.	0.126
"	4112-AE2	17.7	483.	2058. ^b	5.80	3549.	0.112
"	4112-BE1	15.4	425.	1699.	5.80	3073.	0.079
"	4112-BE2	16.6	463.	1902. ^b	5.80	3313.	0.126
"	4113-AE1	17.1	728.	2473. ^b	5.80	3418.	0.267
"	4113-AE2	15.6	729.	2239. ^b	5.80	3116.	0.280
"	4113-BE1	16.0	538.	1965. ^b	5.80	3124.	0.170
"	4113-BE2	15.9	694.	2204. ^b	5.80	3161.	0.210

^oDATA REVISED FROM BNWL-1875.

^bAVERAGE OF CENTERLINE TEMPERATURES DETERMINED FROM EQUILAXED AND COLUMNAR GRAIN BOUNDARIES.

^cTHERMOCOUPLE MEASUREMENT IN ANNULAR PELLETS. ALL OTHER TEMPERATURES CORRESPOND TO SOLID PELLETS GEOMETRY.

sets which have been adjusted to correct the inconsistencies and typographical errors are from the following reports or papers: DTECH ECS-EFC-73-595 (BNES Conf. 1973), ⁽²⁾ HPR-129, ⁽³⁾ AECL-1676, ⁽⁴⁾ and AECL-2662. ⁽⁵⁾ Consequently, some of the data presented in Table 1 differs from those presented in the original reports and BNWL-1875. ⁽¹⁾ Since the original reports were not always clear as to the MeV/fission used for rod powers and burnups, the fission gas yields used for release fractions, and the existence of typographical errors, the primary authors of the above reports were contacted to provide this information. Based on their replies (Appendix A) and the above criteria and methodology for data reduction, we have made the following adjustments.

The DTECH ECS-EFC-73-594 paper has presented burnups based on 184 MeV/fission. In addition, the release fractions are not consistent with the fission yields used in this analysis. To be consistent with our methodology for data reduction, the burnups and release fractions have been recalculated in Table 1 based on 200 MeV/fission and 31 cc/MWd, respectively.

The HPR-129 report has presented rod powers based on total assembly power (i.e., 200 MeV/fission). The rod powers for the two rods in Table 1 have been recalculated based on 182 MeV/fission. It should also be mentioned that rod powers for these rods are not based on time averaged values, but rather those powers which correspond to the temperatures utilized in Table 1. The measured thermocouple temperatures for both rods have also been revised downward by 60°C from BNWL-1875 ⁽¹⁾ to reflect (time) average temperatures during the latter 1/3 of irradiation. The higher temperatures in BNWL-1875 were the peak temperatures measured during the same time period.

The AECL-1676 report gives the effective-full-power days (EFPD) as 16.7 which is a typographical error and should be 16.17 EFPD. Release fractions were also adjusted slightly (~5%) to reflect the updated yields for xenon used in this analysis (26.9 cc/MWd).

The rod powers utilized for the AECL-2662 data in BNWL-1875 were peak (time) powers. The powers presented in Table 1 are average (time) rod powers.

2. High Burnup Data Base and Selection Criteria

As noted above, the low burnup data base did not exceed 19,000 Mwd/Mt. Current commercial reactors reach peak burnups up to 40,000 Mwd/Mt pointing to the need for a data base in the 20,000 to 40,000 Mwd/Mt burnup range. It also came to the attention of the committee that a significant burnup effect may exist above 30,000 Mwd/MTM. (Reference 15 and Appendix B) At this time, the Working Group researched the open literature to find non-proprietary data in the higher burnup range. However, the committee could not find data which could meet the selection criteria used in the low-burnup data base. The major problems for data at high burnups have been the lack of an independent measure of fuel temperature, a significant variation in power history, and that much of the data was derived from mixed-oxide (MOX) fuel. (Appendix C)

Published gas release data (16,17) from fuel irradiated to high burnups (15,000 to 39,000 Mwd/MTM) in the Saxton reactor were examined. However, attempts to calculate fuel temperatures for these fuel rods showed large uncertainties in calculated values. (Appendix D) These data have also been criticized as being inconclusive in quantifying a burnup effect. (Appendix E)

A large high burnup data base was discovered (18) in the Liquid Metal Fast Breeder Reactor (LMFBR) program; however, detailed data were not publicly available. The Nuclear Regulatory Commission subsequently obtained and published (19) these data. Upon examination of these data, the Working Group discovered that some of the data exhibited relatively small variations in power history, and all of the data had a relatively flat axial power profile. Also, the majority of the data have detailed power histories and grain growth measurements. The major problems in comparison with the low burnup criteria were that temperatures were calculated rather than measured independently, and were from $(U_{0.75} Pu_{0.25}) O_2$ rather than from UO_2 .

The temperatures for the LMFBR data were calculated with the SIEX code. (18) This code has been developed exclusively for and correlated against EBR-II fuel irradiations.

The Working Group has attempted to determine if any inherent differences exist between MOX and UO₂ gas release data; however, no data were found which allowed a direct comparison typical of operating conditions in commercial fuel. Calculations by Westinghouse; (Appendix B) however, have indicated that their burnup dependent release model, based on UO₂ data, adequately predicts MOX data. Also, the GESMO report⁽²⁰⁾ concluded that there did not appear to be justification for differences in releases between MOX and UO₂ fuels.

Consequently, the Working Group has accepted selected LMFBR data as the high-burnup data base. These data are the best characterized and controlled of the high-burnup data examined. There has also been a systematic approach in the data reduction.

Similar to the low-burnup data, criteria were used in the selection of LMFBR data. These criteria were:

- Relatively small centerline temperature variations (5200°C) with time as calculated by SIEX.
- Relatively flat axial power profile

$$\left(\frac{\text{Axial Peak Power}}{\text{Axial Avg. Power}} \leq 1.09 \right)$$

The second criterion was met by all EBR-II data since the core length is relatively short (13.5 inches) and the peak-to-average approximately 1.08. The first criterion resulted in only 19 out of 41 LMFBR gas release data points being acceptable. These data are listed in Table 2.

The rod powers and temperatures quoted represent the end-of-life (EOL) calculated values. With the exception of beginning-of-life (BOL) temperatures, these EOL values are at or near the peak temperatures experienced by these rods. An example of a typical centerline and surface temperature history for these fuel rods is given in Figures 1a and 1b.

TABLE 2

HIGH BURNUP DATA BASE AND CALCULATED TEMPERATURES

Rod No.	Heat Rating (Kw/ft)	Fuel Dia. (inches)	Fuel Temperature EOL* (°C)		Fuel Density (% TD)	Burnup MWd/MTM	Grain Growth Radius (inches)		Gas Release (%)
			Surface	Centerline			Columnar	Equiaxed	
PNL 1-6	8.18	0.2120	769	1703	95.1	8070	0.0382	0.0600	12.9
PNL 1-14	8.40	0.2120	762	1723	91.6	8180	0.0244	0.0474	8.2
PNL 1-17	8.95	0.2122	769	1783	93.2	8680	0.0371	0.0550	15.1
PNL 1-18	9.24	0.2122	766	1787	95.0	8950	0.0498	0.0799	18.1
PNL 1-19	9.20	0.2101	855	1838	98.0	9090	0.0568	0.0763	29.9
PNL 3-8	4.85	0.2134	925	1475	93.5	26340	0.000	0.0467	10.7
PNL 3-27	4.71	0.2135	823	1363	90.2	26740	0.000	0.0280	12.5
PNL 3-33	4.75	0.2116	851	1386	92.4	26710	0.000	0.0360	13.1
PNL 4-1	8.55	0.2135	851	1751	94.6	42140	0.0413	0.0707	62.2
PNL 4-26	8.05	0.2135	846	1767	97.0	40980	0.0440	0.0732	64.5
PNL 4-34	7.73	0.2118	967	1851	95.3	39570	0.0536	0.0751	65.4
PNL 7-10	8.46	0.2111	862	1722	95.2	24250	0.0467	0.0742	30.1
PNL 8-11	12.16	0.2115	870	2078	98.0	58200	0.0803	-	92.2
PNL 8-25	11.61	0.2115	853	1999	97.8	57180	0.0822	-	94.3
PNL 8-37	10.77	0.2119	818	1870	96.9	55720	0.0652	-	65.2
PNL 8-38	11.45	0.2120	798	1921	95.6	27760	0.0653	0.0760	53.6
PNL 10-15	8.73	0.1944	866	1788	91.8	60550	-	-	78.7
PNL 10-23	8.34	0.1949	877	1817	93.2	49820	0.0524	0.0691	67.5
PNL 10-63	8.32	0.1948	847	1797	94.6	51960	0.0559	0.0699	71.5

*End-of-Life

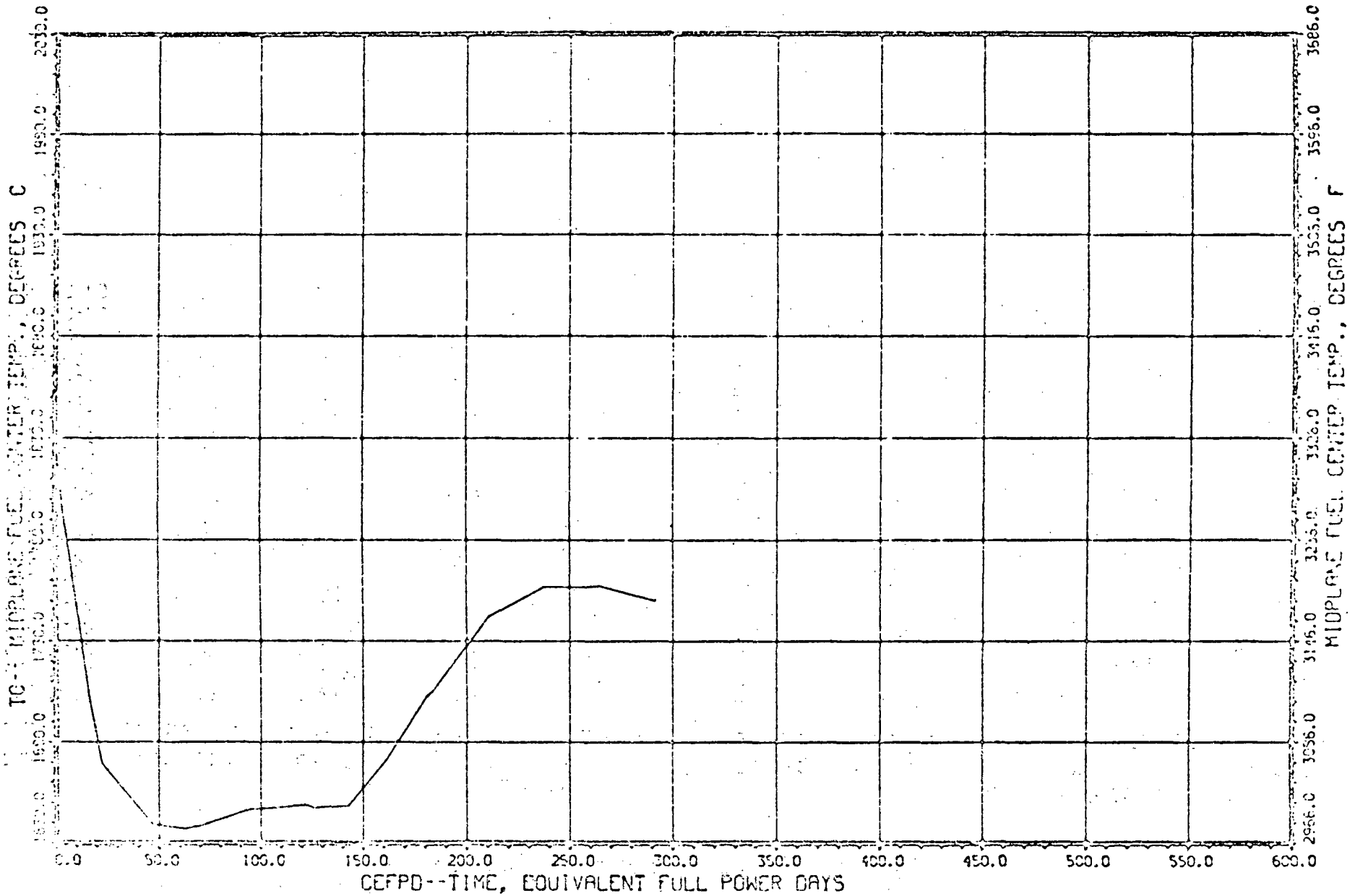


FIGURE 1a. Fuel Centerline Temperature History for PNL 4-1.

All temperatures in Table 2 are taken directly from the SIEX calculations with the exceptions of three rods, PNL 3-8, 3-27 and 3-33. Peak BOL temperatures calculated by SIEX for these rods were unreasonably low ($\sim 300^{\circ}\text{C}$) when compared to their measured equiaxed grain growth. The other 16 rods used in high burnup data base consistently predicted grain growth boundary temperatures of $\sim 1450^{\circ}\text{C}$.[†] Dutt later confirmed that SIEX was underpredicting temperatures for the PNL 3 rods. (21)

In order that temperatures for these three rods be made consistent with the other 16 high burnup rods, the original temperature histories for these rods, as predicted by SIEX, were normalized to calculated BOL temperatures based on a 1450°C grain growth temperature. The EOL temperatures from this normalized temperature history were then used in Table 2.

[†] These grain growth temperatures were estimated from SIEX BOL temperature profiles, which in all but one instance represented the peak temperature during the rod life.

REFERENCES

1. C. E. Beyer and C. R. Hann, Prediction of Fission Gas Release from UO_2 , BNWL-1875, Battelle-Northwest Laboratories, 1974.
2. E. De Meulemeester, et al., "Review of Work Carried out by BELGONCLEAIRE and CEA on the Improvement and Verification of the Computer Code with the Aid of In-Pile Experimental Results," British Nuclear Energy Society International Conference on Nuclear Fuel Performance, DTECH ECS-EFC-73-595, (October 15-19, 1973).
3. J. A. Ainscough, An Assessment of the IFA-116 and 117 Irradiations from Data Obtained from the In-Reactor Instrumentation, HPR-129, (April 1971).
4. M. J. F. Notley, et al., Zircaloy Sheathed UO_2 Fuel Elements Irradiated at Values of $\int_{rod} dQ$ Between 40 and 83 w/cm, AECL-1676, (December 1962).
5. M. J. F. Notley, R. Deshaies, et al., Measurements of the Fission Product Gas Pressures Developed in UO_2 Fuel Elements During Operation, AECL-2662 (1966).
6. M. J. F. Notley and J. R. MacEwan, The Effect of UO_2 Density on Fission Product Gas Release and Sheath Expansion, CRNL Report AECL-2230 (1965).
7. P. Chenebault and R. Dumas, "In Pile Mobility of Fission Gases in UO_2 Fuel Rods," Ceramic Nucl. Fuels. CONF-690512, (1969).
8. Jean-Claude Janvier, et al., Irradiation of Uranium Dioxide in Strong Cladding Effect of Initial Diametral Gap on Overall Behavior, CEA-R-3358, (October 1967).
9. M. F. Lyons, et al., UO_2 Pellet Thermal Conductivity From Irradiation With Central Melting, GEAP-4624, 1964.
10. S. Y. Ogawa, E. A. Lees, and M. F. Lyons, Power Reactor High Performance UO_2 Program, GEAP-5591, 1968.
11. J. C. Maxwell, A Treatise on Electricity and Magnetism, vol. I, 3rd edition, Oxford University Press (1891), reprinted by Dover, New York (1954).
12. A. Eucken, "The Heat Conductivities of Ceramic Refractory, Calculations of Heat Conductivity from the Constituents," Forsch, Gebiete Ingenieurw, B3 Forschungsheft, no. 353, 1932.

REFERENCES

13. C. R. Hann, C. E. Beyer, and L. J. Parchen, GAPCON-THERMAL-1: A Computer Program for Calculating the Gap Conductance in Oxide Fuel Pins, BNWL-1778 (September 1973).
14. J. A. L. Robertson, $\int_{\kappa d\theta}$ in Fuel Irradiations, CRFD-835 (1959).
15. E. Roberts, G. W. Hopkins, W. R. Smalley, M. G. Balfour and E. Deguidt, "Fuel Modeling and Performance of High Burnup Fuel Rods," ANS Program for Meeting Attendees, ANS Topical Meeting on Water Reactor Fuel Performance, May 9-11, 1977, St. Charles, Ill.
16. W. R. Smalley, Saxton Core II Fuel Performance Evaluation, Part I: Materials, WCAP-3385-56, Part I, September, 1971.
17. W. R. Smalley, Evaluation of Saxton Core III Fuel Materials Performance, WCAP-3385-57, July, 1974.
18. D. S. Dutt and R. B. Baker, "SIEX: A Correlated Code for the Prediction of Liquid Metal Fast Breeder Reactor (LMFBR) Fuel Thermal Performance," HEDL-TME 74-55, June 1975.
19. R. O. Meyer, C. E. Beyer and J. C. Vogtleweed, "Fission Gas Release from Fuel at High Burnup." NRC Report, NUREG-0418, March 1978.
20. "Final Generic Environmental Statement on the Use of Recycle Plutonium in Mixed Oxide Fuel in Light Water Cooled Reactors," NRC Report, NUREG-0002, Vol 3, August 1976.
21. D. Dutt, Private communication.

C. Model Fitting

1. Diffusion Theory (ANS 5.4 Model)

(C.S. Rim, Korea Atomic Energy Research Institute)

The stable isotope solution of the burnup dependent diffusion model (Equation 21 in Section II - A2b) was fitted to various stable fission gas release data. The modified diffusion coefficient, D' , was assumed to be a function of temperature and burnup in the following form :

$$D' = (D_0/a^2) e^{-Q/RT} \times 100^{Bu/B}$$

where

T is the local fuel temperature (K)

R is the gas constant (cal/mole K)

Q is the activation energy (cal/mole)

Bu is the accumulated local burnup (MWD/t)

D_0/a^2 , Q and B were determined to meet the following requirements :

- 1) Fit to 45 low burnup data
- 2) Fit to 19 high burnup data
- 3) Low release for low temperature fuel even at high burnup

Low and high burnup data quoted in 1) and 2) above are described in detail in Section II - B. Based on the review of fission gas release data from low temperature fuel (Section III - B), the third requirement was determined to be "less than 0.25% release at 30,000 MWD/ t from a pellet with the centerline temperature of 900°C and a surface temperature of 400°C".

In analyzing the data, the total irradiation period was divided into a series of time steps with a burnup increment of 1,000 MWD/t and the diffusion coefficients were calculated using burnups corresponding to the midpoints of each time step. The pellets were subdivided into 10 radial rings of equal volume, and the average temperature and burnup in each ring were used in determining diffusion coefficients.

For low burnup data, which were obtained from thermal reactor irradiations, detailed radial power distributions were used in calculating local fission gas production rates, burnups and fuel temperatures. A uniform radial power distribution was assumed for high burnup fuel pins which were irradiated in EBR - II, a fast reactor. High burnup data were analyzed using parabolic radial temperature distributions and an axial power distribution with a peak to average power ratio of 1.08.

The steep temperature gradient across the pellet and the nonlinear form of the model have necessitated the use of nonlinear regression techniques to fit the model and data. For a given set of data, many values of D_0/a^2 , Q and B were tried, in order to obtain a small residual sum - of - squares, S_R^2 :

$$S_R^2 = \sum_{j=1}^n (F_j^P - F_j^M)^2$$

where n is the number of data points, F_j^P is the predicted fission gas release for the j^{th} data point, and F_j^M is the measured fission gas release for the j^{th} data point. An effort was also made to obtain

the regression line close to the ideal one, i.e., $F^P = F^M$.

An extensive parametric study resulted in the following parameters which give a best fit to the low and high burnup data sets and meet the low temperature requirement :

$$D_0/a^2 = 0.61 \text{ sec}^{-1}$$

$$Q = 72,300 \text{ cal/mole}$$

$$B = 28,000 \text{ MWD/t}$$

Figure II C - 1 shows a comparison between measured and predicted fission gas release for 45 low burnup data. For this data set, the correlation coefficient is 0.88 and the regression line is

$$F^P = 0.97 F^M + 1.9$$

where F^P and F^M are predicted and measured fission gas release in percent

The goodness of fit to the high burnup data is shown in Figure II C - 2. For this data set, the correlation coefficient is 0.97 and the regression line is

$$F^P = 0.91 F^M + 1.33$$

The fission gas release calculated for low temperature fuel ($T_c = 900^\circ\text{C}$, $T_s = 400^\circ\text{C}$) is 0.23% at 30,000 MWD/t and, therefore, the model satisfies the low temperature requirement. Although the low release restriction was included in order to maintain consistency with the low temperature data, it did not change the goodness of fit to both low and high burnup data significantly.

Fission gas release calculated by the model at constant fuel temperature and power is shown in Figure II C - 3. Figure II C - 4 shows the results with step changes in fuel temperature and power at 20,000 MWD/t. The effect of burnup enhancement factor in the diffusion coefficient is given in Table II C - 1. Also presented in Table II C - 1 are results for pellets with given centerline and surface temperatures and parabolic radial temperature and uniform radial power distributions.

Table IIC-1 Comparison Between Burnup Dependent and Burnup Independent Diffusion Model

Fission Gas Release (%) in PWR Fuel Rods

Temp	Burnup (GWD/t)	1000	5000	10000	20000	30000	40000	50000
1000°C	With Bu Dep { 6 Kw/ft	0.16	0.47	0.91	2.45	5.90	10.60	29.9
	12 Kw/ft	0.72	0.33	0.64	1.73	4.20	9.73	11.77
	No Bu Dep 12 Kw/ft	0.11	0.54	0.54	0.48	0.59	0.63	0.76
1500°C	With Bu Dep 12 Kw/ft	6.41	17.74	32.48	72.11	27.37	99.58	99.95
	No Bu Dep 12 Kw/ft	5.95	13.31	18.08	24.94	29.95	34.00	37.44
T _{CO} = 1500°C	With Bu Dep 12 Kw/ft	0.93	2.62	4.93	12.15	23.02	33.53	42.59
T _{CO} = 1500°C	No Bu Dep 12 Kw/ft	0.36	1.91	2.58	3.74	4.53	5.19	5.76
T _{CO} = 1000°C T _{FS} = 500°C	With Bu Dep 6 Kw/ft	0.03	0.07	0.14	0.38	0.92	2.15	4.86
	No Bu Dep 6 Kw/ft	0.02	0.05	0.07	0.11	0.13	0.15	0.1
T _{CO} = 900°C T _{FS} = 400°C	With Bu Dep 6 Kw/ft	0.01	0.02	0.04	0.10	0.23	0.55	1.26
	No Bu Dep 6 Kw/ft	0.01	0.01	0.02	0.03	0.03	0.04	0.04

48

$Q = 72300 \text{ cal/mole} \quad D_0/a^2 = 0.61 \text{ sec}^{-1}$

$D'(Bu, T) = D'(T) \times 100^{Bu/20000}$

Pellet Diameter = 0.3225", Pellet Density = 95% TD

Fraction of Power Generated in Pellet = 0.974

Figure II C - 1

MEASURED vs PREDICTED FISSION GAS RELEASE

(Low burnup data < 19000 MWD/t)

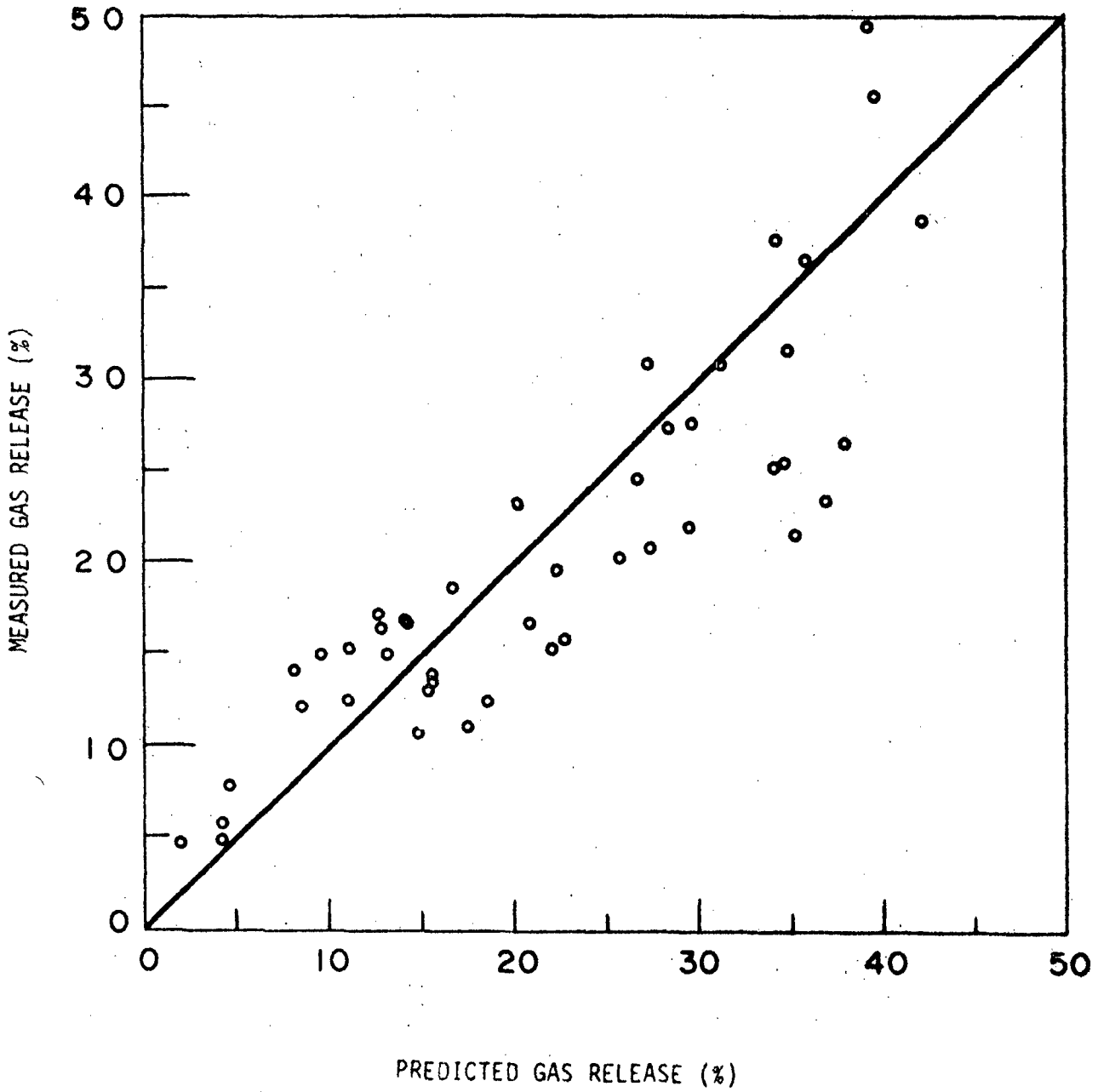


Figure II C - 2

MEASURED vs PREDICTED FISSION GAS RELEASE

(high burnup data < 60600 MWD/t)

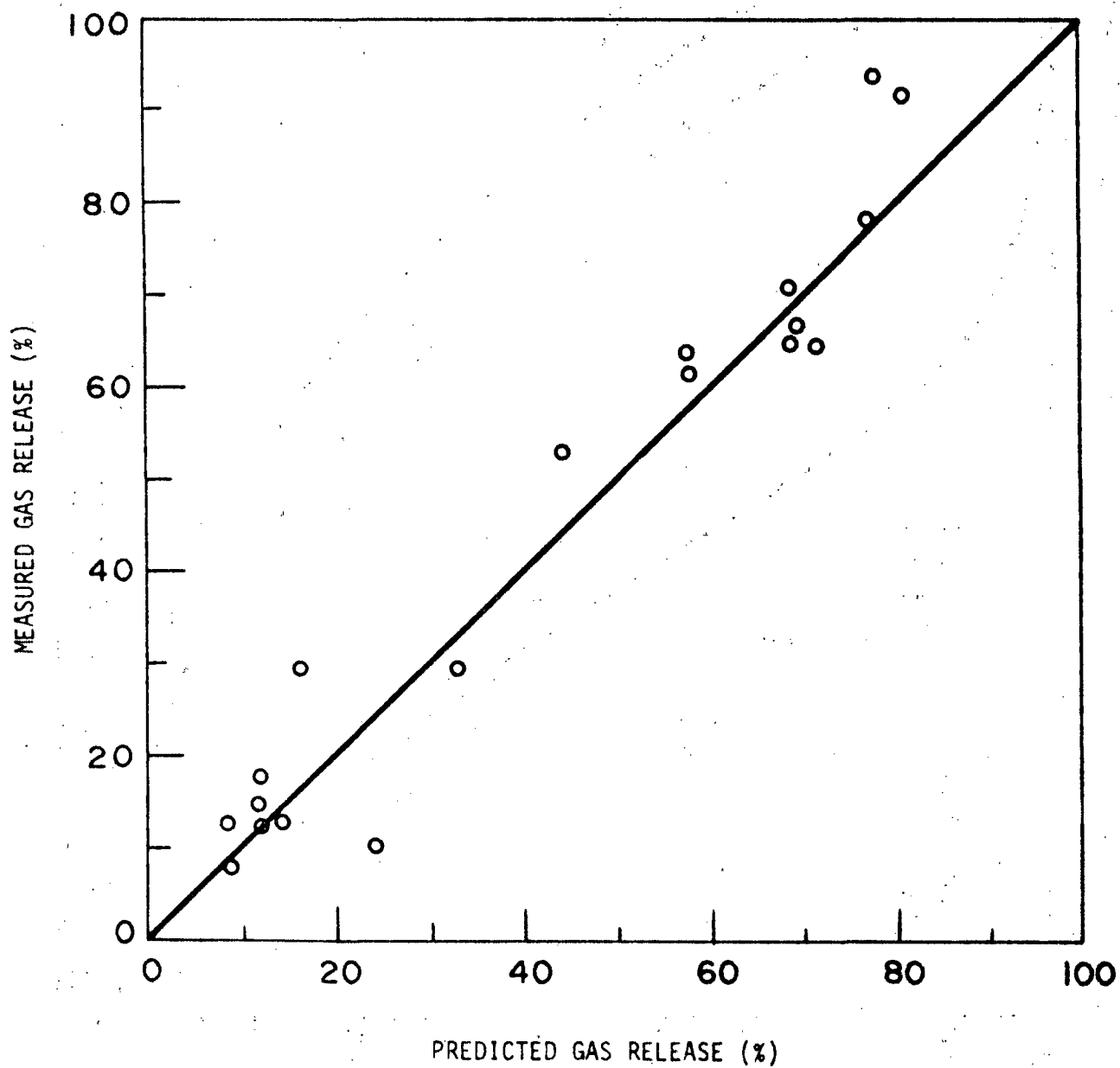


Fig.II C - 3 Fission Gas Release at Constant Temperature and Power

51

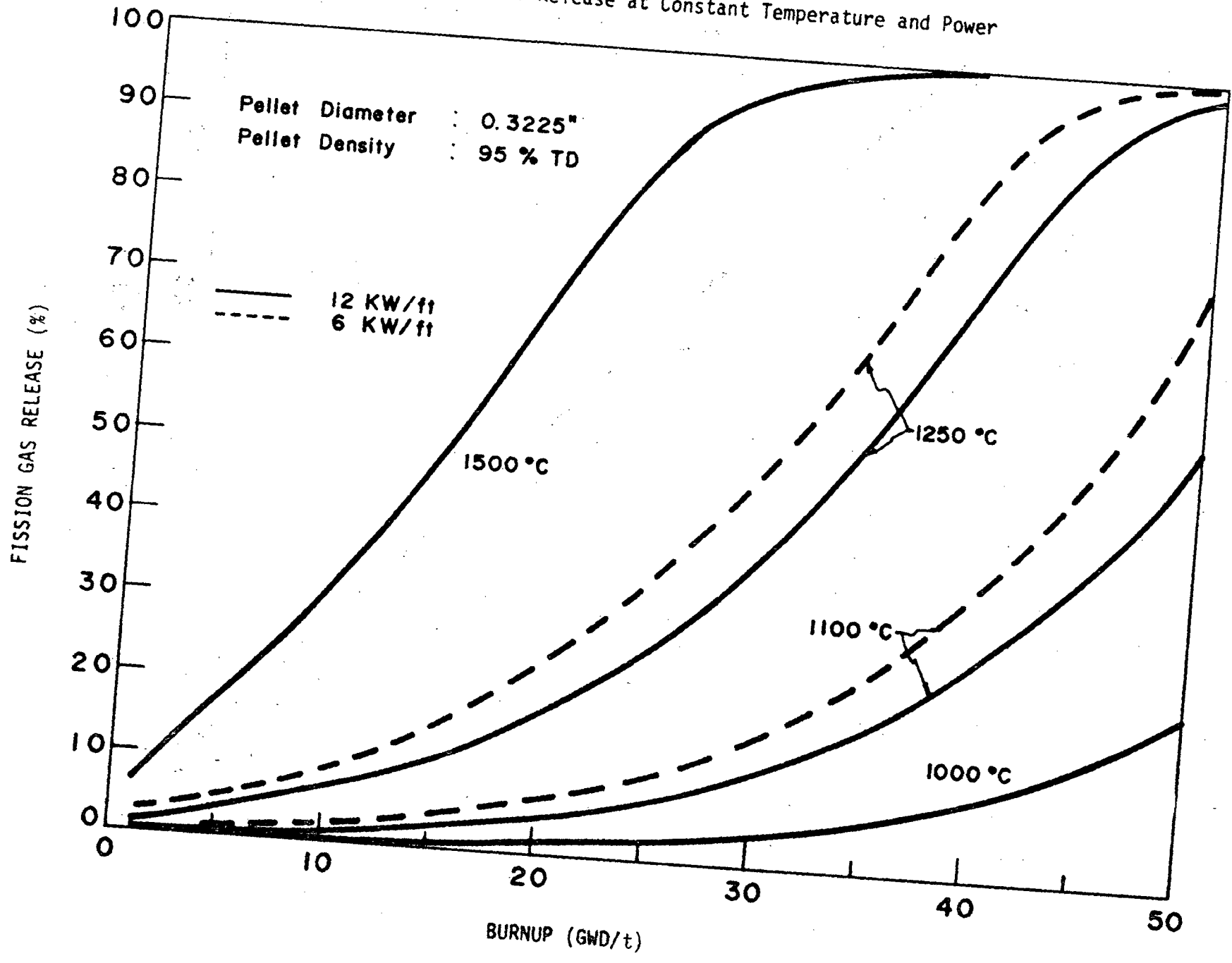
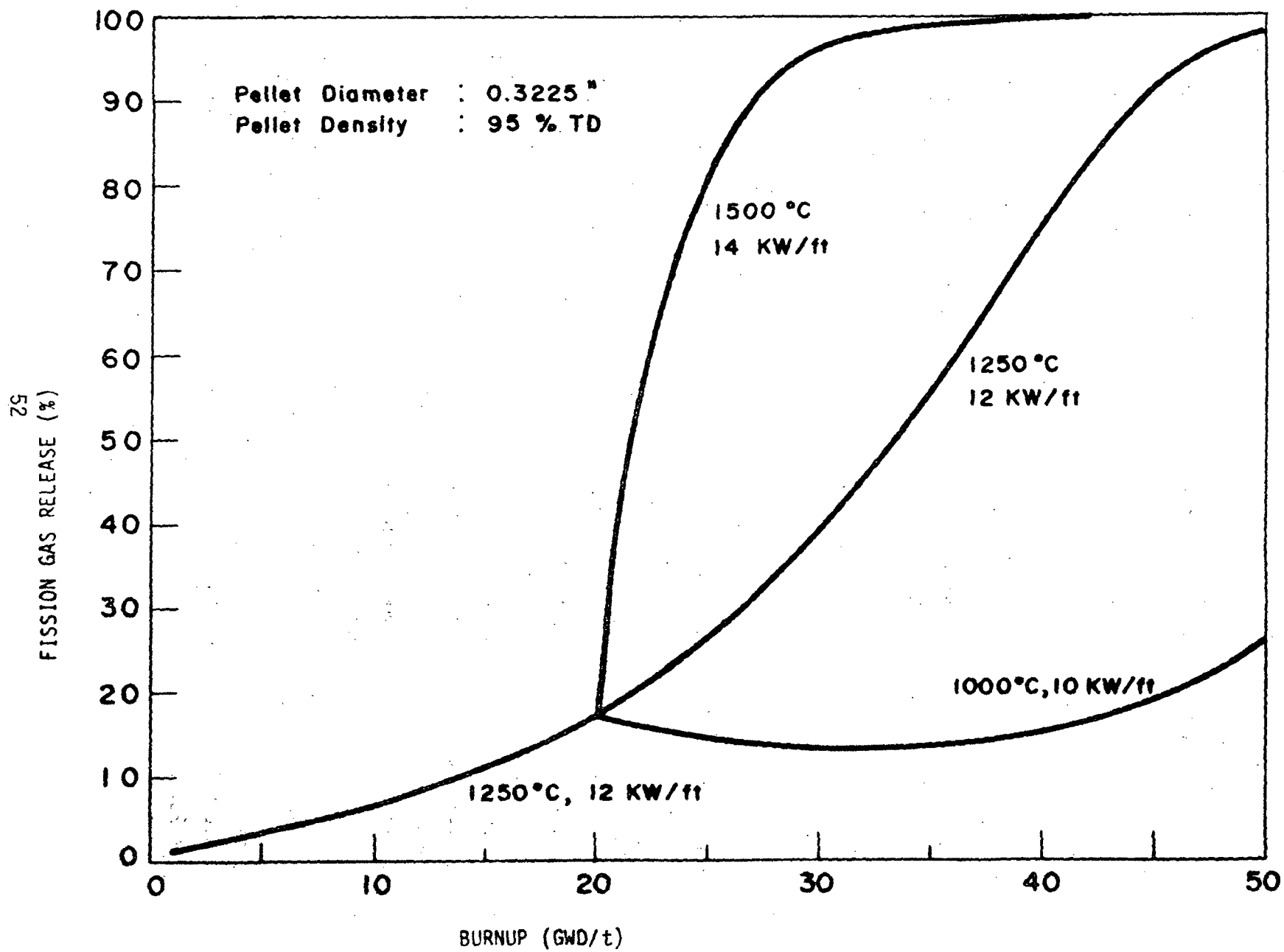


Fig. II C-4 Fission Gas Release with Step Changes in Temperature and Power



2. Comparison with Beyer-Hann/NRC Model
(R. O. Meyer, U.S. Nuclear Regulatory Commission)

Comparisons (using GAPCON-THERMAL-2) have been made of the ANS-5.4 model and the Beyer-Hann fission gas release model. They were expected to agree well in the burnup range below 20,000 MWd/t because both models were based on the same low-burnup data base. However, the ANS-5.4 model overpredicted the Beyer-Hann model significantly above 5,000 MWd/t for high linear power ratings.

These comparisons were continued for burnups above 20,000 MWd/t by using the NRC correction function with the Beyer-Hann model. They were expected to agree in this burnup range as well because both were derived from a second high-burnup data base. Again they do not agree. While the ANS-5.4 model overpredicts the other model significantly at 20,000 MWd/t, the trend reverses at about 38,000 MWd/t, and by 50,000 MWd/t the ANS-5.4 underpredicts the other model significantly. See Fig. 1 for a typical comparison.

The ANS-5.4 Working Group considered two approaches in deriving the release correlation. One approach provided a best-fit to the low-burnup data and made a discontinuous switch to a burn-up dependent function at 20,000 MWd/t. This approach would have resulted in lower gas release predictions below 20,000 MWd/t and would have assured agreement with the Beyer-Hann model. The approach was rejected because there was no fundamental basis for a discontinuity in the model at 20,000 MWd/t, because the low-burnup data base was very sparse above 10,000 MWd/t, and because the burnup dependence would have been stronger than we believed reasonable at high burnups. The second approach, that taken by the ANS-5.4 Working Group, assumes a single continuous function which applies at all burnups. The agreement between this function and the data is good as demonstrated by correlation coefficients of 0.88 (low burnup) and 0.97 (high burnup). This agreement is illustrated in Figures IIC-1 and IIC-2. Nevertheless, there is a suggestion that the use of the high burnup EBR-II data results in overpredictions for the transition range near 20,000 MWd/t, particularly at high power levels.

At the time the ANS-5.4 model was developed, additional data were not available to quantify such overpredictions. The Working Group has concluded that the model is the best candidate for a standard that the present state-of-the-art will allow.

B&W 15X15

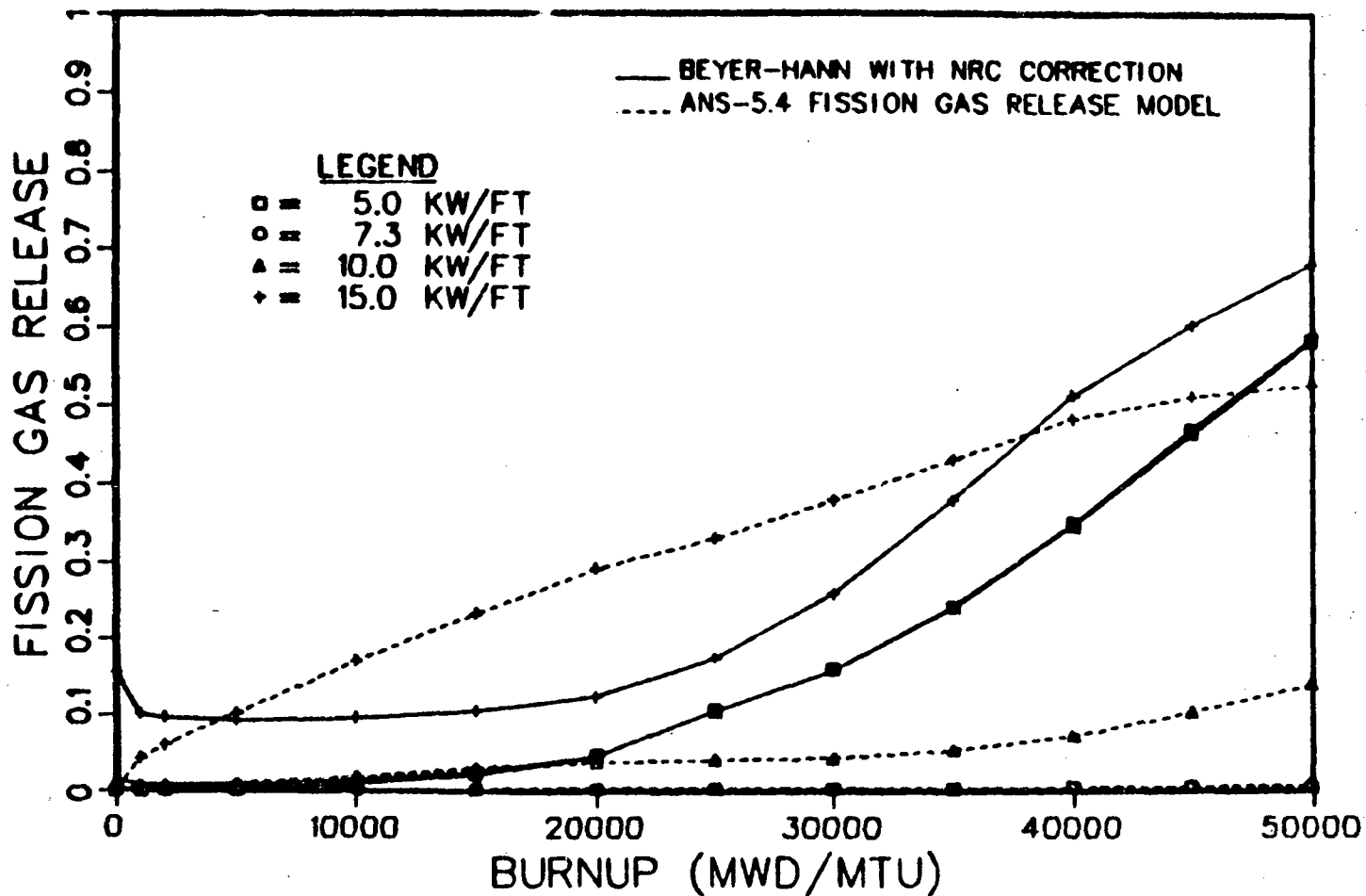


Fig. 1 Fission Gas Release for Two Burnup Dependent Fission Gas Release Models

D. REDUCING APPLICATION ERRORS (L.D. Noble, GE)

The total release within any axial segment of a fuel rod is the integral of the radial release distribution. The error introduced by approximating the integral should not be so large that it contributes significantly to the uncertainty in the calculated fuel rod release. If it is assumed that other uncertainties, such as in the fission gas model itself, in the power and temperature distributions, etc., are of the order of 15%, then the integration error should be \lesssim 7%.

A number of calculations were performed to investigate the error introduced by an integration scheme using N equally spaced nodes. The release fraction in each node was computed using the node average temperature.

A simplified relationship between fuel temperature and power was used:

$$T = 560 + 20P + 95P(1-X)$$

where T is the fuel temperature, (K), at radial location $X = (r/R)^2$, and P is the power in KW/ft. This relation is equivalent, for typical LWR rods, to assuming no pellet flux depression, a constant pellet-to-coolant heat transfer coefficient of 750 Btu/ft²-hr-⁰F, and a fuel thermal conductivity of 0.0273 w/cm-⁰C. Calculations were performed for power levels between 1 and 20 KW/ft at the four different sets of time and exposure shown in Table 1.

The maximum calculated percentage error in the release fraction F for all the cases considered is plotted in Figure 1 as a function of the number of nodes N. (Calculations with N=100 were used as the "correct" answers). The trend in the maximum error was similar, regardless of whether equal volume, or equal radial increment nodes were used. The maximum percentage error for some cases which had equal temperature differences, ΔT , between nodes is plotted in Figure 2.

The results indicate that it is the number of radial nodes, not the temperature difference, which is the primary factor in reducing integration error. Six or more nodes appear sufficient in all cases (in most cases 4 to 5 is acceptable).

TABLE 1: COMBINATIONS USED IN ASSESSING ERROR

<u>TIME</u> <u>(YEARS)</u>	<u>EXPOSURE</u> <u>(GWD/t)</u>	<u>D't 100^{Bu/28}</u>	<u>POWER</u> <u>(KW/FT)</u>	<u>TEMPERATURE</u> <u>(K)</u>
0.1	1	2.28×10^6	1 to 20	560 to 2860
0.5	5	2.20×10^7	"	"
3	25	3.55×10^9	"	"
8	50	5.78×10^{11}	"	"

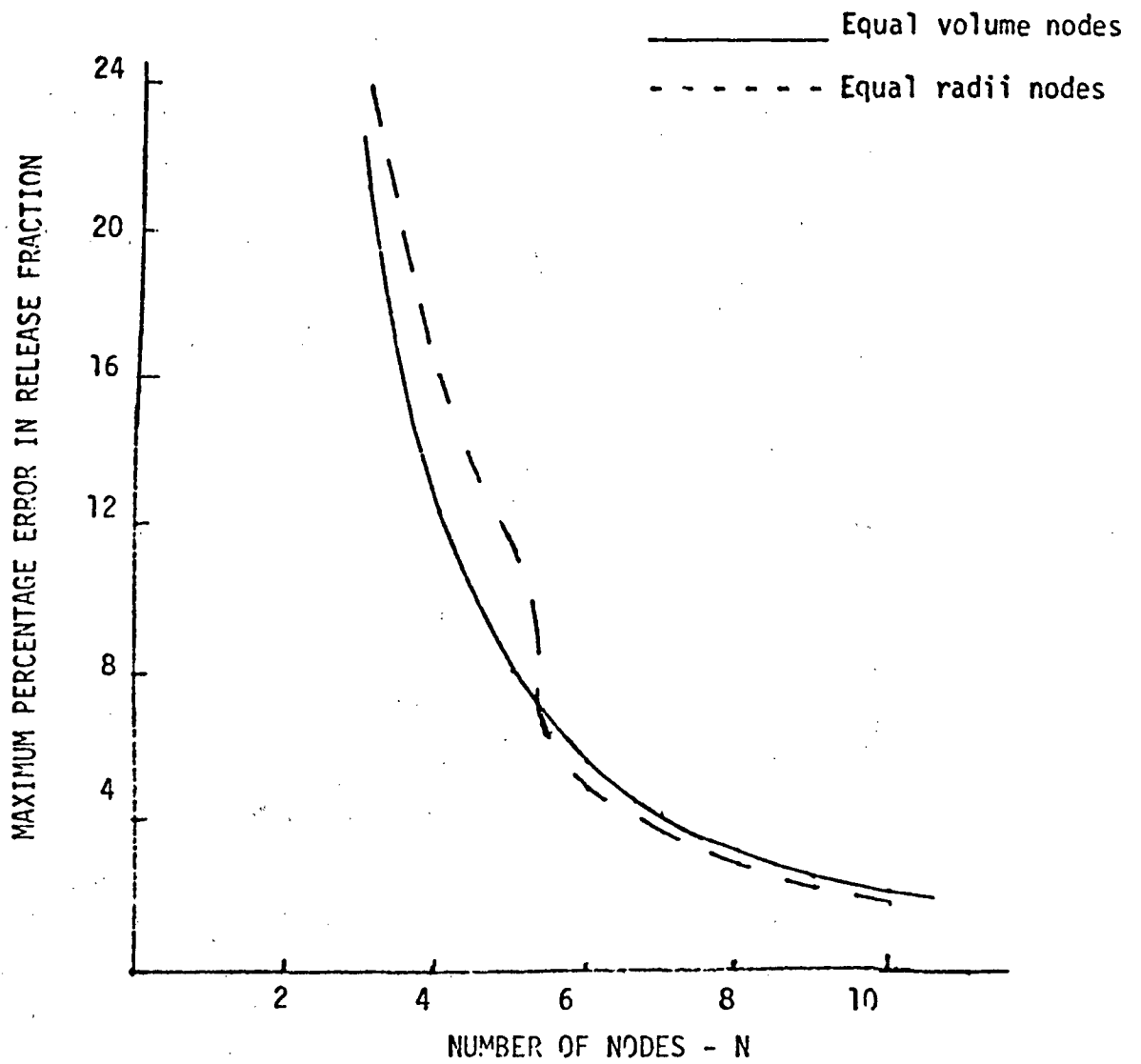


FIGURE 1 : ERROR IN RELEASE FRACTION VERSUS NUMBER OF RADIAL PELLET NODES.

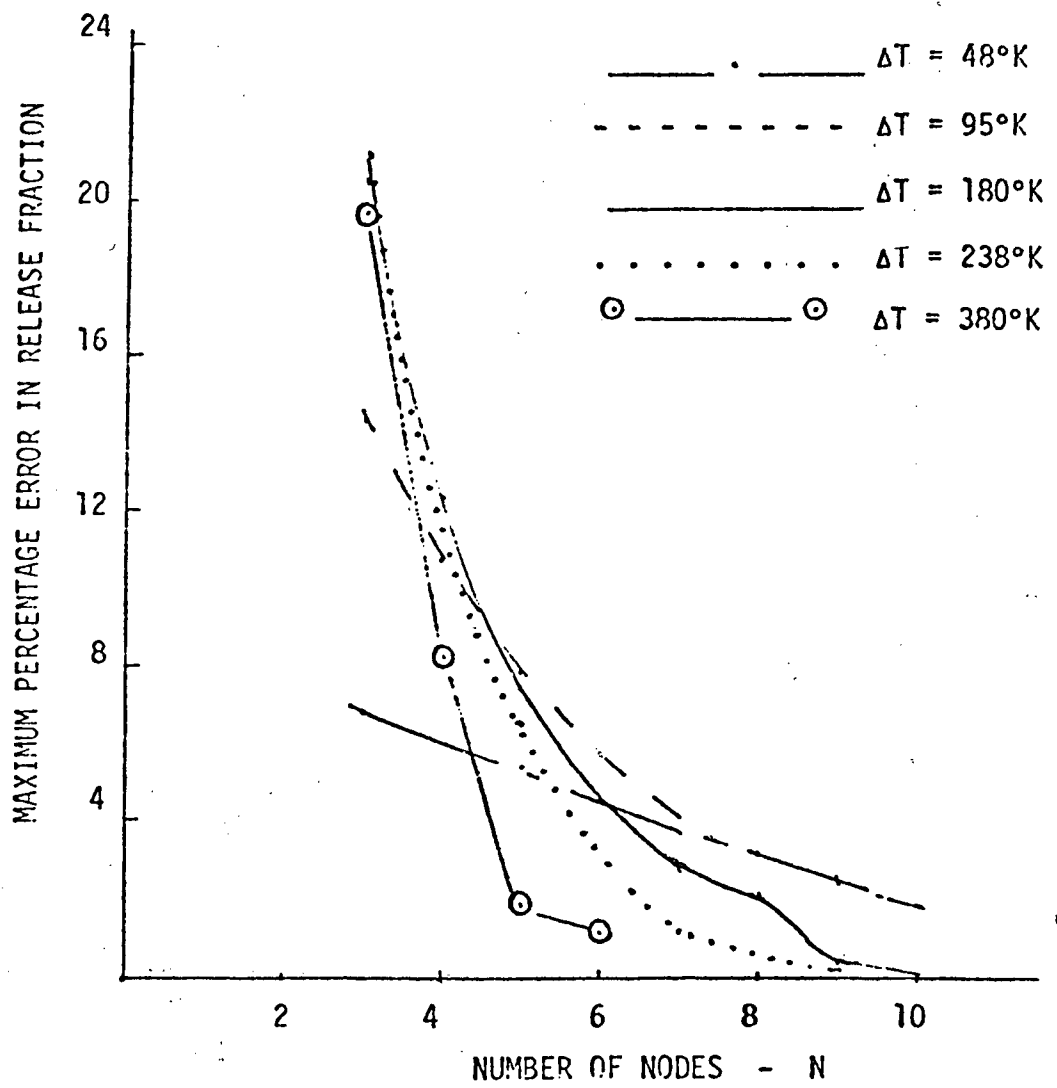


FIGURE 2 : ERROR IN RELEASE VERSUS NUMBER OF NODES FOR VARIOUS CONSTANT TEMPERATURE INCREMENTS.

E. RELEASE OF IODINE, CESIUM, AND TELLURIUM (R. L. Ritzman, SAI)

1. GENERAL

A survey of the literature for the past twenty years revealed about a dozen studies of iodine, cesium, or tellurium release from UO_2 , either in-reactor or out-of-reactor. The data that have been reported were obtained using a variety of techniques and conditions. Only three or four studies represented systematic investigations over a sizeable temperature range with prototypical UO_2 fuel specimens. It was considered impractical to obtain absolute release parameters from this limited data base. A principal factor in this judgment was the absence of differential release rate data in the studies, without which an assessment of the possible "burst release effect" cannot be made. However, since the systematic studies noted above included noble gas release measurements as well as iodine, cesium, and tellurium release measurements, it does appear feasible to obtain relative release parameters for iodine, cesium, and tellurium from the data set. In such a case the "burst release effect" for each of the different species would tend to cancel and its influence on the release parameters would be minimized.

The considerable effort to develop a standard analytical method for the noble gases has resulted in a procedure which is based on diffusion theory.* In order to be compatible, the method for the other volatile fission products should have the same basis. Therefore, the plan for the present work was to use what data are available from the literature to develop diffusion parameter ratios for each fission product relative to xenon. The reference noble gas diffusion parameter (D') could then be multiplied by these ratios to obtain D' values for the other fission products for use in the ANS-5.4 model. Several criteria for data acceptance were formulated to promote applicability of the derived diffusion parameter ratios to the conditions of commercial fuel rod operation. The criteria are listed as follows:

*As described in this report.

- 1) Only fission product and noble gas release data obtained in the same experiment were to be used in deriving sets of diffusion parameter ratios. This is consistent with the relative nature of the procedure.
- 2) Release data for these species were to be limited to measurements made at temperatures above about 1000°C since diffusion release is regarded as important at these higher temperatures.
- 3) The release data were obtained from high density UO₂ samples (greater than about 92% theoretical density) since this is more characteristic of reactor grade fuel.
- 4) The UO₂ samples used in the studies were stoichiometric or slightly hyperstoichiometric in composition since this is also more characteristic of reactor grade fuel.

2. DATA SOURCES

On the basis of the above criteria, two reports from the literature were identified as sources of data for obtaining diffusion parameter ratios. Each of the studies involved post-irradiation heating experiments rather than in-pile tests at elevated temperatures. The first data source was the work of Davies, Long, and Stanaway⁽¹⁾ who measured D'_I/D'_{Xe} , D'_{Cs}/D'_{Xe} , and D'_{Te}/D'_{Xe} ratios for a series of UO_2 sintered compacts, sintered spheroids, and fused spheroids of various densities at temperatures ranging from 1000°C to 2150°C in hydrogen. A total of 19 separate values was reported for samples which had a density of 10.16 g/cc or greater. The results as given by the authors are listed here in Table 1 (Iodine/Xenon), Table 2 (Cesium/Xenon), and Table 3 (Tellurium/Xenon).

The second data source was the work of Parker, Creek, Barton, Martin, and Lorenz⁽²⁾ who measured the fractional release of xenon and the other fission products from reactor-type UO_2 samples (93 - 94% theoretical density) during 5.5 hour anneals at temperatures ranging from 1400°C to 2260°C in helium. From the reported experiments, a group was selected in which the measured fission product release fractions were low enough to allow calculation of D' ratios using the simple diffusion equation. The results of these experiments and calculations are listed in Table 4 (Iodine/Xenon), Table 5 (Cesium/Xenon), and Table 6 (Tellurium/Xenon).

Other reports were identified in which the investigators applied classical diffusion theory to interpret post-irradiation release data. However, these reports either used one of the sets of data noted above or did not provide the basic release data from which the classical diffusion coefficients were derived. Therefore these sources were not included in this analysis.

It should be noted that no specific evidence exists which would confirm that diffusion parameter ratios obtained from out-of-pile heating experiments are applicable for predicting fission product release under in-pile conditions. In-pile irradiation is accompanied by certain phenomena which do not occur out-of-pile such as continuous generation of fission product species, fission-induced re-solution from lattice trapping sites or gas bubbles, and perhaps even fission enhanced transport of species within the solid. However, the ratio approach noted above offers the best potential for compensating for such absolute differences in environmental and mechanistic factors until definitive in-pile data become available. The method utilized here should be applied with the realization that future in-pile work could result in modifications to the parameter ratios or perhaps even to the basic approach.

Table 1. Diffusion Parameter Ratios Obtained for Iodine/Xenon in Reference (1)

Sample Type	Density g/cm ³	Surface Area cm ² /g	Temperature °C	D _I ⁱ /D _{Xe} ⁱ
Sintered	10.3	140	1000	15.2
Compacts	10.3	140	1000	39.7
Compacts	10.3	140	1200	8.4
Compacts	10.3	140	1400	5.3
Compacts	--	100	1600	1.7
Compacts	10.3	10	1600	19.4
Compacts	10.8	5	1600	6.3
Compacts	10.16	4	1300	53.3
Compacts	10.7	7	2000	7.8
Compacts	10.7	7	2150	1.4
Sintered	--	25	1200	4.4
Spheroids	--	25	1400	28.1
Spheroids	--	25	1600	7.3
Spheroids	--	25	1600	16.8
Spheroids	--	25	1600	12.3
Spheroids	--	25	1600	2.0
Spheroids	--	103	1400	6.3
Fused				
Spheroid	10.6	77	1200	4.0
Spheroid	10.6	77	1600	16.8

Table 2. Diffusion Parameter Ratios Obtained for Cesium/Xenon in Reference (1)

<u>Sample Type</u>	<u>Density g/cm³</u>	<u>Surface Area cm²/g</u>	<u>Temperature °C</u>	<u>D'_{Cs}/D'_{Xe}</u>
Sintered	10.3	140	1000	5.76
Compact	10.3	140	1000	26.0
Compact	10.3	140	1200	1.96
Compact	10.3	140	1400	1.96
Compact	-	~100	1600	5.29
Compact	10.3	10	1600	39.7
Compact	10.8	5	1600	0.64
Compact	10.7	7	2000	4.84
Compact	10.7	7	2050	0.83
Compact	10.7	7	2150	0.141
Sintered	-	25	1200	1.0
Spheroids	-	25	1400	21.2
Spheroids	-	25	1600	0.36
Spheroids	-	25	1600	6.25
Spheroids	-	25	1600	0.64
Spheroids	-	25	1600	0.36
Spheroids	-	25	1400	6.25
Fused	10.6	77	1200	1.0
Spheroids	10.6	77	1600	3.24

Table 3. Diffusion Parameter Ratios Obtained for Tellurium/Xenon in Reference (1)

<u>Sample Type</u>	<u>Density g/cm³</u>	<u>Surface Area cm²/g</u>	<u>Temperature °C</u>	<u>D_{Te}'/D_{Xe}'</u>
Sintered	10.3	140	1000	7.84
Compacts	10.3	140	1000	24.0
Compacts	10.3	140	1200	15.2
Compacts	10.3	140	1400	7.29
Compacts	10.3	19	1600	100.
Compacts	10.8	5	1600	121.
Compacts	10.16	4	1300	44.9
Compacts	10.7	7	2000	13.0
Sintered	-	25	1200	6.76
Spheroids	-	25	1400	39.7
Spheroids	-	25	1600	110.3
Spheroids	-	25	1600	196.
Spheroids	-	25	1600	441.
Spheroids	-	25	1600	441.
Spheroids	-	103	1400	10.9
Fused	10.6	77	1200	32.5
Spheroids	10.6	77	1600	259.

Table 4. Diffusion Parameter Ratios Calculated from Release Data for Iodine and Xenon in Reference (2)

Sample Type	% Theo. Density	Temperature °C	Fraction Released in 5.5 Hours		D'_I/D'_{Xe}
			I	Xe	
PWR-UO ₂	93-94	1515	0.058	0.013	19.9
PWR-UO ₂	93-94	1610	0.065	0.027	5.8
PWR-UO ₂	93-94	1710	0.096	0.026	13.6
PWR-UO ₂	93-94	1800	0.12	0.037	10.5
PWR-UO ₂	93-94	1900	0.16	0.097	2.7
PWR-UO ₂	93-94	1400	0.04	0.008	25.0
EGCR-UO ₂	97	1400	0.009	0.008	1.3
PWR-UO ₂	93-94	1400	0.016	0.005	10.2
PWR-UO ₂	93-94	1400	0.23	0.061	14.2
EGCR-UO ₂	97	1610	0.037	0.026	2.0
PWR-UO ₂	93-94	1610	0.055	0.060	0.84
PWR-UO ₂	93-94	1610	0.25	0.14	3.2
PWR-UO ₂	93-94	1780	0.12	0.037	10.5
EGCR-UO ₂	97	1780	0.24	0.12	4.0

Table 5. Diffusion Parameter Ratios Calculated from Release Data for Cesium and Xenon in Reference (2)

Sample Type	% Theo. Density	Temperature °C	Fraction Released in 5.5 Hours		D'_{Cs}/D'_{Xe}
			Cs	Xe	
PWR-UO ₂	93-94	1515	0.014	0.013	1.16
PWR-UO ₂	93-94	1610	0.017	0.027	0.396
PWR-UO ₂	93-94	1710	0.027	0.026	1.08
PWR-UO ₂	93-94	1800	0.032	0.037	0.748
PWR-UO ₂	93-94	1900	0.086	0.097	0.786
PWR-UO ₂	93-94	1980	0.15	0.12	1.56
EGCR-UO ₂	97	1400	0.026	0.008	10.6
PWR-UO ₂	93-94	1400	0.005	0.005	1.0
PWR-UO ₂	93-94	1400	0.21	0.061	11.9
EGCR-UO ₂	97	1610	0.12	0.026	21.3
PWR-UO ₂	93-94	1610	0.20	0.060	11.1
PWR-UO ₂	93-94	1780	0.032	0.037	0.748

Table 6. Diffusion Parameter Ratios Calculated from Release Data for Tellurium and Xenon in Reference (2)

<u>Sample Type</u>	<u>% Theo. Density</u>	<u>Temperature °C</u>	<u>Fraction Released in 5.5 Hours</u>		<u>D' Te/D' Xe</u>
			<u>Te</u>	<u>Xe</u>	
PWR-UO ₂	93-94	1515	0.029	0.013	4.98
PWR-UO ₂	93-94	1610	0.12	0.027	19.75
PWR-UO ₂	93-94	1710	0.20	0.026	59.2
PWR-UO ₂	93-94	1800	0.21	0.037	32.2
PWR-UO ₂	93-94	1400	0.039	0.008	23.8
EGCR-UO ₂	97	1400	0.008	0.008	1.0
PWR-UO ₂	93-94	1400	0.012	0.005	5.76
PWR-UO ₂	93-94	1400	0.16	0.061	6.88
EGCR-UO ₂	97	1610	0.12	0.026	21.3
PWR-UO ₂	93-94	1780	0.21	0.037	32.2

3. ANALYSIS OF THE DATA SOURCES

Inspection of Tables 1 through 6 reveals a total of 33 determinations of D'_I/D'_{Xe} , 31 determinations of D'_{Cs}/D'_{Xe} , and 27 determinations of D'_{Te}/D'_{Xe} as a function of temperature. Assuming D' values for each individual species would follow the expected Arrhenius equation, the form of the D' ratio versus temperature expressions should be:

$$D'_{FP}/D'_{Xe} = D'^0_{FP}/D'^0_{Xe} \exp [(Q_{Xe} - Q_{FP})/RT] \quad (1)$$

or,

$$\ln(D'_{FP}/D'_{Xe}) = \ln(D'^0_{FP}/D'^0_{Xe}) + [(Q_{Xe} - Q_{FP})/RT] \quad (2)$$

where, D'_{FP} = the diffusion parameter for iodine, cesium, or tellurium at temperature T , (sec^{-1})

D'_{Xe} = the diffusion parameter for xenon at temperature T , (sec^{-1})

D'^0_{FP} = the limiting diffusion parameter for iodine, cesium, or tellurium, (sec^{-1})

D'^0_{Xe} = the limiting diffusion parameter for xenon, (sec^{-1})

Q_{FP} = the activation energy for iodine, cesium, or tellurium diffusion, (cal/g-atom)

Q_{Xe} = the activation energy for xenon diffusion, (cal/g-atom)

R = the gas constant, (cal/g-atom, K)

T = the absolute temperature, (K)

Using the form of the expression in equation (2), each set of D' ratio versus temperature determinations was subjected to a linear regression analysis. The results of the analysis are displayed in Figure 1 (Iodine/Xenon), Figure 2 (Cesium/Xenon), and Figure 3 (Tellurium/Xenon). Each figure contains the individual data points, the estimated regression line for the set of data, and the 90% confidence limits for the regression line. The estimated regression lines in the three figures correspond to the following set of D' ratio expressions:

$$D'_I/D'_{Xe} = 5.75 \times 10^{-1} \exp (8900/RT) \quad (3)$$

$$D'_{Cs}/D'_{Xe} = 7.58 \times 10^{-2} \exp (12100/RT) \quad (4)$$

$$D'_{Te}/D'_{Xe} = 1.10 \times 10^3 \exp (-12500/RT) \quad (5)$$

In the ANS 5.4 model, each of the above expressions can be multiplied by the reference Arrhenius expression for noble gases to obtain reference Arrhenius expressions for each of the other volatile fission products.

The constants in Equations (3), (4), and (5) represent expected values. However, these constants are subject to some uncertainty. Therefore, 90% confidence limit values were obtained for each of the constants. The resulting lower and upper limit values are given in Table 7. It is the simultaneous effect of the uncertainty in (D'_{FP}^0/D'_{Xe}^0) and $(Q_{Xe} - Q_{FP})$ that produces the 90% confidence limit curves which are shown in Figures 1, 2, and 3.

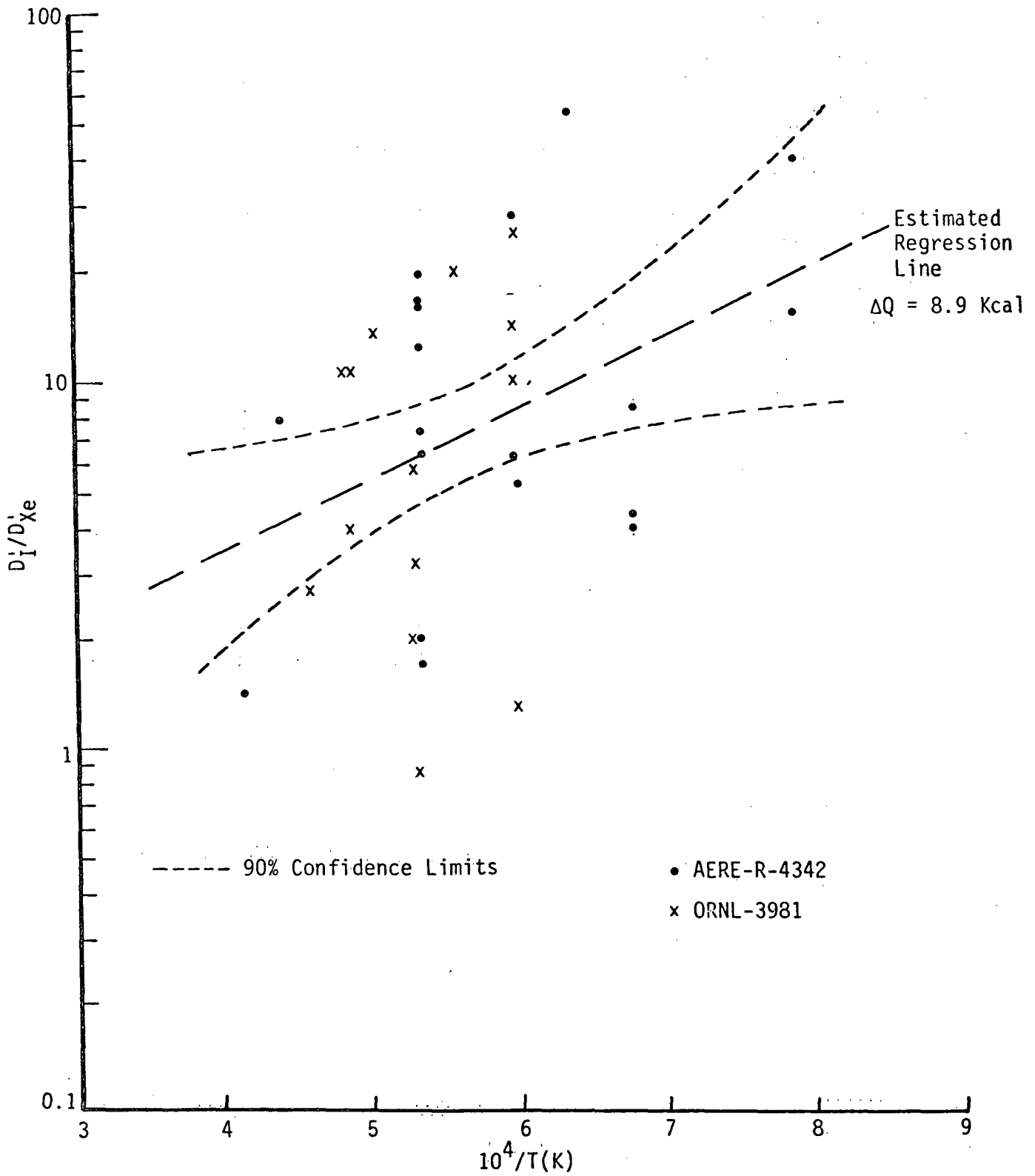


Figure 1. Diffusion Parameter Ratio Data and Regression Analysis Results for Iodine/Xenon

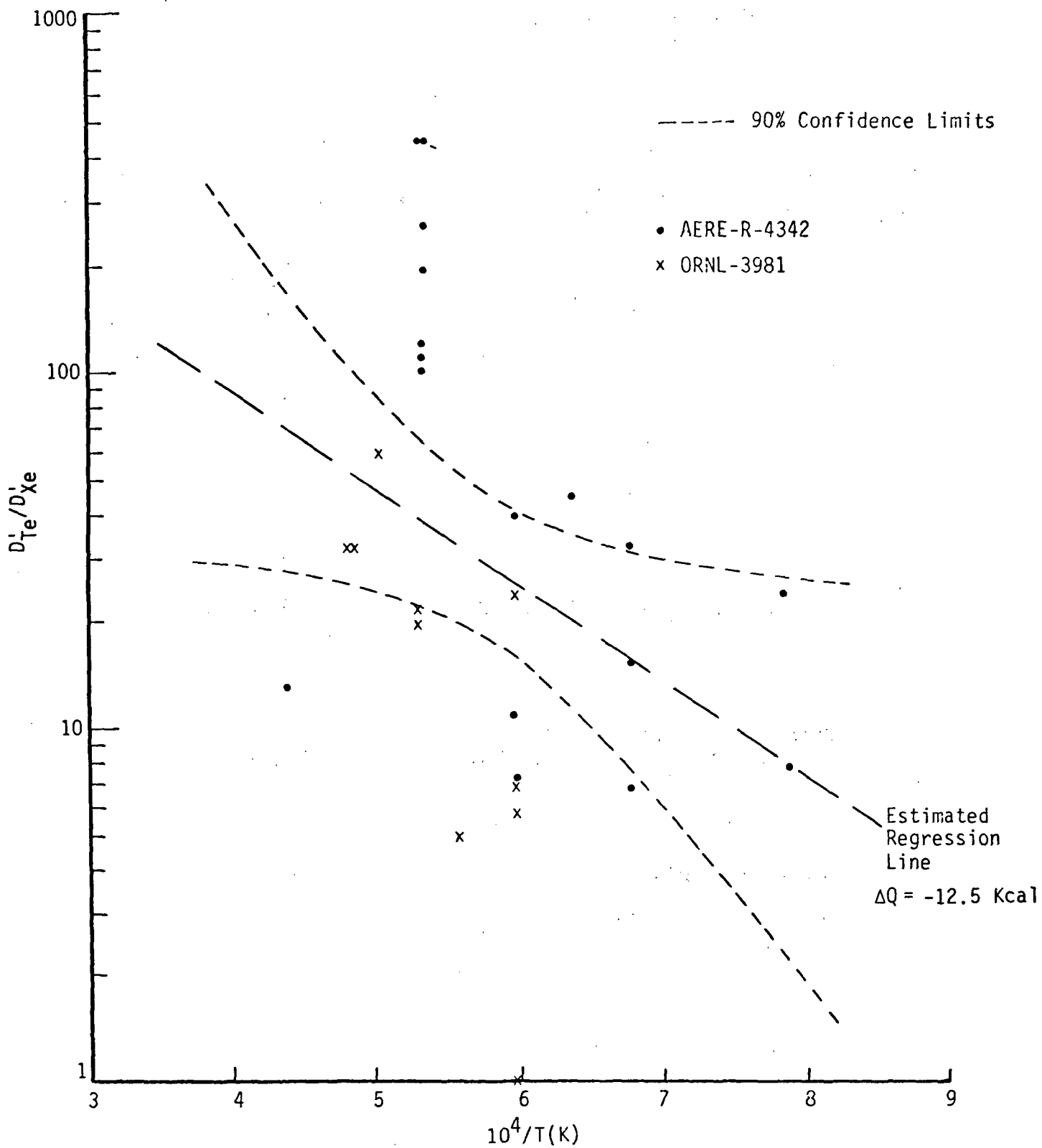


Figure 3. Diffusion Parameter Ratio Data and Regression Analysis Results for Tellurium/Xenon

Table 7. 90% Confidence Limit Values for the Constants in the D' Ratio Expressions

Fission Product FP	$D'_{FP} / D'_{Xe} \text{ (sec}^{-1}\text{)}$		$Q_{Xe} - Q_{FP} \text{ (cal/g-atom)}$	
	Lower Limit	Upper Limit	Lower Limit	Upper Limit
I	8.06×10^{-2}	4.10×10^0	2900	15000
Cs	5.38×10^{-3}	1.07×10^0	2800	21400
Te	4.04×10^1	2.98×10^4	-23600	-1300

Table 8. Fission Product D' Ratio Results Assuming Temperature Independence for the Ratios

Diffusion Parameter Ratio	Geometric Mean Value	Geometric Std. Dev.
D'iodine/D'noble	7.2	2.8
D'cesium/D'noble	2.3	4.3
D'tellurium/D'noble	28.5	4.4

4. DISCUSSION OF RESULTS AND RECOMMENDATIONS

The results of the above analyses are based on limited sets of data and on a particular interpretation of those data. The use of diffusion theory almost certainly represents an oversimplification of a complex migration and release process for these species, but it is thought to be the best approach for the current level of available information. Inspection of Figures 1, 2, and 3 and Table 7 reveals the considerable uncertainties that exist in the derived D' ratio expressions given by Equations (3), (4), and (5). Therefore, these equations should be applied with caution, recognizing the limited precision with which the ANS 5.4 model can be extended to predict releases of iodine, cesium, and tellurium from UO_2 fuel.

Some effort was made in this study to correlate the out-of-pile data with results of a series of relatively recent in-pile experiments reported by Friskney, et al (3,4,5). The data in Ref. (3), while subject to rather large uncertainties, suggest cesium/xenon diffusivity ratios that are both lower and of opposite temperature dependence than shown by the results in Figure 2. Unfortunately, these data were obtained from tiny particles of high-porosity UO_2 which are not prototypical of LWR fuel. The data in Ref. (4) and (5) provide somewhat conflicting results for iodine/xenon diffusivity ratios; at sufficiently high temperatures, data from Ref. (4) indicate ratios which fall among or below the lower values in Figure 1 while data from Ref. (5) indicate ratios which are more consistent with the out-of-pile data in Figure 1. In general, the number of in-pile determinations in either reference are too few to constitute a strong test of the statistical fit shown in the figure. It is well to point out, however, that the in-pile results tend to reinforce the statement made above that the equations derived from the out-of-pile data should be applied with caution.

Because of the large uncertainties, it is attractive to

adopt a much simpler approach for estimating D' ratio values; namely, to ignore the suggested differences in activation energies between species and to treat the D' ratios as a set of temperature independent data. This would be equivalent to assuming that the activation energies for iodine, cesium, and tellurium diffusion are all equivalent to that for xenon diffusion. The results of re-analyzing the three sets of data, using this assumption, are given in Table 8. On the basis of these results the proper D' ratio values (rounded to one significant figure) for use in ANS-5.4 high temperature model would be:

$$\begin{aligned} D'_{\text{iodine}}/D'_{\text{noble}} &= 7 \\ D'_{\text{cesium}}/D'_{\text{noble}} &= 2 \\ D'_{\text{tellurium}}/D'_{\text{noble}} &= 3 \times 10^1 \end{aligned}$$

However, it should be noted (see Table 8) that these values are uncertain by factors of roughly 3 or 4 at the one standard deviation level. Thus the simple approach also yields a rather crude approximation of the diffusion parameters for the non-noble gas species.

In conclusion, it is probably worth emphasizing again that the simple ratios listed above, which were obtained from out-of-pile experiments, may not be applicable under in-pile conditions. In the case of iodine, for example, several studies ^(4,6,7) indicate that the value of the iodine/xenon ratio would be less than one during in-pile irradiation. The in-pile experiments involving cesium release ⁽³⁾ indicate similar behavior for the cesium/xenon diffusivity ratio. These findings, while not conclusive, suggest that the above ratios may be conservatively high. Therefore, as additional data become available, the approach and assumptions adopted for the present analysis should be re-evaluated for compatibility with the new information.

REFERENCES

1. D. Davies, G. Long, and W.P. Stanaway, "The Emission of Volatile Fission Products from Uranium Dioxide". British Report AERE-R-4342, June, 1963.
2. G.W. Parker, C.E. Creek, C.J. Barton, W.J. Martin, and R.A. Lorenz, "Out-of-Pile Studies of Fission-Product Release from Overheated Reactor Fuels at ORNL, 1955 - 1965", ORNL-3981, July 1967.
3. C.A. Friskney, and K.A. Simpson, "The Release of Cesium and Xenon from the Uranium Dioxide Kernels of Irradiated HTR Fuel Particles", J. Nucl. Mater., 57, 341-47, (1975).
4. C.A. Friskney, J.A. Turnbull, F.A. Johnson, A.J. Walter, and J.R. Findlay, "The Characteristics of Fission Gas Release From Monocrystalline Uranium Dioxide During Irradiation", J. Nucl. Mater., 68, 186-92, (1977).
5. C.A. Friskney, and J.A. Turnbull, "The Characteristics of Fission Gas Release from Uranium Dioxide During Irradiation," British Report RD/B/N 4217, January, 1978.
6. J.A. Turnbull, C.A. Friskney, F.A. Johnson, A.J. Walter, and J.R. Findlay, "The Release of Radioactive Gases From Uranium Dioxide During Irradiation," J. Nucl. Mater., 67, 301-6 (1977).
7. J.F. Findlay, F.A. Johnson, J.A. Turnbull, and C.A. Friskney, "Fission Product Release From UO₂ During Irradiation: Diffusion Data and Their Application to Reactor Fuel Pins," personal communication from M.J. Notley, March 25, 1980.

F. EFFECT OF PRECURSORS ON RELEASE OF FISSION PRODUCT GASES

(M.J.F. Notley)

F.1 Release by Diffusion

In the foregoing sections, it is assumed that the production of fission product gases is proportional to the local fission rate in the fuel. However, the gases are daughters of precursors which may themselves move in the fuel before decaying. The fractional release of a particular isotope will be increased if the precursor is able to diffuse before decaying. Thus, decay products having precursors with relatively high diffusivities and half-lives which are a significant fraction of the irradiation time will experience the greatest increase in fractional release.

Friskney and Speight (1) have developed the mathematics for the release of an isotope with radioactive precursors, under constant irradiation conditions. The case of a variable irradiation history is more complex and the mathematics have not yet been developed. However for most practical situations it is usually sufficient to consider only the last period of irradiation, averaging over three half-lives for the isotope under consideration.

Friskney and Speight conclude that for chains with short-lived precursors (of the order of a few minutes) little error should be introduced by ignoring precursor movement. For Xe-135 (with a 6.7 h half-life iodine precursor) release is considerably augmented by precursor diffusion. Even if the precursor and the daughter product have the same diffusion coefficient, releases will be higher than calculated considering the daughter alone.

These deductions are confirmed by experiment. Turnbull et al. (2) show that the release of Xe-135 exceeds that of Kr-85 after several weeks irradiation, even though the half-life of the Kr-85 is greater than that of the Xe-135. This is due to diffusion of the I-135 precursor. In practice, release may be significantly underestimated if the ratio of the decay constant of the precursor to that of the released daughter is less than about 10, particularly if the irradiation period is of the order of the half-life of the longer-lived isotope.

Figure 1 taken from reference 1 indicates the magnitude of the effect of precursor diffusion (in this case I-133 with a half life of 20.9 hours). Section E of this report indicates that D_I/D_{Xe} is approximately 3 at high temperatures, therefore the effect could be significant for both Xe-133 and Xe-135. For example, if the fractional release of Xe-133 were calculated to be

0.07 (by the formalism suggested earlier in this report), then Figure 1 suggests that the release allowing for iodine diffusion would be about 1.5 x higher at this particular temperature (compare curve 1 with curve 7). At higher temperatures the factor decreases (compare curve 6 with curve 8). A more detailed model than that proposed in this standard should attempt to allow for precursor diffusion, since the standard is non-conservative in so far as it ignores the effect. However, integrated over a typical fuel element, the error due to this source is unlikely to be more than about a factor of 1.1.

F.2 Release by Knock Out and Recoil

At low temperatures, precursors as well as daughter products are immobile. Therefore low temperature knock out or recoil releases are not affected by precursor movement.

F.3 Consequences of the Release of a Precursor

If a precursor is released to the gap it will decay and add to the inventory of the daughter, thus apparently increasing the fractional release of the daughter. Assume that the fractional release of the precursor is F_p , then only $(1-F_p)$ of the precursor remains within the fuel to decay to the daughter and to be released subsequently by diffusion or knockout. The released precursor atoms all decay into daughter products, whose effective fractional release by this route will therefore be equal to F_p . The fractional release of the daughters of the atoms remaining in the fuel is F_d , calculated as in this standard, assuming the cumulative yield of the daughter. Thus the effective total fractional release of the daughter

$$F_d' = F_d (1 - F_p) + F_p \dots \dots \dots (1)$$

This equation applies to both high and low temperature release mechanisms, but in practice for the low temperature calculations can be reduced to

$$F_d' = F_d + F_p$$

since both F_d and F_p are small ($<10^{-4}$).

When considering the high temperature releases, the release of the precursor should be calculated and the above correction made to the effective release of the daughter. However, we do not have reliable estimates for the diffusion coefficient for bromine (see Section E) so are unable to correct the calculations for krypton release. The bromine isotopes of interest have very short half lives (<1900 sec.) so their fractional release is likely to be low and have little effect.

References

- (1) Friskney, C.A., and Speight, M.V., "A Calculation on the In-Pile Diffusional Release of Fission Products Forming a General Decay Chain", J. Nucl. Mat. 62 (1976) 89-94.
- (2) Turnbull, J.A., Friskney, C.A., Johnson, F.A., Walther, A.S., and Findlay, J.R., "The Release of Radioactive Gases From Uranium Dioxide During Irradiation", C.E.G.B. Report RD/B/N3607 (1976).

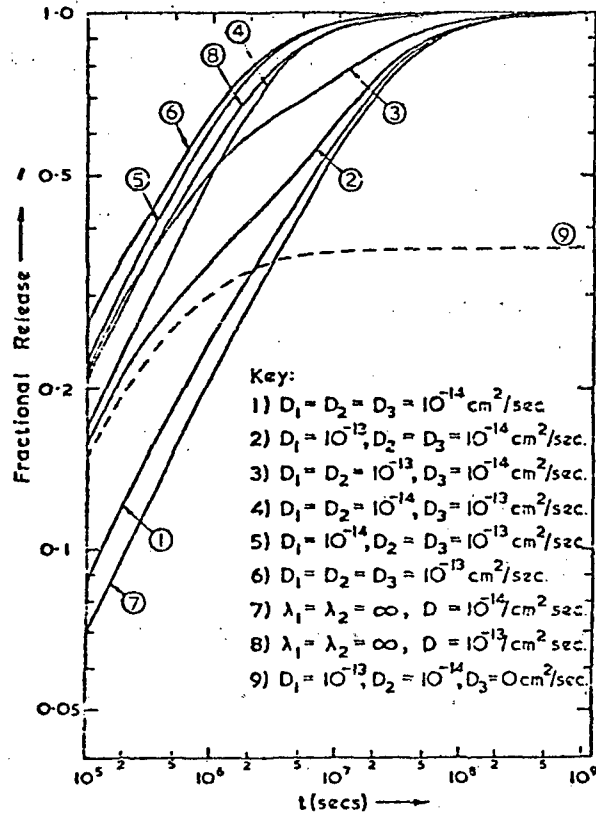
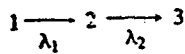


Fig. 1. Fractional release vs time for the final stable isotope (3) in the chain:



(for the case of $^{133}\text{I}, ^{133}\text{Xe}, ^{133}\text{Cs}$, $\lambda_1 = 9.255 \times 10^{-6}$, $\lambda_2 = 1.522 \times 10^{-6}/\text{sec}$).

(From reference 1; Friskney and Speight, J. Nucl. Mat. 62 (1976))

III. LOW TEMPERATURE FISSION PRODUCT RELEASE

A. Mathematics of the Knockout Model (R. A. Lorenz, ORNL)

The classical knockout model states that the rate of knockout (release) of an isotope per unit of geometrical surface area is proportional to the volumetric concentration of the isotope and the volumetric fission rate:

$$\frac{R}{S} = C_1 \left(\frac{N}{V} \right) (f) \quad (1)$$

where

R = knockout (release) rate of an isotope, atoms/sec,

S = geometrical surface area of fuel pellet, cm²,

C₁ = a proportionality constant, cm⁴/fission,

N = number of atoms of the isotope in the fuel,

V = volume of fuel, cm³, and

f = volumetric fission rate, fissions/cm³·sec.

Fuel of density less than theoretical may contain open porosity of size sufficient for knockout atoms to escape, thus requiring an addition to the geometrical surface area.

For radioactive isotopes at production-decay equilibrium,

$$\frac{R}{S} \approx C_1 \left(\frac{B}{\lambda V} \right) (f) \quad (2)$$

where

B = birth rate, atoms/sec, and

λ = decay constant, sec⁻¹

since the total number of atoms of an isotope = B/λ, atoms/cm³, and the number of atoms escaping is relatively very small.

An alternative form of Eq. (2) is:

$$\frac{R}{S} \approx C_1 \frac{f^2 Y}{\lambda} \quad (3)$$

where

Y = the isotopic yield, atoms/fission,

since $B/V = fY$.

The fractional release of radioactive isotopes is obtained directly from Eq. 2.

$$F = \frac{R}{B} \approx C_1 \frac{Sf}{V\lambda} \quad (4)$$

where

F = fraction of an isotope existing outside (released from) the fuel.

An alternative form of Eq. (4) is:

$$F \approx C_2 \frac{P}{\lambda} \quad (5)$$

where

C_2 = a proportionality constant calculated for $S/V = 6.0 \text{ cm}^{-1}$,*

in units of metric tons per space megawatt second, and

P = specific power, MW/t (megawatts per metric ton).

For stable isotopes or those with very long half-lives, the concentration increases with time. If we assume a constant production rate, neglect the small fraction released, and assume uniform concentration throughout the fuel, the concentration is given by

$$\frac{N}{V} \approx fYt \quad (6)$$

where

$\frac{N}{V}$ = the concentration of a stable isotope, atoms/cm³,

t = irradiation time, sec.

* A typical value for commercial LWR fuel pellets.

In analogy with Eq. 1, the release rate of a stable isotope at irradiation time t is given by

$$\frac{R}{S} = \frac{dN/dt}{S} \approx C_1 (fYt) (f) \quad (7)$$

where

C_1 = the same proportionality constant used in Eqs. 1, 2, 3, and 4.

The total number of atoms of the isotope released from start of irradiation to time t is given by

$$N_o = C_1 S f^2 Y \int_0^t t dt = C_1 S f^2 Y \frac{t^2}{2} \quad (8)$$

The total number of atoms of the isotope produced is

$$N_T = fYtV \quad (9)$$

The fraction released from start of irradiation to time t is therefore

$$F = \frac{N_o}{N_T} = \frac{C_1}{2} \frac{S}{V} ft \quad (10)$$

Since the quantity ft is proportional to burnup, the fraction released can be expressed as

$$F = C_3 \frac{S}{V} Bu \quad (11)$$

where

C_3 = proportionality constant, $\frac{\text{cm} \cdot \text{t}}{\text{MWd}}$, and

Bu = burnup, MWd/t.

For commercial fuel pellets where $S/V \approx 6 \text{ cm}^{-1}$,

$$F = C_4 Bu \quad (12)$$

where

$C_4 = 6C_3$, t/MWd.

B. Low Temperature Data Base (R. A. Lorenz, ORNL)

The data sources for fission gas release at low temperature are divided into two groups: (1) stable gas and long-lived isotopes, e.g. ^{85}Kr , and (2) short-lived active gas release. In the case of stable gas release, emphasis has been in gathering data at high burnup. Irradiation temperatures were not always available. The accuracy and consistency of published temperatures were not evaluated.

1. Stable Fission Gas Release

Five groups of fuel rods were found which provided useful stable fission gas release results, (Refs. 1-8 and Appendix F); data from these rods are summarized in Table 1. It was not possible to determine which of these rods (if any) experienced gas release as a result of only low temperature release mechanisms. Where the irradiation conditions varied within a given group (DIDO, Yankee-Rowe, and VBWR-Dresden), it was clear that a direct correlation existed between either calculated centerline temperature or linear heat rating and the amount of gas released, especially when other rods (not included in Table 1 because of high fission gas release) were considered.

In order to help determine selection criteria for the purpose of discerning which fuel rod gas release data were relatively unaffected by high-temperature release mechanisms, the data of Bellamy and Rich (DIDO) were plotted as shown in Fig. 1. This set was chosen since data from a large number of fuel pins were available with fairly complete temperature information. Centerline temperature was plotted as a function of burnup since Bellamy and Rich had observed that fission gas release increased with

Table 1. Fuel samples exhibiting low release of stable fission gas and ^{85}Kr at high burnup^a

Facility	Fuel rod No.	Peak heat rating ^b (w/cm)	Peak centerline temperature (°C)	Burnup (MWd/MT)		Fission gas release (%)	
				Avg.	Peak	Xe	^{85}Kr
DIDO ^c	5029		943	14,250	14,960 ^c	0.09	
	5032		927	15,680	16,460	0.10	
	5034		-	13,210	13,870	0.12	
	5030		1072	14,060	14,760	0.12	
	5037		943	18,340	19,260	0.15	
	5031		1033	15,490	16,260	0.16	
	5038		1061	19,290	20,250	0.195	
	5025		-	17,860	18,750	0.22	
	5023		1068	21,000	22,050	0.22	
	5024		-	23,250	24,410	0.25	
	5033		1357	13,780	14,470	0.895	
	5028		-	10,925	11,470	0.92	
	5020		1279	8,075	8,480	1.145	
	5019		~1465	19,000	19,950	1.48	
	5026		~1250	19,570	20,550	2.36	
	5022		~1160	35,340	37,100	2.53	
	5039		~1150	40,000	42,000	3.16	
H. B. Robinson ^d	H-1	327-292-244	850	28,000	30,500	0.14	
	K-7	327-292-244	850	28,000	30,500	0.16	
	K-9	327-292-244	850	28,000	30,500	0.19	
	K-4	327-292-244	850	28,000	30,500	0.19	
	M-4	327-292-244	850	28,000	30,500	0.19	
	L-4	327-292-244	850	28,000	30,500	0.29	
H. B. Robinson ^e	D-12	327-292-244	850	28,000	30,500	0.22	0.33
	H-15	327-292-244	850	28,000	30,500	0.25	0.42
BETT ^f	79-163	313-305-306	1350		16,400 ^g	0.18	
Yankee-Rowe ^h	H3-C-f1	98-103-85		7,440	9,870	0.050	
	H3-C-a6	120-97-103		9,320	12,020	0.058	
	K4-C-f6	45-47-39		3,560	4,350	0.067	
	E6-C-a6	157-147-113		28,700	33,870	0.071	
	F5-SW-d6	157-149-189		18,300	22,140	0.083	
	F4-C-f6	157-183-185		12,260	16,850	0.100	
	F5-C-a1	133-167-157		20,100	24,320	0.100	
	E6-C-f1	156-146-111		28,400	33,510	0.107	
	F5-NW-d4	159-177-198		19,720	23,860	0.117	
	F4-SW-d2	190-110-206		10,700	14,640	0.142	
	K5-C-a1	61-77-63		5,710	6,980	0.175	
	F4-SW-a5	217-234-235		12,240	16,740	0.192	
	F5-NW-a1	192-192-240		23,860	28,870	0.367	
	F4-NE-f1	210-320-198		15,160	20,740	1.442	
H5-NW-a1	200-239-193		14,820	19,800	1.608		

Table 1 (continued)

Facility	Fuel rod No.	Peak heat rating (w/cm)	Peak centerline temperature (°C)	Burnup (MWd/MT)		Fission gas release (%)	
				Avg.	Peak	Xe	⁸⁵ Kr
VBWR- DRESDEN ⁱ	A46	5J-R2D10	341-257	24,200	27,800	0.076	0.06
	B70	16J-R5D15	375-252	22,200	27,800	0.88	0.08
	A1	5J-R2D7	304-229-192	35,400	37,500	~0.10	~0.08
	A7	16J-R5D29	375-259-218	36,200	40,150	~0.11	0.10
	B52	4J-R2D23	291-219-184	32,800	36,100	~0.11	~0.07
	A35	5J-R2D1	348-262-220	31,700	33,900	~0.12	~0.08
	-	14J-R4D17	422	~9,000	~12,000	0.33	0.29
	A9	12J-T6D80	463-259-218	35,400	38,600	0.38	0.25
	-	12J-T6D8	510	~10,500	~15,000	0.47	0.46
	A13	11J-R2D93	446-277	28,200	32,700	0.51	0.58
	B76	12J-R2D86	463-374	24,600	32,000	0.54	0.50
	A18	14J-R4D18	422-241-203	35,100	39,300	~0.56	~0.35
	A11	13J-R4D5	429-254-214	36,600	40,300	0.66	0.43
	A37	11J-R1D73	446-277-233	37,300	41,000	~0.88	0.51
	A41	11J-R6D14	446-297	26,400	31,350	0.92	0.93
	B90	11J-R1D69	446-297-250	36,500	41,250	1.04	0.69
	-	11J-R1D71	402	~9,600	~12,500	2.43	2.00
	-	12J-R2D88	463	~4,700	~6,900	~2.62	2.63
	-	11J-T2D25	490	~10,900	~15,900	5.05	4.80

^aExcept for peak heat rating, conditions listed are for end of irradiation.

^bRatings listed are for three successive thirds of burnup. For SA-1 rods, ratings are for burnup increments ~0 to 10,000; ~10,000 to 22,000; and ~22,000 to 34,000 MWd/MT.

^cPeak burnup assumed to be 1.05 times average. Ref. 1.

^dRef. 3.

^eRef. 2. Used stable Xe production of 28.2 cm³ (STP)/MWd/t. Used ⁸⁵Kr content at end of irradiation of 0.191 cm³ (STP)/MWd.

^fRef. 4 and Appendix F

^gBurnup at fuel rod centerline. Burnup at surface 32,000 MWd/t.

^hRef. 5.

ⁱRefs. 6 to 8. First rod number is Dresden SA-1 designation; second is VBWR.

68

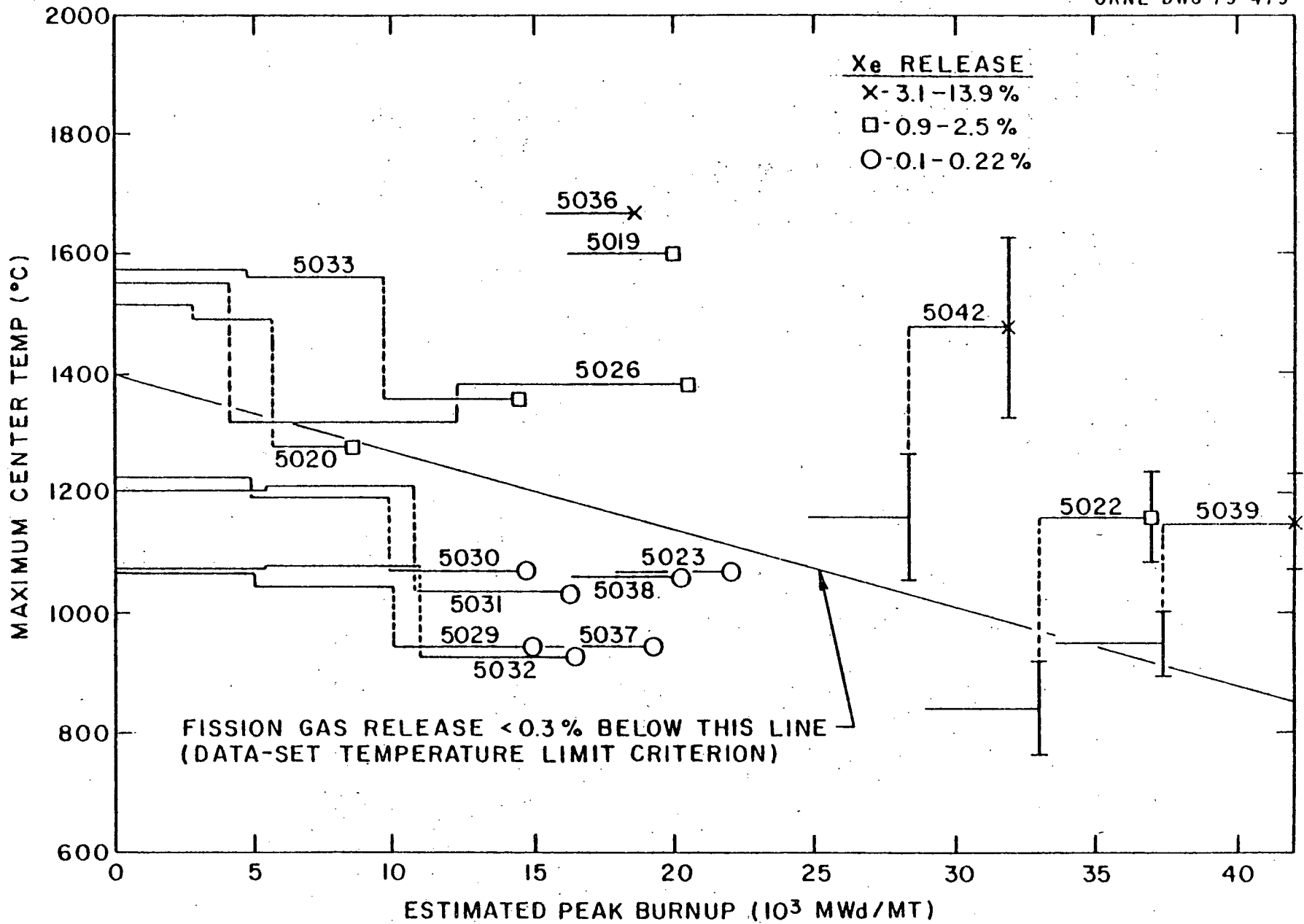


Fig. 1. Maximum Temperature and Xenon Release: Bellamy and Rich Data.

burnup for fuel irradiated at centerline temperatures near 1250°C.¹

Supplemental temperature data were employed. (Ref. 1 and Appendix F).

The data in Fig. 1 are shown separated by a sloping straight line which divides fuel pins releasing <0.3% of the fission gas from those releasing >0.8%. Those fuel pins in the low gas-release group had centerline temperatures which remained below the line for their entire irradiation. These data suggest that an upper temperature limit similar to that shown in Fig. 1 may be sufficient to determine which irradiations should be relatively unaffected by high temperature fission gas release.

Centerline temperatures for the H. B. Robinson fuel rods⁹ were plotted in the same manner in Fig. 2 along with the suggested upper temperature limit. It is clear that the H. B. Robinson fuel rod centerline temperature lay below this temperature limit for almost the entire irradiation period. The calculated temperatures shown in Fig. 2 are biased high toward end-of-life because the inclusion of an unrealistically high fission-gas-release model resulted in low calculated gap thermal conductivity.

The temperature data for fuel pin BETT 79-163 (Ref. 4, Appendix F) are plotted in a similar manner in Fig. 3. A number of the centerline temperature peaks penetrated the upper limit. Interpretation of data from this fuel pin is complicated by high-enrichment uranium causing a significant flux depression within the pin. Burnup at the fuel pellet surface was almost twice that at the centerline.

Centerline temperature data for the Yankee-Rowe and VBWR-Dresden fuel rods were not available. For both sets of data there is a trend toward lower fission gas release with lower linear heat rating (lower centerline temperature). These data are useful in that they do confirm the occurrence of low fission

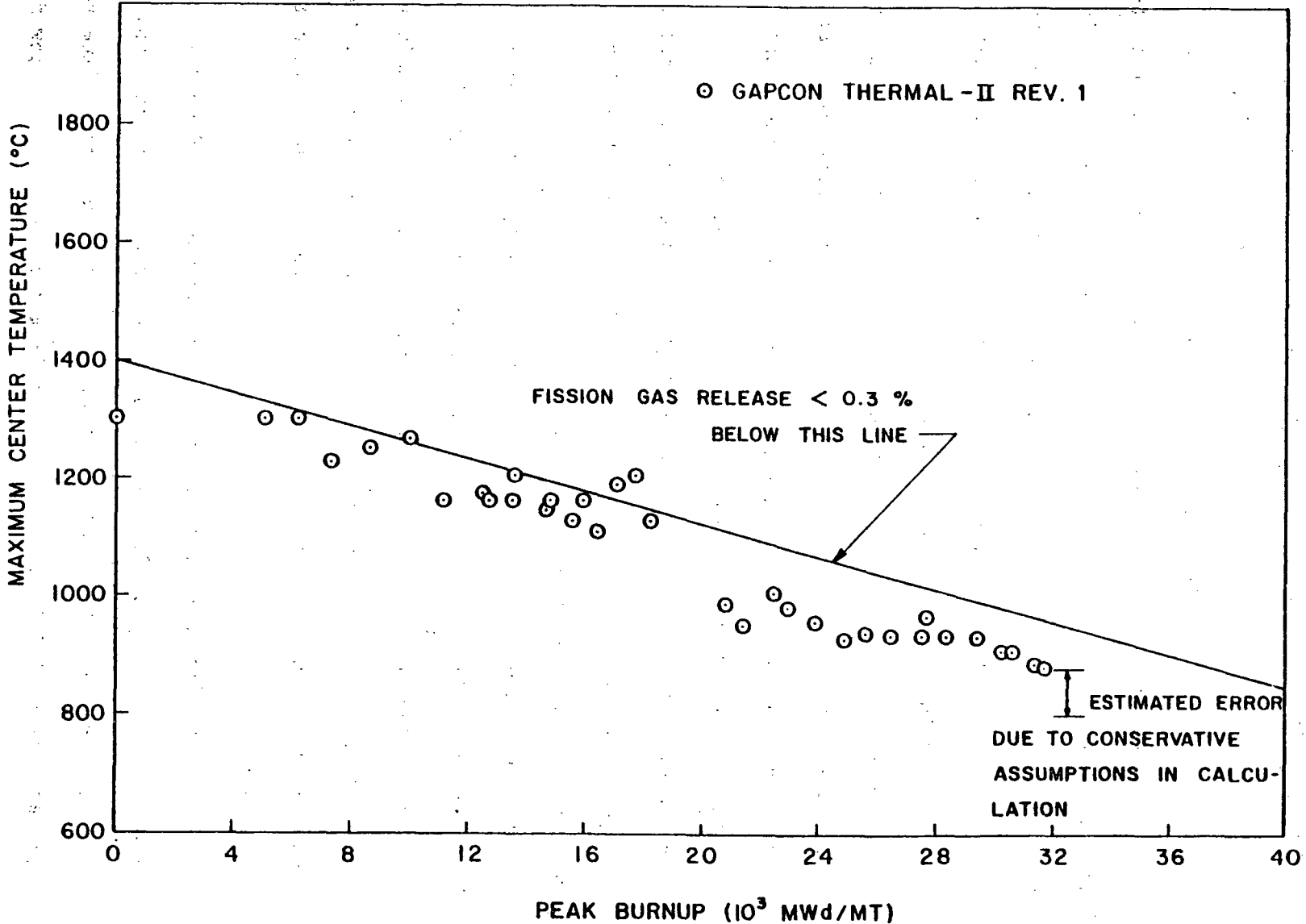


Fig. 2. H. B. Robinson Bundle B05 temperatures vs. burnup at peak axial location.

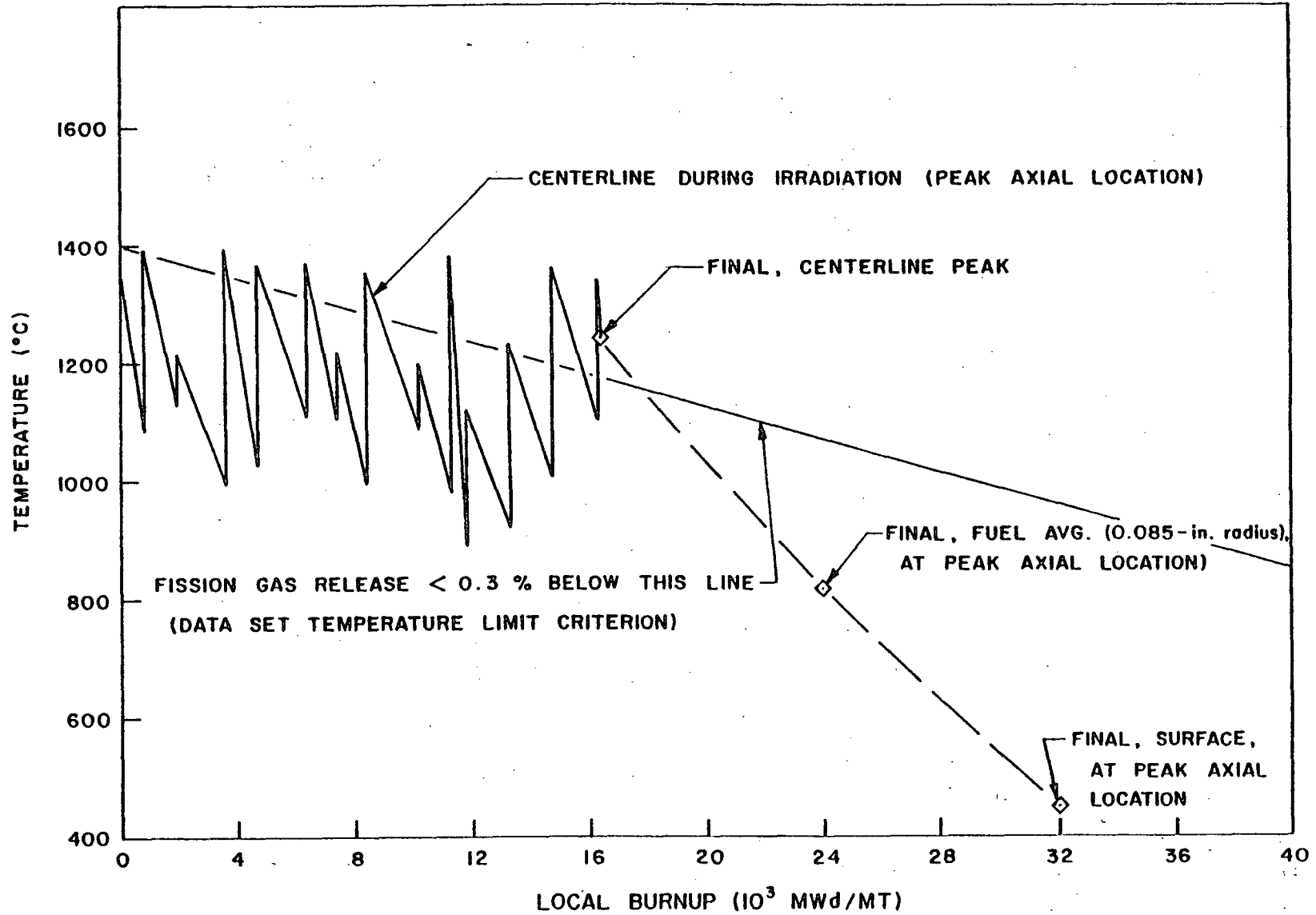


Fig. 3. Local temperature vs. local burnup for fuel rod BETT 79-163 at peak axial location.

gas release (several tenths of a percent or less) at peak burnups of the order of 30,000 to 40,000 MWd/t for rods irradiated at sufficiently low heat ratings.

2. Radioactive Fission Gas Release at Production-Decay Equilibrium

The release of radioactive fission gas is usually measured by sweeping helium over small samples of bare fuel. Seven references¹⁰⁻¹⁶ provided the data listed in Table 2. Most of the data were obtained at low fission rates. Commercial fuel operating at a heat rating where low temperature release might be important would have a fission rate of the order of 10^{13} fissions/cm³·sec.

The criteria for selection of data demonstrating low temperature release of radioactive fission gas are as follows. The exposure temperature was limited to a maximum of 800°C. Soulhier¹³ believed that some of the release observed at 800°C was a result of high-temperature diffusion. The fuel density range was 10.08 to 10.96 g/cm³. Lower density fuel released a much larger fraction of the fission gas presumably because of extensive open porosity.^{12,13} Burnup was not a criteria for selection, although most samples exhibited an initial gradual decrease in release rate. According to Carroll,¹⁷ "the decrease is usually not significant after 30 days of irradiation and the subsequent gas release is about 1/3 to 1/2 the starting release." Data taken under conditions of temporarily abnormal fuel geometry (high exposed surface area resulting from power cycle-induced cracking¹⁵ or the opening of tunnels¹⁶) were not included. Subsequent irradiation tends to heal the cracks¹⁷ even in unconstrained fuel, and the tunnels close,¹⁸ especially in constrained fuel.

Table 2. Release of radioactive fission gas at low temperature

Researcher	Fuel characteristics			Surface-to-volume ratio ^a (cm ² /cm ³)	Temperature (°C)	Irradiation time (d)	Isotope	Fractional release (atoms/sec rel.) (atoms/sec born)	Release rate ^b (atoms/cm ² ·sec)	Fission rate ^c (fissions/cm ³ ·sec)	Concentration x fission rate	
	Test	Type	Density (g/cm ³)								(atoms/cm ³) ^d	(fissions/cm ³ ·sec)
Melehan '63	A	Sintered pellet	10.08 (initial)	9.45	320		¹³³ Xe	5.0×10^{-3}	3.86×10^6	1.10×10^{11}	5.29×10^{26}	
	C	Sintered pellet	10.85	9.45	430	30-60	¹³³ Xe	$\sim 9.6 \times 10^{-5}$	6.94×10^4	1.10×10^{11}	5.29×10^{26}	
Jackson '64	2	Sintered pellet	10.49	13.3	800		⁸⁸ Kr	2.6×10^{-5}	2.36×10^4	3.50×10^{11}	6.15×10^{25}	
					800		¹³³ Xe	1.14×10^{-4}	1.84×10^5	3.50×10^{11}	4.46×10^{27}	
Carroll '65	CI-9	Single-crystal discs	10.69	22.9	600	0	⁸⁸ Kr	6.1×10^{-5}	1.01×10^5	1.10×10^{12}	6.09×10^{26}	
					600	30	⁸⁸ Kr	4.2×10^{-5}	7.32×10^4	1.10×10^{12}	6.09×10^{26}	
					600	90	¹³³ Xe	1.3×10^{-4}	3.77×10^5	1.10×10^{12}	7.29×10^{28}	
							⁸⁸ Kr	2.3×10^{-5}	3.83×10^4	1.10×10^{12}	6.09×10^{26}	
							¹³³ Xe	6.2×10^{-5}	1.80×10^5	1.10×10^{12}	7.29×10^{28}	
							⁸⁸ Kr	7.5×10^{-6}	1.25×10^4	1.10×10^{12}	6.09×10^{26}	
600	180	⁸⁸ Kr	6.8×10^{-6}	3.28×10^4	3.2×10^{12}	5.15×10^{27}						
Soulhier '66		Sintered pellet	10.26	7.07	230	0-5	⁸⁸ Kr ^e	5.0×10^{-5}	6.12×10^4	2.5×10^{11}	3.14×10^{25}	
							¹³³ Xe ^f	2.6×10^{-4}	6.09×10^5	2.5×10^{11}	1.37×10^{27}	
							⁸⁸ Kr ^e	1.8×10^{-5}	2.20×10^4	2.5×10^{11}	3.14×10^{25}	
							¹³³ Xe ^f	6.0×10^{-5}	1.41×10^5	2.5×10^{11}	1.37×10^{27}	
							⁸⁸ Kr ^e	1.2×10^{-5}	1.47×10^4	2.5×10^{11}	3.14×10^{25}	
		Sintered pellet	10.41	7.07	230	0-5	¹³³ Xe ^f	3.5×10^{-5}	8.21×10^4	2.5×10^{11}	1.37×10^{27}	
Carroll '66	CI-12	Fine-grain discs	10.96	22.5	<600		⁸⁸ Kr	5.5×10^{-6}	6.14×10^4	1.85×10^{12}	1.72×10^{27}	
					<600		⁸⁸ Kr	5.4×10^{-6}	1.93×10^5	6.00×10^{12}	1.81×10^{28}	
Carroll '69	CI-20 ^B	Sintered hollow cylinder, fine grain	10.78	16.2	~600		⁸⁸ Kr	1.23×10^{-5}	1.84×10^4	7.0×10^{11}	2.46×10^{26}	
					~600		⁸⁸ Kr	3.0×10^{-5}	1.08×10^5	1.7×10^{12}	1.45×10^{27}	
Carroll '69	CI-21	Fused-crystal enr. spheres	10.96	60.2	~600		⁸⁸ Kr	6.6×10^{-5}	4.93×10^5	1.3×10^{13}	8.50×10^{28}	
					~600		⁸⁸ Kr	6.6×10^{-5}	3.45×10^6	9.1×10^{13}	4.17×10^{30}	
Turnbull '78		Fine, coarse-grain spheres		49.9	~725	0-42	⁸⁸ Kr	7.5×10^{-5}	2.34×10^5	4.5×10^{12}	1.02×10^{28}	

^aThe S/V ratio of commercial pellets lies in the range 4 to 10 cm²/cm³.

^bRelease rate based on geometrical surface area.

^cAssumes natural uranium enrichment and fission rate (f/cm²·sec) = 0.10 x thermal neutron flux (n/cm²·sec) except for Carroll '69 test CI-21 and Turnbull '78.

^dConcentration of ⁸⁸Kr = 503 x fission rate and concentration of ¹³³Xe = 43,800 x fission rate except for Souhier '66.

^eRelease rate of ⁸⁸Kr obtained by extrapolation.

^f¹³³Xe concentration assumed to be one-half of production-decay equilibrium.

^BData for test CI-19 with a single-crystal hollow cylinder, S/V = 12.7: fractional release and release rate were 78% of values shown for fine-grain hollow cylinder at same fission rate.

C. Model Fitting-Low Temperature Release (R. A. Lorenz, ORNL)

The data base for low temperature release of stable fission gas consists of seven fuel pins from the DIDO irradiation (Table 1 and Fig. 1), eight fuel rods from H. B. Robinson-2 bundle B05 (Table 1 and Fig. 2), and rod 79-163 from the BETT irradiation (Table 1 and Fig. 3). These fuel pins all meet the temperature limit criterion shown in Figs. 1, 2, and 3; the release data for these pins are plotted in Fig. 4 as a function of burnup. The measured fractional releases for the DIDO pins listed in Table 1 were reduced to give expected fractional release for $S/V = 6^{-1}$ cm since the actual S/V values ranged from 10.7 to 12.1 cm^{-1} . The S/V values for the H. B. Robinson fuel and BETT fuel were within 10% of 6.0 cm^{-1} , so the measured fractional releases were not adjusted.

In accordance with the form of Eq. 12, the line $F = 7 \times 10^{-8}$ Bu fits the data reasonably well. From this the following values for the proportionality constants can be calculated:

$$\begin{aligned}C_4 &= 7 \times 10^{-8} \text{ t/MWd,} \\C_3 &= 1.17 \times 10^{-8} \text{ cm}\cdot\text{t/MWd} \\C_2 &= 1.62 \times 10^{-12} \text{ t/MW}\cdot\text{sec, and} \\C_1 &= 8.96 \times 10^{-25} \text{ cm}^4/\text{fission.}\end{aligned}$$

When the data for radioactive isotope release are plotted in the manner of Eqs. 2 and 3, as shown in Fig. 5, it can be seen that although the knockout model does not provide a satisfactory correlation, the data tend to lie in a narrow band with slope ≈ 0.5 .

When the release of stable isotopes is examined in the same manner (Eq. 7), Fig. 6, good agreement is obtained with the knockout model equations both in magnitude and slope. Furthermore, the release of stable isotopes merges with the high end of the radioactive release data.

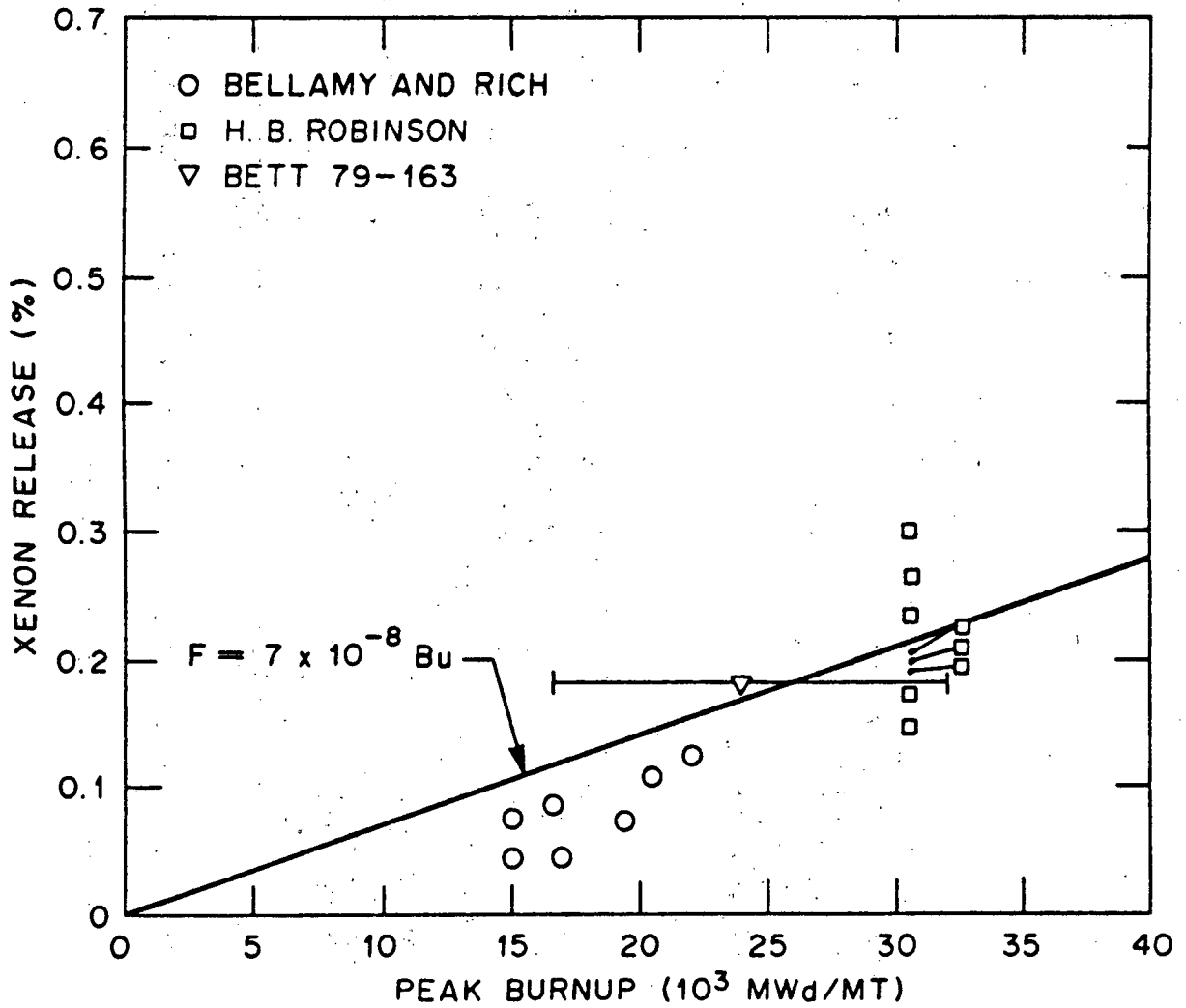
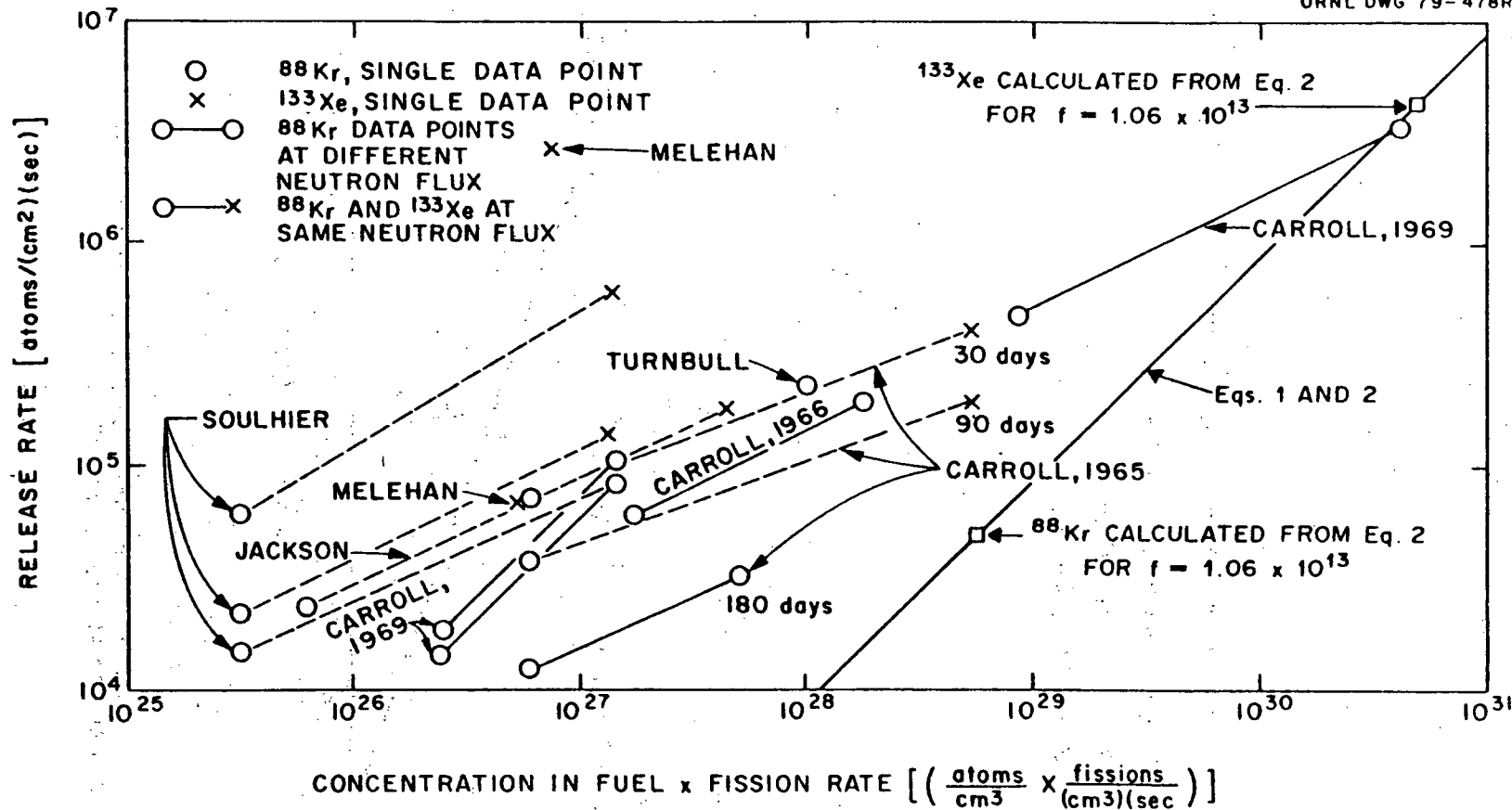


Fig. 4. Xenon release from fuel pins meeting data-set temperature criterion.



RELEASE OF RADIOACTIVE FISSION GAS

Fig. 5. Release of short half-life radioactive fission gas.

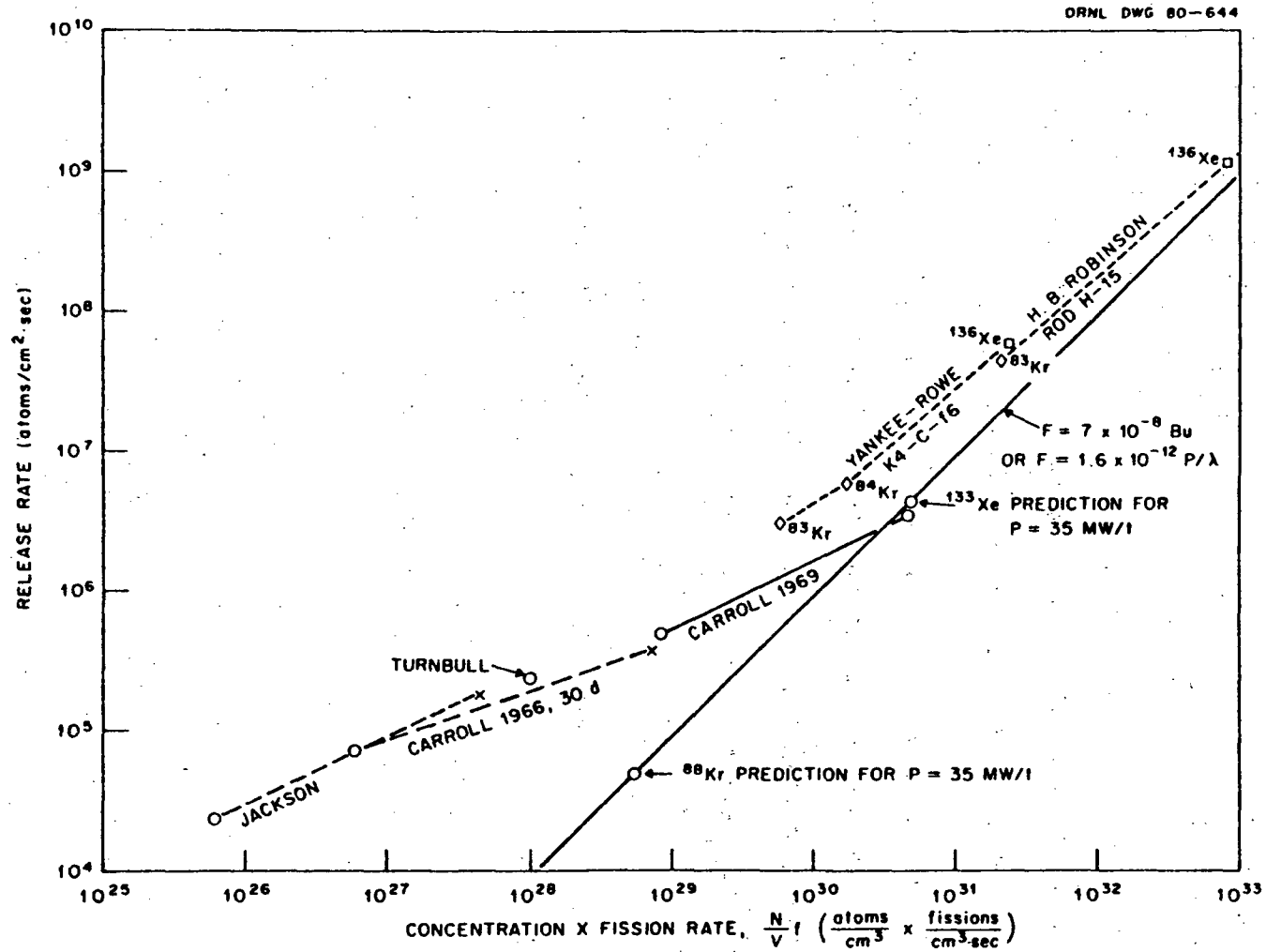


Fig. 6. Release of stable isotopes compared with radioactive isotopes.

The knockout model underpredicts the release rate for values of $(nf/V) < 10^{30}$, a condition that will apply to isotopes with half lives < 1 day in power reactors where low temperature release might be important.

An empirical addition to the knockout equation was formulated and is expressed in the following form.

$$F = 10^{-7} (\lambda)^{-0.5} \quad (13)$$

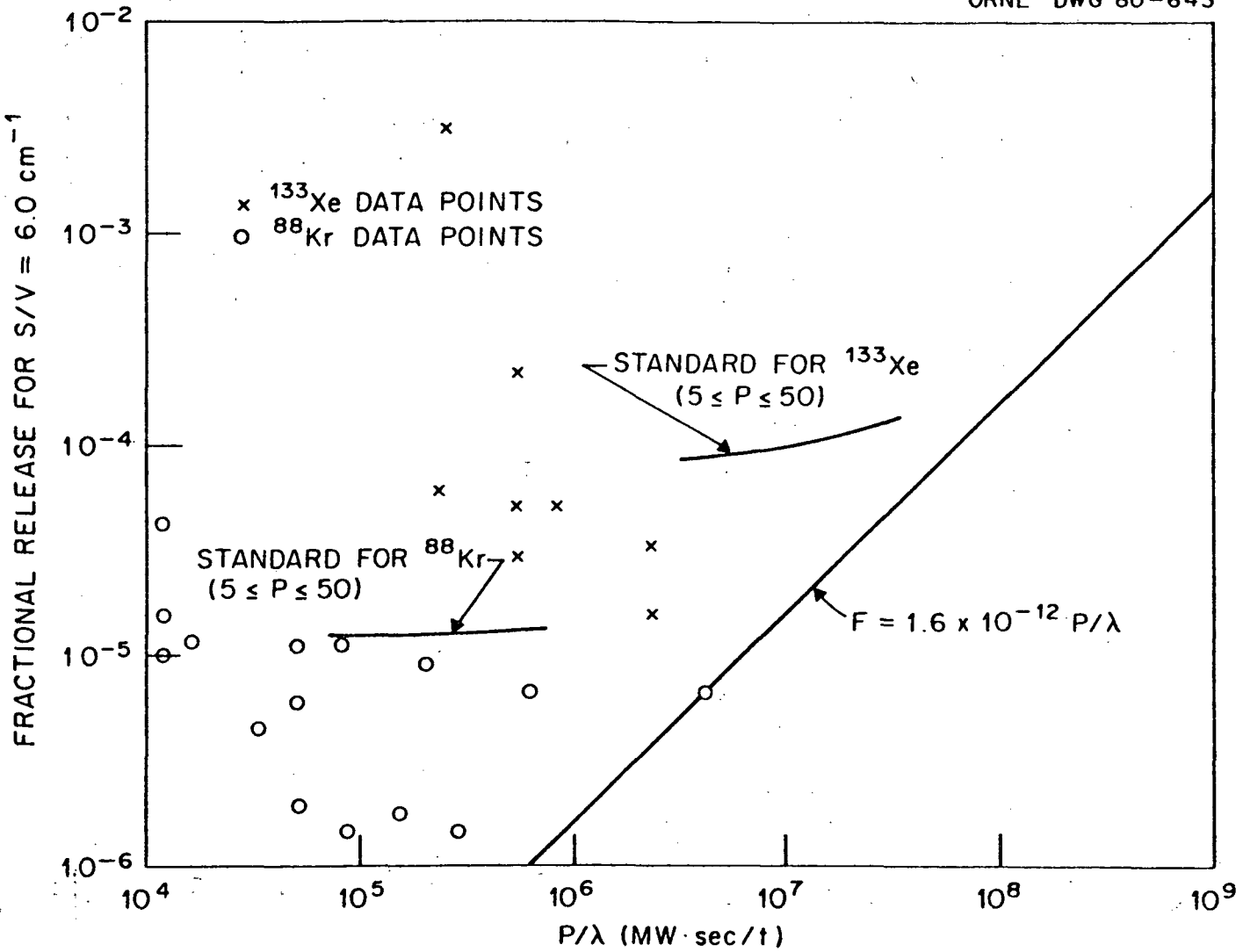
where

F = fractional release of radioactive isotopes at production-decay equilibrium for fuel with $S/V = 6.0 \text{ cm}^{-1}$.

The magnitude of this correction is shown in Fig. 7 along with the knockout model in the form of Eq. (5). The best-estimate low-temperature release of radioactive isotopes reaching production-decay equilibrium from fuel with $S/V = 6.0 \text{ cm}^{-1}$ is therefore the sum of Eqs. 13 and 5:

$$F = 10^{-7} (\lambda)^{-0.5} + 1.6 \times 10^{-12} \frac{P}{\lambda} \quad (14)$$

For the equations given in this section, P should be evaluated at 200 Mev/fission.



FRACTIONAL RELEASE OF RADIOACTIVE ISOTOPES FOR $S/V = 6.0 \text{ cm}^{-1}$

Fig. 7. Comparison of empirical model for radioactive isotopes (Eq. 14) with data base.

100

References

1. R. G. Bellamy and J. B. Rich, "Grain-Boundary Gas Release and Swelling in High Burn-Up Uranium Dioxide," *J. Nucl. Mater.* 33, 64-76 (1969).
2. R. A. Lorenz, J. L. Collins, A. P. Malinauskas, O. L. Kirkland, and R. L. Towns, Fission Product Release from Highly Irradiated LWR Fuel, NUREG/CR-0722 (ORNL/NUREG/TM-287/R2) (February 1980).
3. S. J. Dagbjartsson, B. E. Murdock, D. E. Owen, and P. E. MacDonald, Axial Gas Flow in Irradiated PWR Fuel Rods, TREE-NUREG-1158, pp. 64-67 (September 1977).
4. J. T. Engel and H. B. Meieran, Performance of Fuel Rods Having 97 Percent Theoretical Density UO₂ Pellets Sheathed in Zircaloy-4 and Irradiated at Low Thermal Ratings, WAPD-TM-631 (July 1968).
5. W. A. Bezella, Analyses of the Fission Gases Released Within Spent Yankee Fuel Rods, WCAP-6087 (February 1968).
6. F. H. Megerth, C. P. Ruiz, and U. E. Wolff, Zircaloy-Clad UO₂ Fuel Rod Evaluation Program Final Report, November 1967-June 1971, GEAP-10371 (June 1971).
7. C. J. Baroch, J. P. Hoffmann, H. E. Williamson, and T. J. Pashes, Comparative Performance of Zircaloy and Stainless Steel Clad Fuel Rods Operated to 10,000 MWD/T in the VBWR, GEAP-4849, p. 4-37 (April 1966).
8. F. A. Megerth, Zircaloy-Clad UO₂ Fuel Rod Evaluation Program, Quarterly Progress Report No. 3, May-July 1968, GEAP-5667, p. 19 (1968).
9. Frank Panisko, Battelle Pacific Northwest Laboratories, personal communication (March 1978).
10. J. B. Melehan, R. H. Barnes, J. E. Gates, and F. A. Rough, Release of Fission Gases from UO₂ During and After Irradiation, BMI-1623 (March 1963).
11. G. Jackson, D. Davies, and P. Biddle, Fission Gas Emission from UO₂ During Irradiation at 800-1000°C, AERE R-4714 (1964).

12. R. M. Carroll and O. Sisman, "In-Pile Fission Gas Release from Single-Crystal UO_2 ," Nucl. Sci. Eng. 21, 147-158 (1965).
13. R. Soulhier, "Fission-Gas Release from UO_2 During Irradiation up to 2000°C ," Nucl Appl. 2, 138-141 (April 1966).
14. R. M. Carroll and O. Sisman, "Fission-Gas Release During Fissioning in UO_2 ," Nucl. Appl. 2, 142-150 (April 1966).
15. R. M. Carroll, J. G. Morgan, R. B. Perez, and O. Sisman, "Fission Density, Burnup, and Temperature Effects on Fission-Gas Release from UO_2 ," Nucl. Sci. Eng. 38, 143-155 (1969).
16. J. A. Turnbull and C. A. Friskney, "The Relation Between Microstructure and the Release of Unstable Fission Products During High Temperature Irradiation of Uranium Dioxide," J. Nucl. Mater. 71, 238-248 (1978).
17. R. M. Carroll and O. Sisman, Evaluating Fuel Behavior During Irradiation by Fission-Gas Release, ORNL-4601 (September 1970).
18. C. J. Greatley and R. Hargreaves, "The Measured Emission of Fission-Product Gases from Operating UO_2 Fuel," J. Nucl. Mater. 79, 235-245 (1979).

APPENDIX A

SOCIETE ANONYME
RUE DU CHAMP DE MARS 20
B-1050 BRUXELLES (Belgique)

RECEIVED
JAN 5 1975
NUS CORPORATION
SOUTHEAST REGION
OPERATIONS

V. REF:

N. REF: 032.00/-/1/151 - NH/BR.

DATE: Le 29 décembre 1975.

Mr. S.E. TURNER,
Chairman, ANS 5.4 Committee,
N.U.S. Corporation,
2536 Countryside Boulevard,
Clearwater, Florida 33515.

Dear Mr. Turner,

We are pleased to answer your letter dated October 15. It reached us, in fact, on beginning of December and Mr. Hoppe was in the States at that time.

The burn-ups quoted in ref. DTECH ECS-EFC-73-595 are comparable to the burn-ups we used in our calculations, i.e. an integration of the specific thermal power generated within the fuel ; they are deduced from experimental measurements using 184 MeV per fission. The usual burn-ups (energy generated by the fuel) can be deduced by multiplying the quoted figures by approximately 200/184. Assuming 0,31 fission atom per fission (including the yield of 136 Xe from 135 Xe by neutron capture), that gives 34 cm³ STP of fission gas per MWd (thermal energy generated in the fuel).

The whole report should be consistent with these definitions and figures except when otherwise quoted. It appears indeed that fractional release values from Figure 7 are not correct, e.g. 26 % for ELP9 instead of 23.2 %. The figure of 27.3 CC/MWd and the resulting fractional release quoted in some Figures (12, 14, 15) were derived neglecting the 136 Xe yield from 135 Xe by neutron capture and are not used anymore.

These experiments were performed by CEA/Saclay and we do not know if they have any additional data since the 1973 BNES conference.

We have ourselves worked on the modelling aspect and we enclose two papers and a working graph which could be interesting. We are further cross-checking with our own experiments.

./.

./.

For example, we use a model where the local fission rate can be a major parameter instead of the temperature depending on the temperature level. This is completely different from classical models based on a temperature effect. In addition, this model can take the history of the irradiation (power level for instance) into account.

It is implemented in our COMETHE code. For the columnar grain growth region during the time where evaporation condensation proceeds, we consider 100 % fission gas release. From our experience, it is impossible to obtain a good correlation of fission gas release from global parameters which could be valid for a large range of application. As an example, since we have introduced in-pile densification and fission gas bubble swelling and a kinetics model for columnar grain growth in the code, the resulting temperature evolution of the fuel is very different of what we obtained previously. Moreover, the grain growth affects also the release so that we have to calibrate again the fission gas release model. Preliminary results are very satisfactory but final conclusions will not be drawn before some months.

To illustrate the differences with usual models, we predict in some cases a lower release in the equiaxed grain growth region than in periphery of the pellet despite the fact that the temperatures are higher.

Please note that in Figure 3 of the ASME paper, the burn-up is the integration of the local specific power and it can be much higher than the mean burn-up of the pellet in case of a heterogeneous fuel. This figure results from the attached working graph.

We think therefore that it will be difficult to find a "standard" for calculating the fission gas release in operating fuel rods. That standard should not be a function of temperature, otherwise it will depend on how to calculate these temperatures. In the case of very low temperatures, Figure 3 of ASME paper and the working graph can be used for such kind of standard.

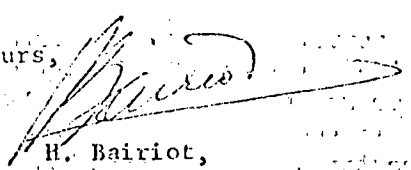
We are of course very interested by your attempt to normalize the calculation of fission gas release. As you see, it is a subject we have thoroughly considered for years and we judge we have reached a good methodology ; indeed it agrees with experimental results as well for thermal reactor fuels as for LMFBR and GCFR fuels.

We hope to hear further from your work.

Sincerely yours,


N. Hoppe,

Chef de Service Adjoint.


H. Bairiot,

Chef de Département Principal.

Enclosures : BN 7311-02,
ASME 75-WA/HT-75,
working graph

A-2



THE REACTOR GROUP
 REACTOR FUEL ELEMENT LABORATORIES

Springfields,
 Salwick,
 Preston.
 PR4 ORR.

TELEGRAMS: "ATEN," SALWICK, PRESTON

TELEX: LAB SPRINGFIELDS 67545

PRESTON 728351

Your Ref.

Our Ref.

Ext. 521

19 November 1975

Dr R O Meyer
 US Nuclear Regulatory Commission
 WASHINGTON DC 20555
 U S A

Dear Ralph

Thank you for your letter of October 17 and the notes of your ANS committee meeting. It seems that you, too, find IFA-116 and 117 to be very interesting experiments. I was interested to see that your calculations of burn-up in IFA 116/5 and 117/1 differ from mine, one being higher and the other lower. Is this because you have a different estimate of days at power, or do they cover a different period from that considered in HPR-129?

Now to try and answer your questions.

The expression built into our computer code to calculate rate of production of stable krypton and xenon (including ^{85}Kr) is

$$R = 3.05 \times 10^{-10} \left[1 + \frac{0.242}{(1 + 7.684 \times 10^{12}/\beta)} \right] \text{cm}^3 \text{W}^{-1} \text{s}^{-1}$$

3.051×10^{-10} is the rate of production of stable Kr and Xe plus ^{85}Kr assuming a yield of 26.01% from the fission of ^{235}U .

0.242 is factor to give the additional yield of ^{135}Xe in which neutron capture can subsequently occur to give ^{136}Xe .

7.684×10^{12} is the ratio of the decay constant of ^{135}Xe to its capture cross section and β is the neutron flux.

These gases, together with the original filling gas, were assumed to be the only contributors to the pin internal pressure. Iodine was not included.

The conversion of temperature and pressure readings from the IFA 116 and 117 instrumentation into fractional gas releases was, to some extent, done the other way round. Having related temperature to rating by the arguments spelled out in Appendix C, I fed the rating history from Tables VI and VII into our computer code together with a set of assumptions as to gas release such as 4% from fuel operating below 1650°C and 100% from fuel above the temperature. This then gave me a pressure history for the pin on the basis of certain assumptions

concerning the temperature distribution in that pin. The program also prints out a fractional release. So, by comparing the observed internal pressure at any time (end of instrumentation life so far as Table IX was concerned) with that calculated and making due allowance for the filling gas pressure, I could calculate the fractional release corresponding to the observed internal pressure.

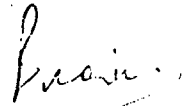
The gas storage temperatures assumed in the program are as follows: fuel/clad gap - average of can inner surface and fuel outer surface temperatures, centre (thermocouple) hole - pellet bore temperature, end dishes - the mean temperatures of the fuel annuli are extended into the dishes and the gas in each annulus assumed to be at the temperature of the underlying fuel. The plenum temperature was taken as 252°C (Table VIII).

Gas storage volumes are calculated from the thermal expansion equations for fuel and clad and the swelling parameters given in Table VIII.

An obvious source of error is the axial rating distribution which I assigned to the pins. If this is in error, gas generation is certainly in error and the release is almost certain to be wrong also. Another uncertainty could arise in having to cope with fuel stacks which were composed partly of hollow and partly of solid pellets. The program was not designed to do this and I mention the way I tried to handle the problem on p.42 of HPR-129. I think also that it is clear from the paper that I divided each pin axially into six zones for the purpose of calculating temperature burn-up, gas release, etc. The appropriate rating factors for these zones were obtained from equation 1 of Appendix C.

Finally, to answer your last question, I did not take gamma heating into account in any of the calculations I did.

Yours sincerely


J B AINSWORTH



Atomic Energy
of Canada Limited

L'Énergie Atomique
du Canada, Limitée

Chalk River
Nuclear Laboratories

Laboratoires nucléaires
de Chalk River

Chalk River, Ontario,
Canada, K0J 1J0
(613) 594-3311

Fuels and Materials Division
Fuel Materials Branch

22 January 1976

Dr. C. Beyer
Fuels Design and Development
Pacific Northwest Laboratories
Battelle Boulevard
Richland, Washington, 99352
USA

Dear Carl:

This is to confirm our recent telephone conversations regarding AECL report 1676. There is an error in the value of equivalent full power days printed in the report, it should read 16.17 days rather than 16.7 days. This brings the quoted power outputs in line (subject to round-off errors) with the quoted burnups. You point out that the xenon produced seems to have been calculated on the basis of approximately 25.5 atoms per 100 fissions rather than the (more recently) accepted value of 26.9 atoms. I cannot confirm whether this is so, but suggest you recalculate on the basis of 26.9.

Thank you very much for your assistance in getting in touch with the ANS fission gas working party. I hope to meet you in that context before too long.

Sincerely,

M.J.F. Notley

/cl

APPENDIX B

APPENDIX B

Evidence For A Strong Burnup Effect (J. V. Miller, Westinghouse)

A. Fission Gas Release Predictions for High Burnup Saxton Rods

Having formulated the equations to be used for fission product release and having established the required empirical constants using the prescribed data base, it is now necessary to determine how well the model predicts the fission gas release of fuel rods not contained in the data base. For this purpose, the Saxton reactor was identified as the most likely source of data since the information was available and covered a reasonably wide range of fuel burnup (15 - 39,000 MWD/MT).

Since the Saxton reactor was not operated at a constant power level (Figure V-1), it was first necessary to derive equations which would account for the time varying behavior of the fuel rods. Rim and Preble derived the appropriate equations (see Section III-B) and these, in turn, were used to evaluate the predicted fission gas release for a representative sample of the Saxton data.

Tables V-1 and V-2 show the results of applying the diffusion equation to the Saxton data. It can be seen from the tables that the predicted fission gas release is significantly lower than the measured values. The ratio of measured-to-predicted fission gas release ranges from 1.3 to 4 with an average value of 2.2.

It should be noted that the diffusion constants (D' and E) used in the calculations are different for the two tables. This is because the calculations were performed during the period when the values of the empirical constants were being finalized. Rather than repeat all the calculations for the cases shown on Table V-1, several check cases were run to determine the effect of changing the value of the diffusion constants (Table V-3). Although the change in predicted fission gas release associated with the different constants is small, resulting values would change the min., max. and average of the measured-to-predicted ratio quoted above. However, the conclusion remains the same: the diffusion constants derived from the uniform power, relatively low burnup data do not adequately predict the fission gas release of high burnup (i.e., > 15,000 MWD/MT) fuel rods with time varying power histories.

B. Possible Reasons for Model Discrepancy

Although it appears that there is a burnup effect which is not accounted for by the diffusion type equation, several other possible reasons for the apparent discrepancy have been suggested. First of all it is possible that the computer program used to calculate the fission gas release from the Saxton rods was biased. This could, in fact, mean that the difference between the predicted and measured fission gas release was caused by the computer model rather than explicitly due to a burnup effect.

To test this theory, two of the fuel rods used in the original data base were evaluated using the computer program. The results are shown below:

<u>Fuel Rod</u>	<u>Fission Gas Release, %</u>	
	<u>Measured</u>	<u>Predicted</u>
ELP-6	23.7	23.5
ELP-9	25.8	30.4

Based upon these results it was concluded that the computer model was not biased.

A second theory suggested that the reason for the apparent discrepancy was related to the fact that the Saxton fuel rods were mixed oxides. The discrepancy was then either due to the fact that the PuO_2 particles were operating at a much higher temperature or due to the fact that there was a basic difference between the fission gas release from oxide fuels and mixed-oxide fuels. To investigate this possibility, a calculation was performed (Section VI) in which the temperature rise in a PuO_2 particle was determined based upon representative Saxton geometry. Based upon these calculations it was determined that the maximum temperature in a PuO_2 particle was less than 11°F greater than the temperature of the UO_2 matrix and therefore could not be the cause of the apparent inconsistency in the fission gas release.

The suggestion that there may be some basic difference between oxide and mixed-oxide fission gas release was also investigated. This was accomplished in two ways: first by comparing the measure and predicted fission gas

release using the Westinghouse design model for fission gas release for some of the Saxton data and secondly by evaluating the diffusion equation prediction for several high burnup UO_2 fuel rods. Figure V-2 shows the results of the first comparison. The results show that the Westinghouse design model, which was normalized to UO_2 data, adequately predicts the fission gas release from the mixed oxide fuel rods. Conversely, the results obtained using the diffusion equation (also shown on Figure V-2), are consistently below the measured fission gas release.

Table V-4 illustrates a similar trend when the diffusion equation and the Westinghouse design equation are applied to several high burnup UO_2 fuel rods. While the fission gas release predicted by the Westinghouse model is in good agreement with the measured data, the diffusion equation underpredicts the fission gas release by a factor of 15 to 20.

It is again concluded that there is an effect of burnup on fission gas release.

C. Burnup Dependent Diffusion Coefficient

The previously described burnup effect on fission gas release is obviously not described by a diffusion coefficient which is only temperature dependent. However, the mathematical formulation (Section III-B) is capable of handling a diffusion coefficient of any functional form provided the coefficient is constant over a given time step or calculational interval.

Parker* suggests that D' be increased one order of magnitude for each 15000 MWD/MT of accumulated burnup but notes that a recent study indicates that this correction may be overly conservative.

To test the validity of this type of correction, six fuel rods were selected at random: four rods from Table V-2 and two rods from Table V-4. These six rods were then reevaluated by correcting the local value of D' according to the equation

$$D'_B = D'_0 \cdot F$$

where D'_B is the value corrected for burnup

D'_0 is the uncorrected (temperature dependent) value

F is the correction factor.

Two values of F were used in the study

1) $F = 100^{BU/30000}$

2) $F = 100^{BU/50000}$

These correction factors (Figure V-3) increase D' by an order of magnitude every 15000 MWD/MT or every 25000 MWD/MTU, respectively. The results of applying the correction factor in the analyses are given on Figure V-4 and in Table V-5. It can be seen that the 15000 MWD/MT order of magnitude correction brings the predicted fission gas release in line with the measured values.

* G. W. Parker, "Release of Radioactive Fission Products," Appendix VII-C, WASH-1400, August 1974.

The average ratio of measured-to-predicted fission gas release for the six rods is 0.86 indicating that the correction is overly conservative as indicated by Parker.

It should be noted that in doing these analyses no attempt was made to study the effect of the size of the timestep used in the calculations. Thus the use of a constant value of D' over an interval in which the burnup changed significantly may have affected the results obtained. Nevertheless, the basic objective of the exercise was accomplished. That is, the use of a burnup dependent diffusion coefficient does improve the predictive capability of the model at high burnups.

Table V-1
FISSION GAS RELEASE DATA FROM SAXTON CORE III MIXED OXIDE RODS⁽¹⁾

Rod I.D. No./Type	Initial Fuel True Density (% T.D.)	Diam. Gap (Mils)	Power During Core II (kw/ft)		Power During Core III (kw/ft)		Total Irrad. Time (Hours)	Rod Average Burnup (MWD/MTU)	Fission Gas Release (%)	
			Instant Peak Pellet	Rod Avg. Time Avg.	Instant. Peak Pellet	Rod Avg. Time Avg.			Meas.	Pred. ⁽²⁾
RR/70-I	93.7	8.3	12.3	7.4	14.7	9.8	11,660	25,070	34.3	16.3
BO/MOL	93.9	8.3	8.0	4.3	19.3	14.9	13,950	25,840	37.0	24.9
FS/MOL	94.6	7.1	9.1	5.3	14.3	9.6	13,950	25,500	26.0	11.7
GL/MOL	94.7	7.8	10.8	6.0	15.6	8.8	13,950	26,500	27.3	11.6
LZ/MOL	95.8	7.8	13.2	8.0	16.6	10.7	13,950	33,680	32.4	15.1
NI/MOL	93.4	7.8	10.0	5.0	17.7	11.2	13,950	27,020	34.0	20.5
RD/MOL	93.9	8.3	8.9	5.2	17.0	10.4	13,950	26,110	32.7	21.2
BE/EOL	94.1	7.4	8.0	4.5	17.4	9.7	16,730	30,200	34.2	15.8
BK/EOL	93.6	7.4	8.5	4.7	17.9	11.2	16,730	33,300	36.1	20.3
FI/EOL	94.1	8.0	11.3	7.3	9.8	6.4	16,730	30,900	19.2	8.1
IM/EOL	94.0	6.8	12.9	7.7	15.7	9.9	16,730	39,030	28.0	16.1
LS/EOL	95.7	6.7	12.3	7.4	11.1	6.8	16,730	33,780	18.2	5.4
PF/EOL	94.7	8.4	13.4	7.2	15.6	9.8	16,730	37,560	32.2	22.0

(1) All rods pressurized to 15 psia (90% Helium + 10% Argon) initially.

(2) Diffusion model using D' (1400°C) = $5.8 \times 10^{-10} \text{ sec}^{-1}$ and $E = 45 \text{ Kcal/mole}$.

SAXTON CORE II PLUTONIUM PROGRAM FISSION GAS RELEASE DATA⁽¹⁾

	Initial Fuel True Density (% T.D.)	Diametral Gap (mils)	Power (kw/ft)		Rod Avg. Burnup (MWD/MTU)	Fission Gas Release (%)	
			Time Avg. Rod Avg.	Peak Pellet		Meas.	Pred. (2)
TI	94.8	7.3	7.1	13.3	18460	30.3	11.0
TP	94.9	7.8	7.6	13.7	19750	30.7	13.5
TT	94.7	7.3	7.8	13.4	20400	32.3	11.5
QE	94.4	7.3	8.3	13.4	21540	23.9	12.2
TE	94.7	7.3	8.3	13.5	21590	28.4	12.2
LA	92.8	7.3	6.4	12.3	17020	22.7	8.8
MY	93.7	7.8	5.9	9.7	15660	12.0	3.0
RI	93.8	7.8	6.0	9.8	15820	5.1	1.8
JF	94.4	7.8	6.0	9.6	15630	3.7	2.9
A	94.4	7.8	7.9	18.3	16360	35.1	19.1
B	94.5	7.8	7.2	17.7	15050	38.2	18.4
CH	94.0	7.8	8.3	13.6	21640	26.7	14.4

(1) Total irradiation time = 9592 hours for all rods except A and B (irradiation time for A and B = 7638 hours). All rods pressurized to 15 psia (90% helium and 10% argon) initially. Pellets contained 6.6% PuO₂ - 93.4% UO₂.

(2) Diffusion model using D' (1400°C) = 7.1×10^{-10} sec⁻¹ and $E = 49.7$ Kcal/mole.

Table V-3

EFFECT OF DIFFUSION CONSTANTS ON PREDICTED GAS RELEASE

<u>Fuel Rod</u>	<u>Measured</u>	Fission Gas Release (%)	
		<u>A*</u>	<u>B**</u>
LZ/Mo1	32.4	15.1	17.0
IM/EOL	28.0	16.1	18.4

* $D'(1400^{\circ}\text{C}) = 5.8 \times 10^{-10} \text{ sec}^{-1}$; $E = 45 \text{ Kcal/mole}$

** $D'(1400^{\circ}\text{C}) = 7.1 \times 10^{-10} \text{ sec}^{-1}$; $E = 49.7 \text{ Kcal/mole}$

Table V-4

TYPICAL FISSION GAS RELEASE
HIGH BURNUP* UO₂ FUEL RODS

<u>Rod</u>	Fission Gas Release, %		<u>Ratio</u>
	<u>Measured</u>	<u>Predicted**</u>	<u>Measured/Predicted</u>
1	19.9	1.06	18.8
2	23.9	1.53	15.6
3	22.6	1.18	19.2
4	13.2	0.86	15.3

* Burnup in Range of 54 - 55,000 MWD/MT

** Diffusion Model with $D' = 7.1 \times 10^{-10}$; $E = 49.7$ Kcal/mole

Values Predicted with Westinghouse Design Model

<u>Rod</u>	<u>Predicted</u>	<u>Measured/Predicted</u>
1	15.3	1.3
2	24.8	.965
3	21.2	1.06
4	15.0	.88

Table V-5
EFFECT OF INCREASING DIFFUSION PARAMETER WITH BURNUP

Fuel Rod	Burnup (MWD/MTU)	Measured Release (%)	Predicted Release (%)		
			$(D'_B/D'_0) = 1$	$(D'_B/D'_0) = 100$	$(D'_B/D'_0) = 100$
				$\frac{BU}{50000}$	$\frac{BU}{30000}$
SAX - LA	17020	22.7	8.8	16.3	23.7
SAX - QE	21540	23.9	12.2	23.6	34.4
SAX - RI	15820	5.1	1.8	3.5	5.6
SAX - TP	19750	30.7	13.5	24.6	34.7
1	55400	19.9	1.06	5.2	21.6
2	54100	23.9	1.53	8.8	29.8

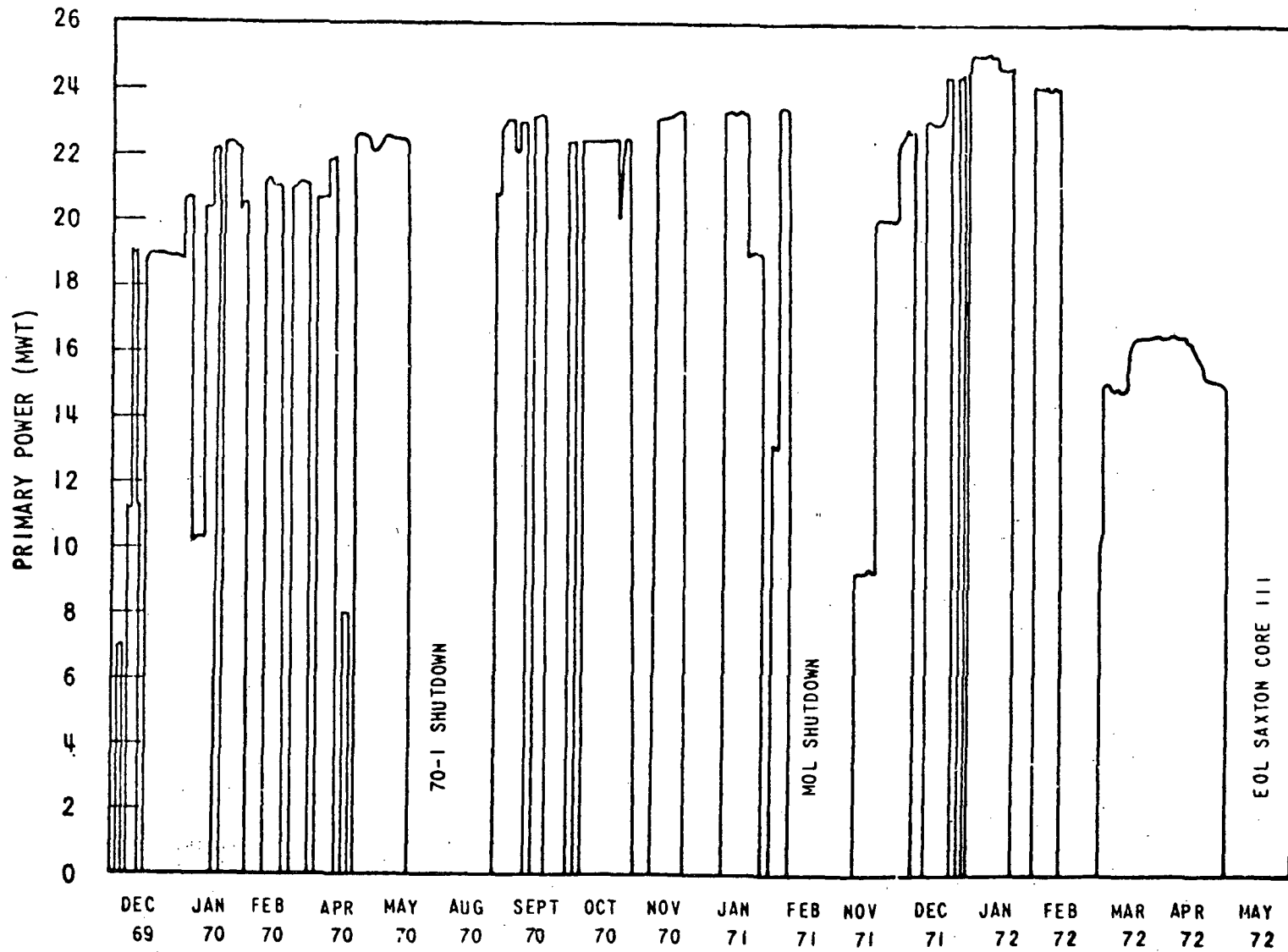


Figure V-1 Schematic Summary of Reactor Power History - Saxton Core III

Figure V-2
Saxton Core II Plutonium Program
Fission Gas Release

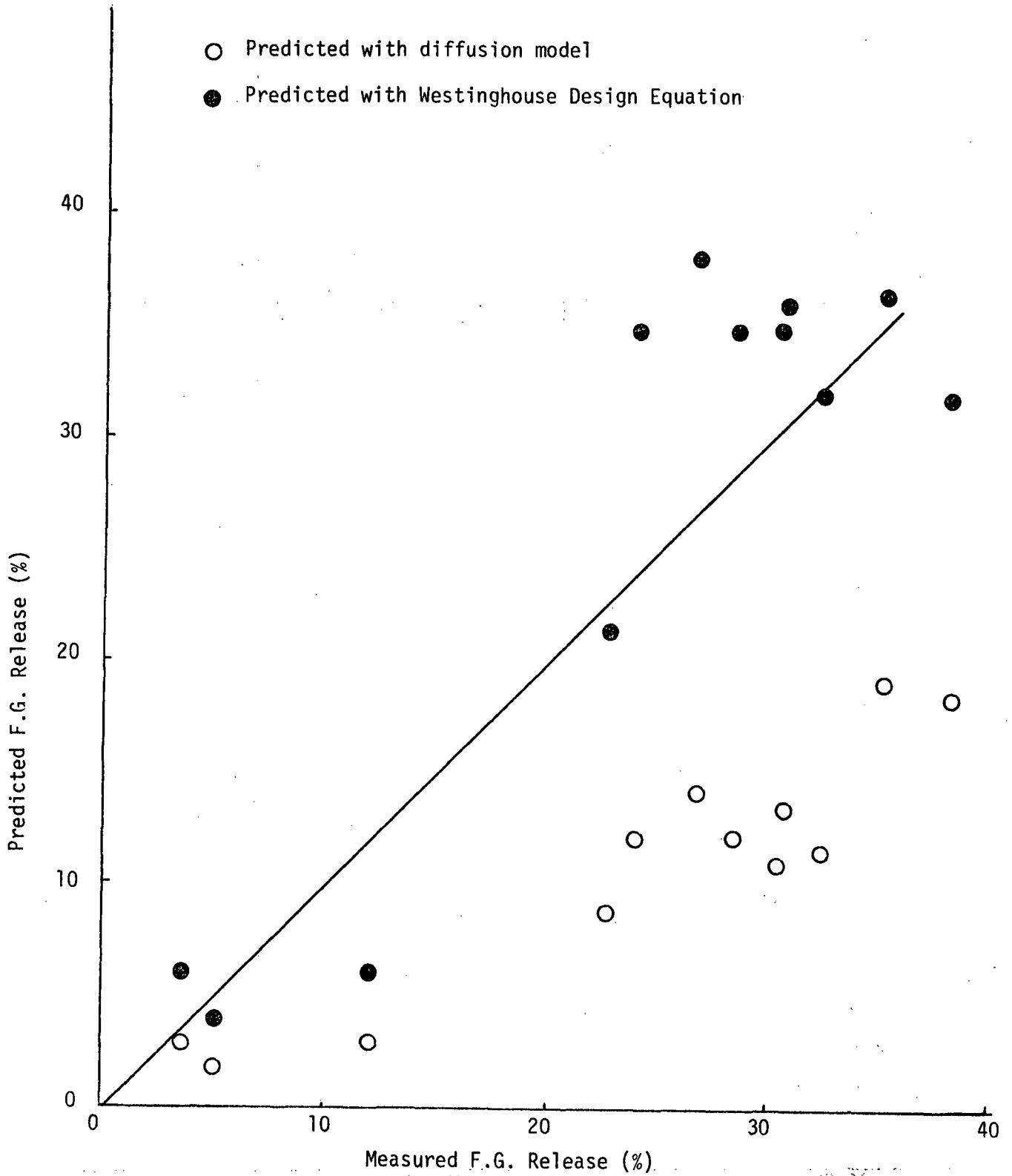


Figure V-3

Assumed Burnup Dependent Increase
in Diffusion Parameter D'

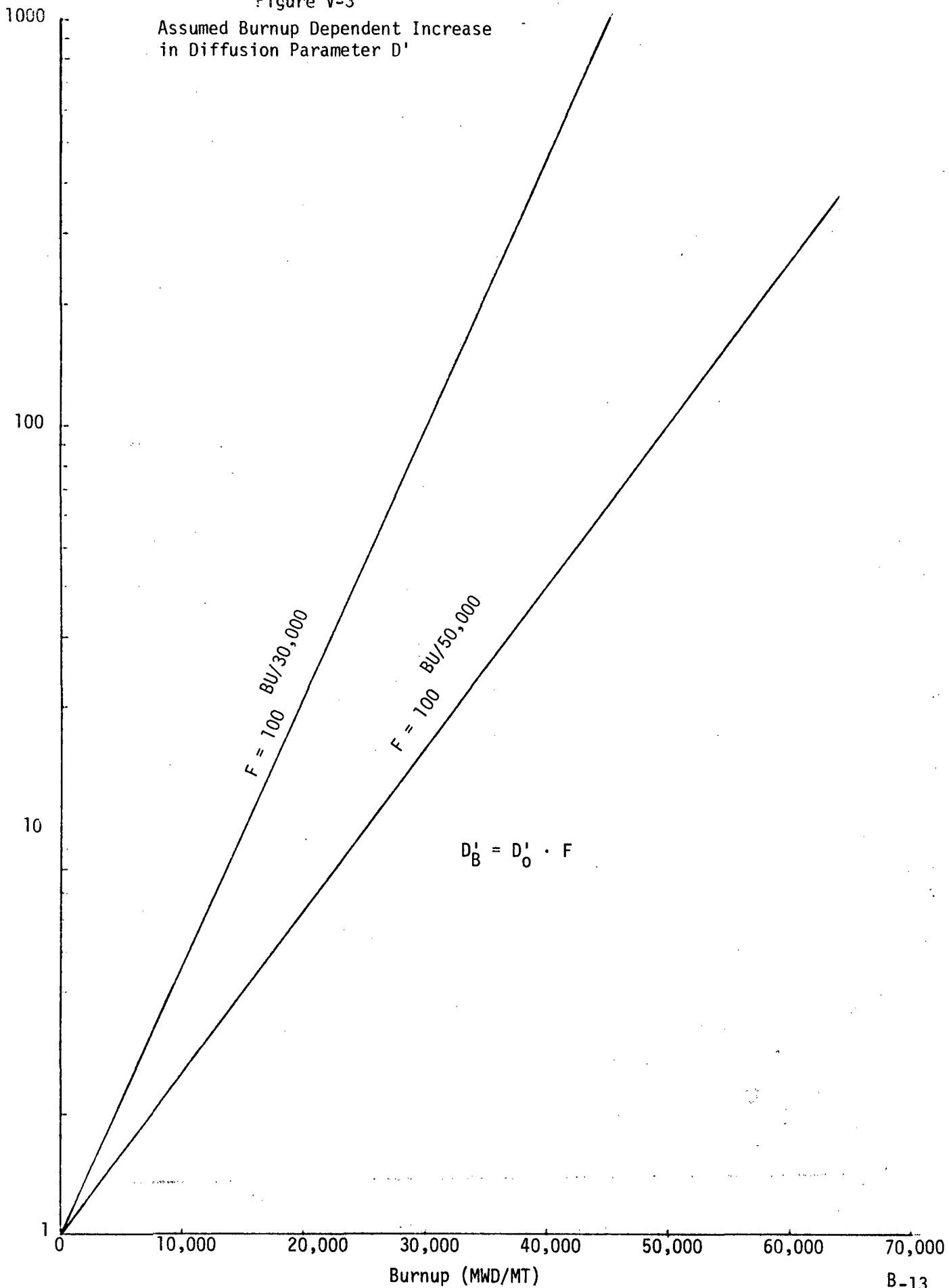
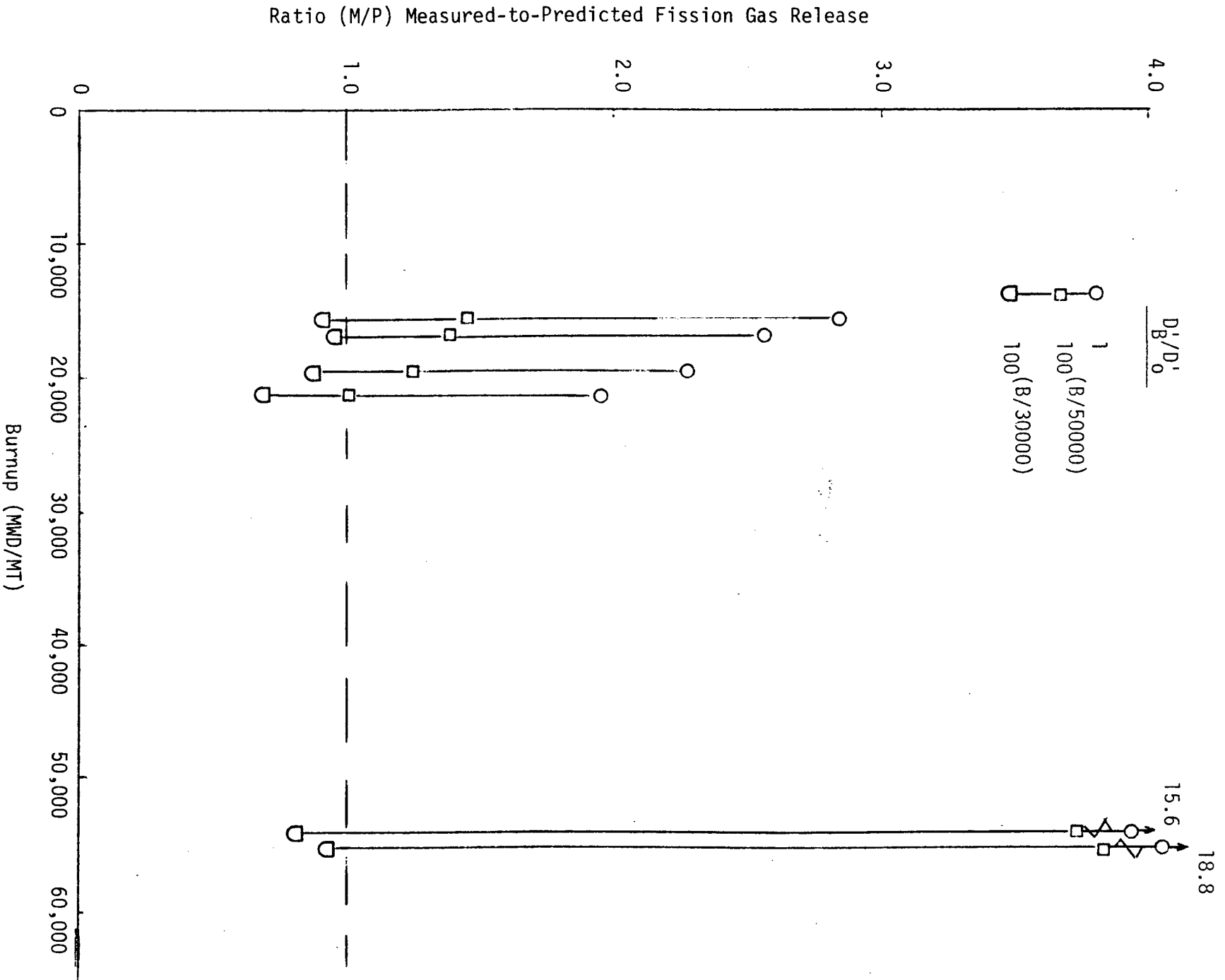


Figure V-4
 Effect of Burnup Dependent
 Diffusion Parameter



APPENDIX C

APPENDIX C

I. Calculation of Temperature Rise in a Spherical Particle having Internal Heat Generation (J. V. Miller, W)

The temperature rise in a spherical particle having internal heat generation is given by⁽¹⁾:

$$\Delta T_f = \frac{Q''' a^2}{6K}$$

where ΔT_f is the temperature rise [°F]

Q''' is the internal heat generation rate [BTU/HR-FT³]

a is the radius of the sphere [ft]

K is the thermal conductivity [BTU/hr-ft-°F]

If we assume that for a mixed-oxide fuel pellet the volume fraction of the fuel which is PuO₂ particles is V_f , then the heat generation in the particles can be related to the linear heat rating (q) by

$$Q''' = \frac{q(\text{kw/ft}) \cdot 3413 \left(\frac{\text{BTU}}{\text{hr-kw}}\right) \cdot 144}{(\pi/4) (.3374)^2 v_f}$$

$$Q''' = 5.5 \times 10^6 q/v_f$$

where .3374 inch is the typical diameter of a Saxton fuel pellet.

The manufacturing specification for the Saxton fuel rods required that the PuO₂ particles be less than 44 microns. Therefore,

$$a = \frac{d}{2} = \frac{44 \times 10^{-6} \text{ meter}}{(2) (.3048 \text{ meter/ft})}$$

$$a = 7.218 \times 10^{-5} \text{ feet} \quad (8.66 \times 10^{-4} \text{ inch})$$

Conservatively assuming that v_f equals 0.05* and that $K = 1$ BTU/hr-ft-°F**, we have

$$\Delta T_f = \left(\frac{5.5 \times 10^6 q}{0.05} \right) \frac{(7.218 \times 10^{-5})^2}{(6 \times 1)} = .096 q$$

At ten kilowatts per foot ($q=10$), we then find that

$$\Delta T_f \approx 1 \text{ } ^\circ\text{F.}$$

It is concluded that the temperature drop through a PuO_2 particle is negligible.

Surface Heat Flux and Associated Temperature Drop

The heat flux at the surface of the particle is

$$\phi = \frac{Q''' \frac{4}{3} \pi a^3}{4\pi a^2} = \frac{Q''' a}{3}$$

At 10 kw/ft,

$$\phi = (5.5 \times 10^6) \left(\frac{10}{.05} \right) \left(\frac{7.218 \times 10^{-5}}{3} \right)$$

$$\phi \approx 26,500 \text{ BTU/hr-ft}^2$$

Dean⁽²⁾, for example, showed that the contact conductance between two surfaces increased as the surface roughness decreased and as the contact pressure increased (Fig. C-I-1). In the case of PuO_2 particles intimately embedded in a UO_2 matrix, the effective surface roughness should be quite small and the contact pressure quite high. From Figure C-I-1 it would therefore appear that the contact conductance would be (at least) on the order of 3000 BTU/hr-ft-°F.

* The Saxton rods were typical 6.6 % PuO_2

** Value would typically be between 1.2 and 2.0

The temperature drop at the surface of the particle is then given by

$$\Delta T_S = \phi/h_{\text{con}} = \frac{26,500}{3000} \approx 10^\circ\text{F}.$$

The total temperature rise would then be given by

$$\Delta T = \Delta T_S + \Delta T_f = 10 + 1 = 11^\circ\text{F}.$$

Figures C-I-2 and C-I-3 show that a 100°F increase in fuel temperature only has a significant (relative) impact on fission gas release at low temperatures (e.g., in going from 1500°F to 1600°F the release increased from 1.5 percent to 2.7 percent). At high temperatures the increase in release due to a 100°F change in fuel temperature is relatively quite small (e.g., the release increased from 59 percent to 69 percent in going from 2500°F to 2600°F).

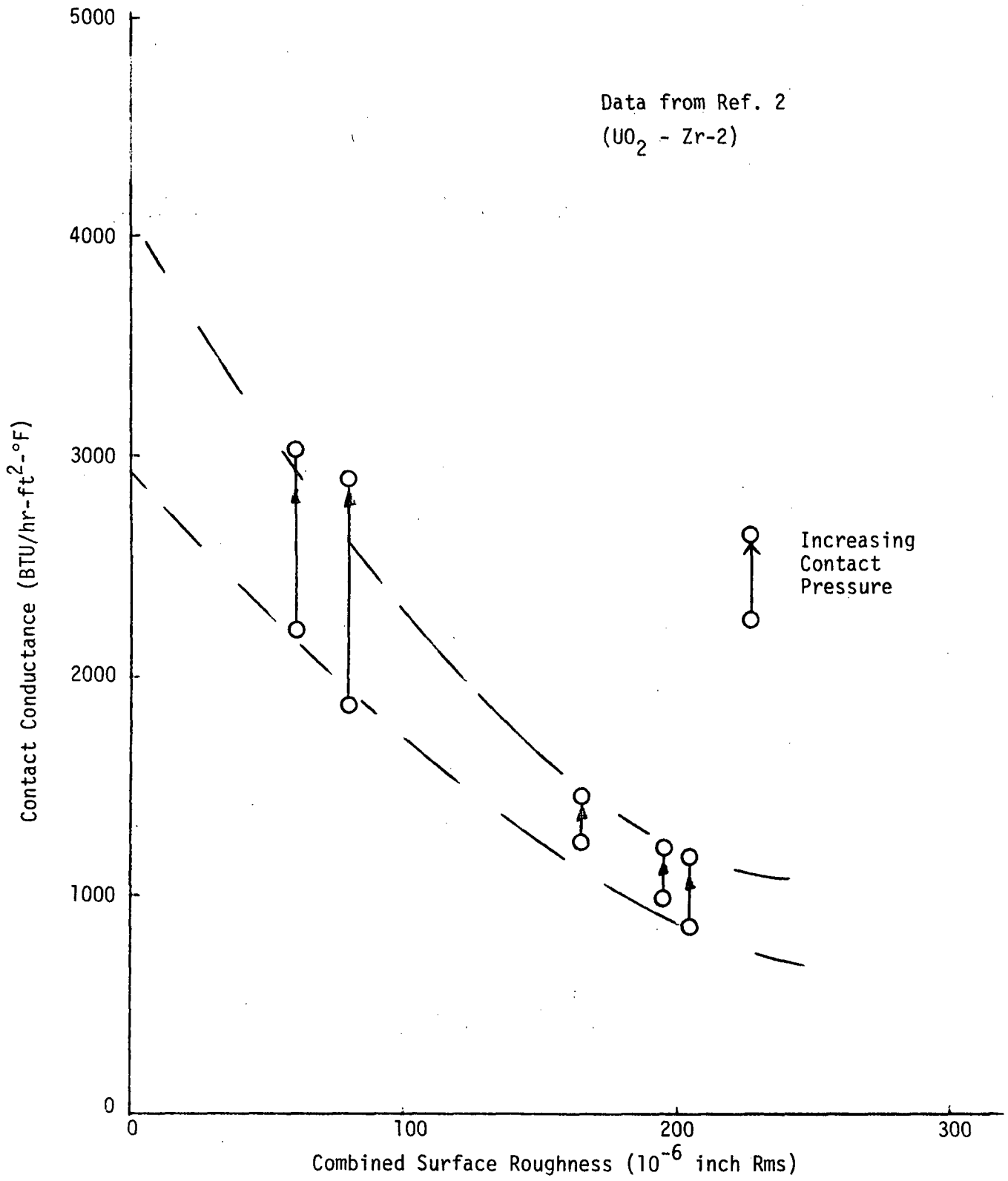
It is concluded that the above described 11°F temperature increase attributed to the PuO_2 particle would not account for the factor of two or three difference between the Westinghouse prediction and the measured fission gas release.

It is also important to note that the central portion of nearly all of the Saxton mixed-oxide fuel rods did not contain discrete particles of PuO_2 throughout their operating history. Autoradiographs^(3,4) taken at various levels of fuel burnup show that thermal diffusion effectively homogenized about half of the cross-sectional area. Discrete PuO_2 particles could only be detected in the outer (colder) region of the fuel. Thus, the region of highest temperature (and highest gas release) had, in fact, a nearly uniform matrix free of discrete particles.

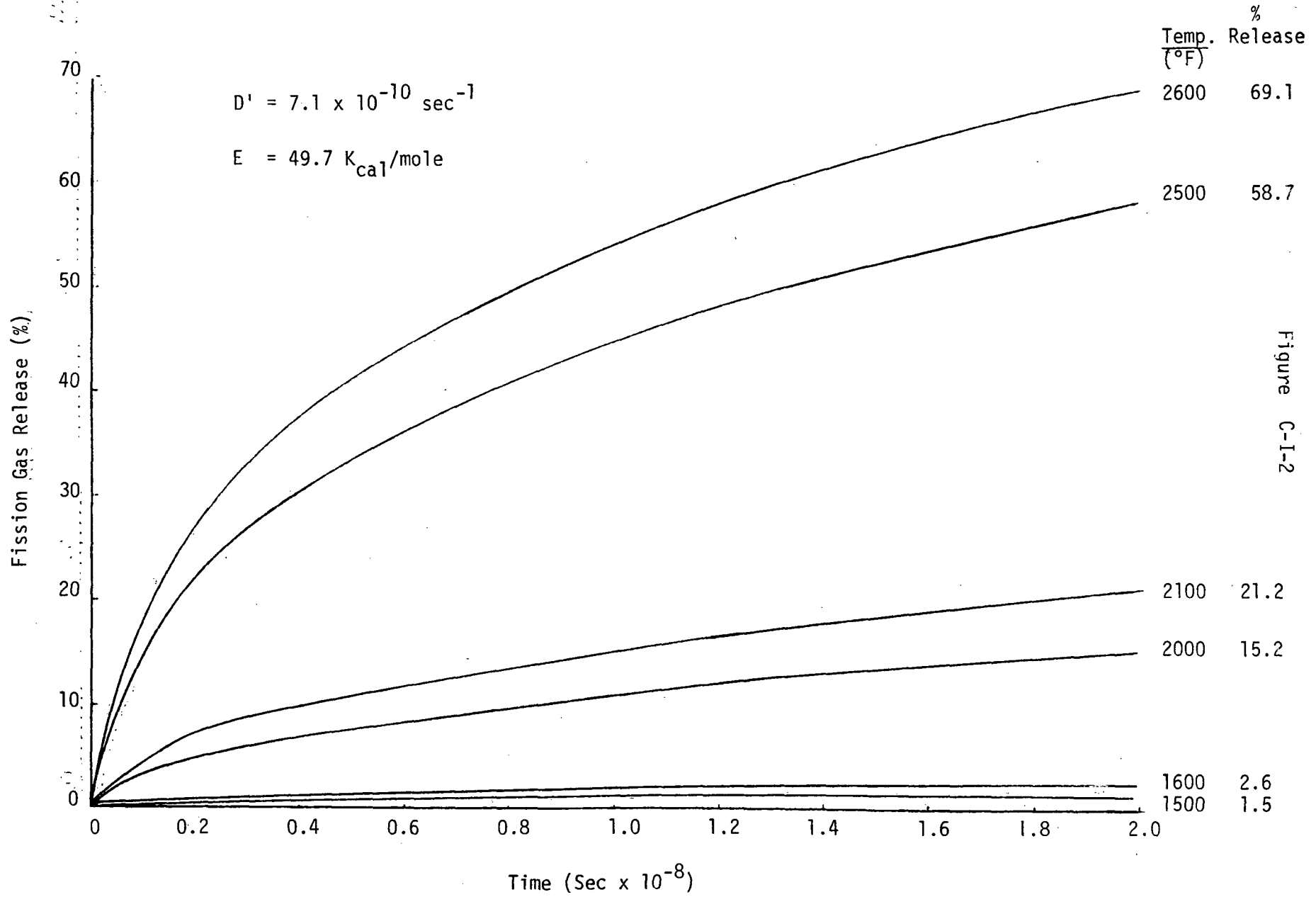
References:

- 1) Carslaw and Jaeger, Conduction of Heat In Solids, Second Edition, 1959 (p. 246).
- 2) R. A. Dean, Thermal Contact Conductance Between UO_2 and Zircaloy 2, CVNA-127, May 1962.
- 3) W. R. Smalley, Saxton Core II Fuel Performance Evaluation, Part I: Materials, WCAP-3385-56, Part I, September, 1971.
- 4) W. R. Smalley, Evaluation of Saxton Core III Fuel Materials Performance, WCAP-3385-57, July, 1974.

Figure C-I-1
Effect of Surface Roughness
on Contact Conductance



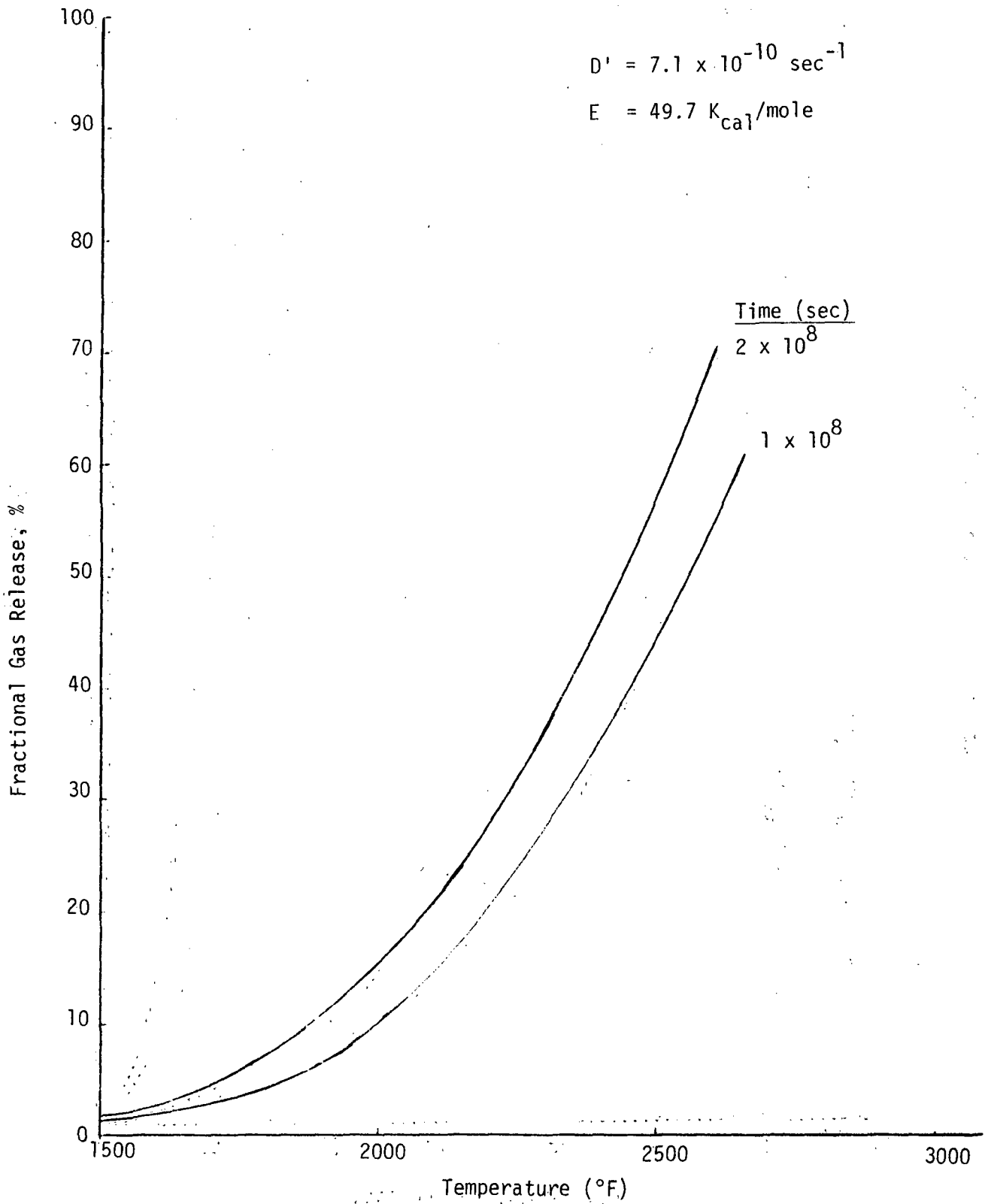
Effect of a 100°F Change in Temperature
on Predicted Fission Gas Release



C-6

Figure C-I-2

Figure C-I-3
Effect of Time & Temperature
on Predicted Fission Gas Release



II. Fission Gas Release From Blended Mixed Oxide Fuel (B.J. Buescher, B&W)

Aside from any intrinsic differences between the fission gas release rate of homogeneous (U, Pu) O₂ mixed oxide fuels and UO₂ fuels, it is quite likely that blended mixed oxide fuel pellets such as those in the Saxton rods will exhibit a different gas release dependence on burnup from that of UO₂ fuel. The Saxton fuel was fabricated by pressing and sintering pellets from blended powder containing 6.6 wt% PuO₂. The maximum particle size of the PuO₂ in the finished pellets was specified to be less than 44 microns. Fissioning in this blended fuel will not be homogeneous on a microscopic scale but will take place primarily in the plutonium rich regions. The resulting large concentration of fission products in the plutonium rich regions gives an effective burnup on a microscopic scale far larger than than the average macroscopic burnup. The magnitude of the local burnup will depend on the particle size illustrated by the following calculation.

For simplicity, the following assumptions were made:

- 1) The PuO₂ particles have a spherical shape and are uniformly dispersed in the matrix.
- 2) All of the fission events occur in the PuO₂ particles.
- 3) The temperature of the region is less than 1200°C.

With these assumptions, the local burnup can be considered to be given by the concentration of fission products produced by the PuO₂ particle spread over a region somewhat larger than the initial particle. The spreading will be due to both the finite range of the fission products, about 5 microns¹, and diffusional migration at low temperatures. The diffusion rate of noble gases in irradiated UO₂ at fission rates of 10¹³ f/cm³ sec has been found to be about 10⁻¹⁶ cm²/sec.² The random walk expression for the mean square displacement of the gas atoms normal to the particle surface is:

$$R^2 = 2Dt.$$

Assuming a nominal burnup of 20,000 MWD/MTM and a nominal pellet density of 94% TD, the total fission/cm³ are 4.9×10^{20} fissions/cm³. This gives a nominal mean square displacement of

$$R^2 = 9.8 \times 10^{-9} \text{ cm}^2,$$

or an average displacement of 1 micron for a fission gas atom implanted in the matrix.

Thus, for a 20 micron diameter particle, the fission products from that particle will be found to be localized to a region roughly 32 microns in diameter.

Assuming a macroscopic burnup of 20,000 MWD/MTM, this 32 micron diameter region will have a fission product concentration equivalent to that of a burnup of about 80,000 MWD/MTM.

The burnup in the region was calculated as follows:

$$\text{Region Burnup} = \frac{\text{Macro-Burnup}}{\text{Fraction of Pu}} * \frac{\text{Particle Volume}}{\text{Region Volume}}$$

A calculation of the local burnup versus particle size was made and is shown in Figure C-II-1. For particles below about 8 microns, the pellet would contain a large number of small particles with overlapping regions resulting in an uniform fission product density. Above about 8 microns, discrete regions are calculated and the local burnup increases with particle sizes up to a microscopic burnup of 147,000 MWD/MTM for 44 micron particles.

For the Saxton rods, an examination of the microstructure published in Reference 3 indicates that the particle sizes were on the order of 20 to 30 microns, giving a local burnup between 70,000 and 110,000 MWD/MTM. The examination of these cross sections also indicates that a high local concentration of porosity is also present, indicative of a large local concentration of fission products. A local burnup enhancement such as this can lead to a pronounced increase in the gas release in mixed oxide fuels at even moderate burnups as has been noted previously.⁴ Such an effect is not present in the UO₂ fuel, and gas release data from mixed oxide is therefore

not representative of the gas release from UO_2 fuel.

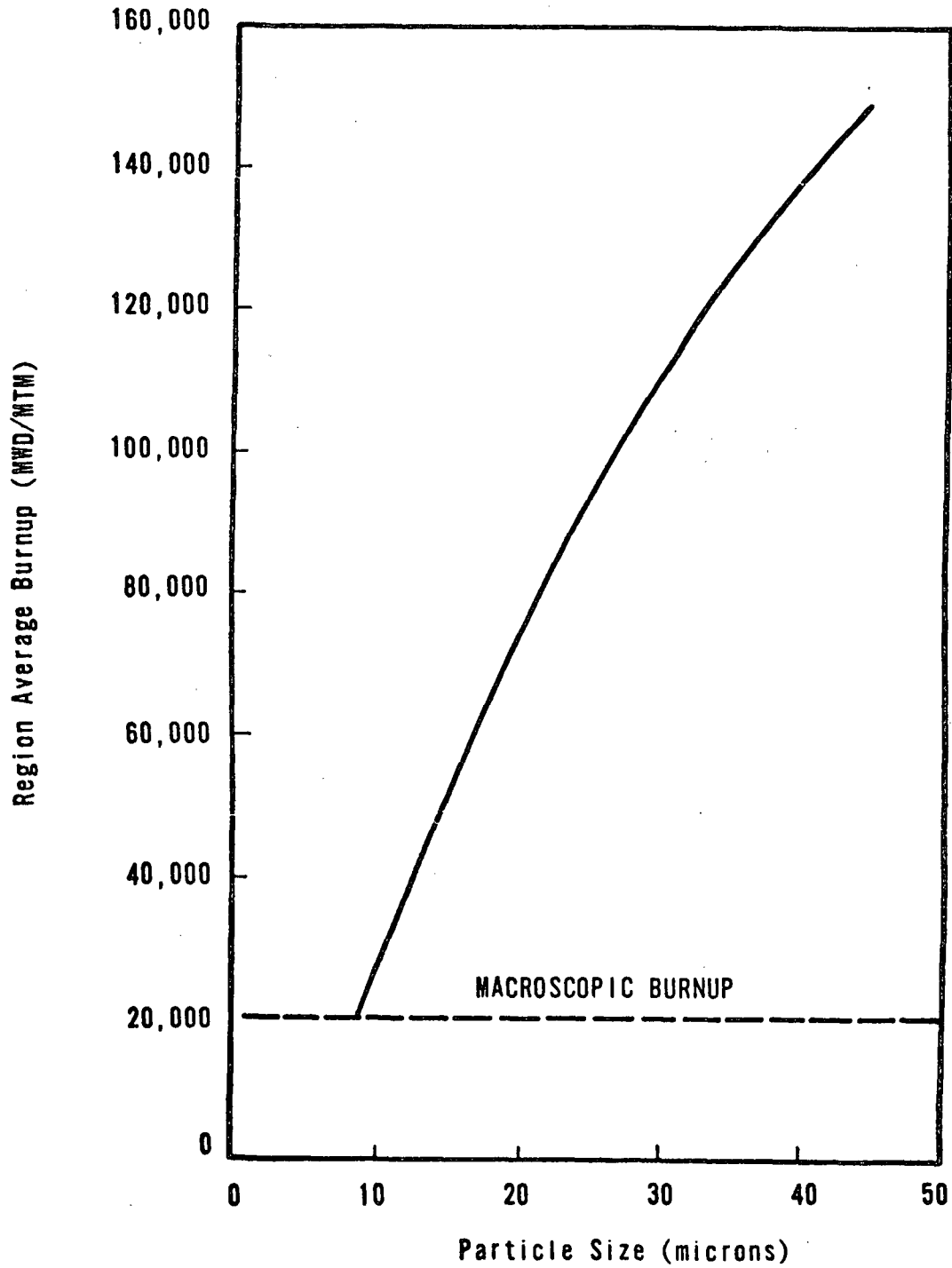
It could be argued that the large gas release seen in Saxton mixed oxide fuels was not due to particle size effects as homogenization had occurred in the high temperature regions of the fuel. Although all of the data obtained in the Saxton Program is not presented in the Saxton reports, a fairly comprehensive presentation of the metallographic data obtained from rod QE is given in Reference 5. This rod was irradiated to ≈ 21000 MWd/t and the gas release measured in this rod was 24% (Appendix B). Homogenization of the Pu particles took place at the peak power location out to about 1/3 of the pellet radius or $\approx 10\%$ of the volume. Examination of the microstructure in the published edge to center composite of the peak section indicated equiaxed grain growth to roughly 1/2 of the pellet radius.

Based on the microstructure, the $1400^{\circ}C$ boundary in the fuel at the peak power position extends out to 1/2 of the pellet radius, and the $1700^{\circ}C$ boundary is estimated to extend out to almost 1/3 of the pellet radius. For this fuel rod, Westinghouse predicted a release of 12% using a gas release rate based on Beyer-Hahn results, and an enhancement ratio of 2 to 1 was observed between the measured and predicted release rate. The release fraction is already 80% at temperatures above $1700^{\circ}C$, where plutonium homogenization is seen to occur. Since this only occupies $\approx 10\%$ of the fuel volume (even at the peak power location) substantial enhancement of the release rate appears to be occurring in the lower temperature regions of the fuel where homogenization does not occur. Based on this, the particle size effect cannot be ruled out by the homogenization seen in high temperature regions of the fuel.

REFERENCES

- ¹ J. Belle, "Uranium Dioxide, Properties and Nuclear Application," USAEC, 1961, p. 654.
- ² HJ Matzke, "Application of the Ion Bombardment Technique to Study the Behavior of Rare Gases in UO₂" in "Physics of Ionized Gases," B. Novinsek Ed. (1970).
- ³ W. R. Smalley, "Saxton Plutonium Program Semi-Annual Progress Report for the Period Ending June 30, 1969," (1969) WCAP 3385-20, pp. 3-29 to 4-4.
- ⁴ H. Stehle et. al., "Uranium Dioxide Properties for LWR Fuel Rods," Nucl. Eng. & Design 33 (1975) p. 230-260.
- ⁵ W. R. Smalley, "Saxton Plutonium Program Semi-Annual Progress Report for the Period Ending June 30, 1969"; WCAP 3385-20.

Figure C-II-1 REGIONAL (MICROSCOPIC) BURNUP VERSUS PARTICLE SIZE
CALCULATED FOR AN AVERAGE (MACROSCOPIC) BURNUP OF
20,000 MWD/MTM



APPENDIX D



Pacific Northwest Laboratories
Battelle Boulevard
Richland, Washington 99352
Telephone (509) 946-2526
Telex 32-6345

January 19, 1977

Mr. F.D. Coffman
Reactor Safety Branch
U.S. Nuclear Regulatory Commission
Washington, D.C. 20555

Dear Mr. Coffman:

Attached are six copies of the December monthly activities report for the Fuel Operational Performance Program. Efforts are now underway on all four of the program tasks.

Sincerely yours,

A handwritten signature in cursive script that reads "Stan Goldsmith".

Stanley Goldsmith, Manager
Fuels Design & Development
Section

SG:vm

Attachments

cc: R Lobel (RSB-DOR)
LS Rubenstein (NRR)
HE Ransom (RL-ERDA)

bcc: CR Hann
WJ Bailey
SR Wagoner
FE Panisko
ER Bradley
EL Courtright
file/lb

Battelle, Pacific Northwest Laboratories
Monthly Activities Report
December 1976
Fuel Operational Performance Program
C.R. Hann, Project Manager

Task A - Fuel Operational Experience - *W.J. Bailey, L.J. MacGowan*

The literature search to locate descriptive material that will aid in the assessment of poolside inspection techniques (Phase 1 of Task B) is continuing. To aid in the search and evaluation in the areas of ultrasonic and eddy current testing, work was initiated in PNL's Nondestructive Testing Section.

A preliminary investigation of existing data base management systems (DBMSs) was initiated. Of particular interest are those DBMSs that may be applicable to the data bank and the associated evaluation of design parameters and operating modes on fuel performance (Phase 2 of Task B). Advantages and disadvantages of the pertinent DBMSs are being compiled during the investigation. Also as part of Phase 2, the routine surveillance of certain current publications* is continuing and clues to sources of data on fuel performance experience are being tabulated.

Task B - On-Call Assistance - *C.R. Hann, S.R. Wagoner, F.E. Panisko*

The GAPCON-THERMAL-2 code was used to simulate the behavior of selected Saxton fuel rods. Four gas release correlations were used in the simulation in which predicted and reported gas releases were compared. The four models were:

1. Beyer - Hann
2. Beyer - Hann with a high burnup multiplier
3. Proposed ANS subcommittee gas release model
4. Proposed ANS submittee model with high burnup

The results of modification are tabulated in the following table:

In addition to the Saxton rods, both a 15 x 15 and a 17 x 17 PWR rod were modeled with the first two correlations.

*Atomic Energy Clearing House, Accessions by NSIC, Accessions of Unlimited Distribution Reports by USERDA Technical Information Center (TID-4401), and Report Additions to Technical Information Files (PNL).

SAXTON ROD IDENTITY

	RI	QE	LA	TP	LZ	IM
Ave. Rod Burnup, (MWD/MT)	15820	21540	17020	19750	33680	29799
Measured Fission Gas Release (%)	5.1	23.9	22.7	30.7	32.4	28.0
Model 1 (%)	2.0	5.0	5.0	18.9	25.8	50.0
Model 2 (%)	2.0	9.0	5.0	21.3	52.6	70.0
Model 3 (%)	8.4	27.8	17.3	36.6	55.1	58.4
Model 4 (%)	8.4	23.5	17.2	34.7	75.7	79.2

Task C - Fuel Rod Volatiles Inventory - E.R. Bradley, C.R. Hann

Parametric studies to establish the influence of gaseous iodine and cesium on the calculated fuel rod internal pressures and fuel temperatures have been completed. The results show that including iodine and cesium release in the calculations increases both the fuel temperature and the fuel rod internal pressure. In the case of iodine release, the magnitude of the increase is less than 10% for the conditions studied. Substantially larger increases are found for cesium release, especially at low power levels. Work on evaluating the chemical and physical state of cesium and iodine in the fuel-cladding gap has been initiated.

Task D - FRAP-T - Evaluation and Utilization - C.R. Hann, S.R. Wagner, L.J. Panchen

Efforts on this task were delayed due to on-call assistance requests.

APPENDIX E

APPENDIX E

Applicability of Saxton Data (R.L. Ritzman, SAI)

The failure of the burnup independent diffusion equation to predict sufficiently large fission gas releases for high burnup Saxton fuel rods has been cited as evidence for a strong burnup effect. Therefore one would expect to observe an increasing disparity between measured and predicted gas releases in these data as the burnup increases. This expectation was checked by plotting the ratio of measured to predicted gas release values versus burnup for Saxton Core III and Core II fuel rods as given in Tables B-1 and B-2 of Appendix B. The results are shown in Figure E-1.

Inspection of Figure E-1 reveals no clear trend of the gas release ratio with burnup, although the measured release fractions are approximately twice the predicted values. Since the varied thermal performance of the different rods was taken into account in the gas release prediction calculations, the lack of a burnup dependent trend should not be due to unaccounted for power history differences in the data set. Therefore, the Saxton data apparently contain no clearly discernable burnup dependence for fission gas release. This particular result does not, by itself, refute the existence of a burnup effect, but it does indicate that the Saxton data are probably of little use for either establishing or quantifying the effect.

E-2

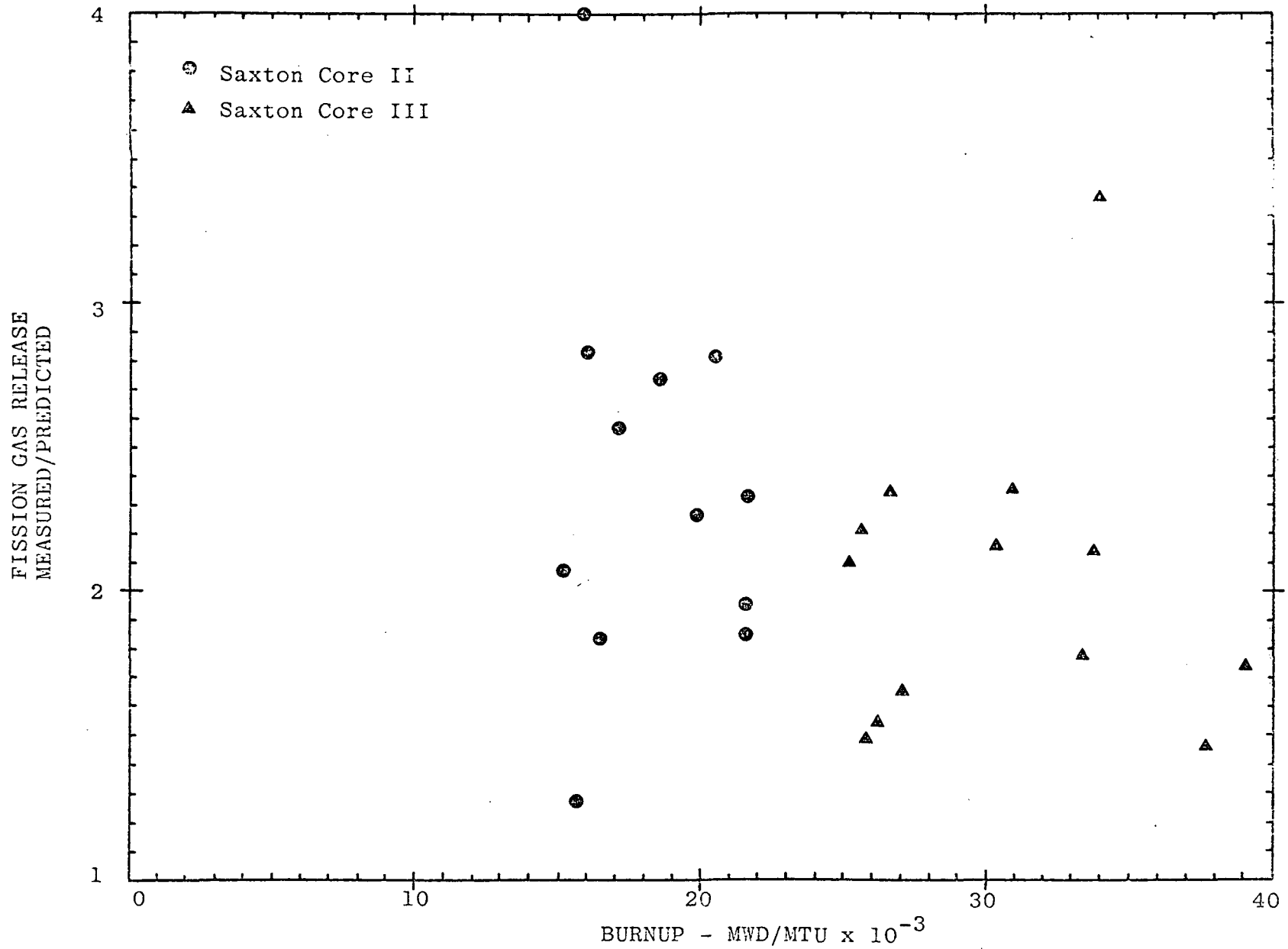


Figure E-1. Burnup dependence of measured/predicted gas release ratios for Saxton data.

APPENDIX F

HARWELL

AERE Harwell, Didcot, Berkshire

OX11 0RA

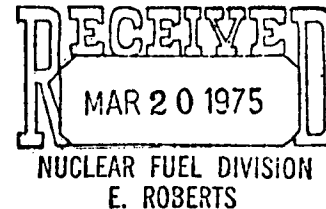
Telephone: Abingdon 4141, Ext. 4316

Telegrams: Aten, Abingdon

Telex 83135

Date 13th March 1975

Dr. E. Roberts
WNES Nuclear Center
Monroeville
Pittsburgh, Pa
USA



Dear Dr. Roberts,

In reply to your Telex received 11th March I enclose a table expanding the data presented in Fig 10 of our paper in Journ.Nuclear Materials V33, pp 64 - 76, 1969. I have some other data which may be of interest to you in the report on which the paper is based, but this requires administrative processing. I will forward them as soon as clearance is obtained. Regrettably I destroyed the file containing my original notes (in February of this year) and there may be some minor gaps, such as the detailed temperature history of pins 5050 and 5049.

Our conclusion that fission gas release from dense UO_2 is insensitive to irradiation temperature below $1250^{\circ}C$ was largely based on the regularity of the points plotted in Fig 10, which despite a wide variation in centre temperatures display a substantially linear relationship with burn-up up to a critical value, above which the increase is quite smoothly exponential. This athermal relationship is quite compatible with non-diffusional release mechanisms such as recoil and knockout which we may expect at low burn-ups below $1250^{\circ}C$. An irradiation enhanced diffusion mechanism of gas release could also conceivably exist, but I would expect this to be fission rate dependent and also athermal below $1250^{\circ}C$, by analogy with the work of D.J. Clough (AERE R 6627, D.J. Clough 1970) on the irradiation creep of fuel. Both fission gas diffusion and irradiation creep are linked to the vacancy diffusion coefficient. In these experiments the range of fission rates was comparatively small (140 - 200 W/g UO_2) and we did not look for a fission rate dependence. At lower fission rates I would expect the temperature limit for athermal behaviour to be lower than $1250^{\circ}C$; in effect there is a greater time per unit of burn-up for thermal diffusion processes to become significant. As all our pins with maximum centreline temperatures not exceeding $1250^{\circ}C$ contained high density fuel pellets (~ 98% TD) we have no evidence of the effect of fuel pellet density on gas release in this temperature range.

I have ascribed the increased gas release above about 3% burn-up to an increase in effective surface area due to grain boundary gas bubble linkage, or to grain boundary weakening followed by intergranular cracking due to thermal stress. This critical grain boundary condition must also be achieved through diffusion processes, which by the arguments adduced above should be athermal below 1250°C at these ratings; i.e. the critical burn-up will not be sensitive to fuel temperature. Again I would expect the limiting temperature for athermal behaviour to fall at reduced fission ratings, which is borne out by much of the UKAEA work on AGR fuel, e.g. "UO₂ Fuel in the Mk 11 Gas Cooled Reactor (AGR)", G.B. Greenough, J.S. Nairn, J.B. Sayers, Paper No. 2.10(6), Fourth ICP UAE, Geneva, 1971.

I hope these comments are of use.

Yours sincerely,

pp. R.G. Bellamy.

R.G. Bellamy

Metallurgy Division
Building 393.7
Extn. 4316

14th March 1975

cc Mr. J.B. Rich
Mr. J.B. Sayers
Dr. M. Hayns
Dr. J.D.C. Mole

Pin identification and maximum fuel centreline temperatures for the points of Fig.10, JNM V33, p 72, 1983.

Pin No.	Mean B.U., at %	Fractional Xe release, %		Assumed fuel/clad resistivity (°C/W.cm ²)	Maximum centre temperature during each reactor cycle °C									
					1 Start	1 end	2	3	4	5	6	7	8	9
5030	1.48 14060	0.12	-	1.0	931	974	960	872						
				1.5	1047	1101	1079	971						
				2.0	1163	1224	1195	1072						
5029	1.50 14250	0.08	0.10	1.0	824	856	848	781						
				1.5	919	959	945	860						
				2.0	1017	1066	1044	943						
5031	1.63 15485	0.17	0.15	1.0	981	938	943	816						
				1.5	1123	1073	1078	925						
				2.0	1264	1207	1212	1033						
5032	1.65 15675	<0.1	<0.1	1.0	870	835	840	743						
				1.5	997	955	960	835						
				2.0	1124	1074	1079	927						
5037	1.93 18335	0.15	-	1.0	671	684	757	758	744	795				
				1.5	750	768	838	839	820	869				
				2.0	828	852	919	920	897	943				
5038	19285 205	0.19	0.20	2.0	967	1000	1047	1049	1020	1061				
5023	20945 21	0.22	0.22	1.5	1016	966	980	948	918	965				
				2.0	1163	1102	1081	1064	1025	1068				
5022	33340 372	2.61	2.44	2.0	1188	1240	1194	1170	1180	1118	990	961	920	1238

See Cont'd

5039	4.21 39 495	3.24	3.08	1.5 2.0	1147 1252	1100 1200	1089 1188	1149 1241	1134 1223	1070 1153	977 1048	934 1000	946 1005	114 122
5050	45.600 4.80	4.08 (4.8)	-	Detailed calculations are not available; irradiated for 10 cycles with centre temperature not exceeding 1250°C.										
5049	48.355 5.09	7.09 (7.9)	-											

J. Nucl. Mat., 33 (1969) p.70

1146
1228

Committee Correspondence

Committee: ANS 5.4 Working Group
Fuel Plenum Gas Activity
(N218)

Reply To:

Subject: Fission Gas Release from
Bettis Rod 79-163

Date: March 9, 1978

To: ANS 5.4 Working Group Members

Please find attached an analysis of the fuel temperatures
calculated for Bettis test rod 79-163.

BJB:lsf

cc: w/o attachments

J. S. Tulenko
H. W. Wilson
W. R. Gray
J. R. Smotrel
R. A. Turner



w/ attachment

J. R. Davis

Bettis Rod 79-163

A calculation of the fuel temperatures was performed for the Bettis test rod 79-163. The as-built dimensions, the operating history and the results of the post irradiation examination are given in Reference 1. The fuel temperatures were calculated using the TACO thermal analysis code (Reference 2). This rod was fabricated using high density fuel with a small initial diametral gap (\approx 1 mil). The fuel temperatures were calculated assuming stable fuel and a constant gap conductance of $0.7 \text{ watts/cm}^2\text{ }^\circ\text{C}$. The centerline temperatures versus burnup which were calculated for this rod are shown in Figure 1. At the final cycle of operation the center temperature of the test rod was found to 1240°C . This occurred at a rod average burnup of 24,000 MWd/mtU.

This rod was highly enriched compared to commercial LWR fuel and had a strong radial dependence on the burnup. The polynomial fit to the radial burnup data is shown in Figure 2. Using this fit as the best estimate the burnup at the centerline of the fuel is 16,400 MWd/mtU.

Since the gas release measured for this rod is 0.2% this analysis gives an additional point for establishing a transition temperature between knockout and enhanced low temperature gas release.

References

1. J. T. Engel and H. B. Meieran, "Performance of Fuel Rods Having 97 Percent Theoretical Density UO_2 Pellets Sheathed in Zircaloy-4 and Irradiated at Low Thermal Ratings," WAPD-TM-631, July, 1968.
2. R. H. Stoudt et al., "TACO - Fuel Pin Performance Analysis," BAW 10087A, August 1977.

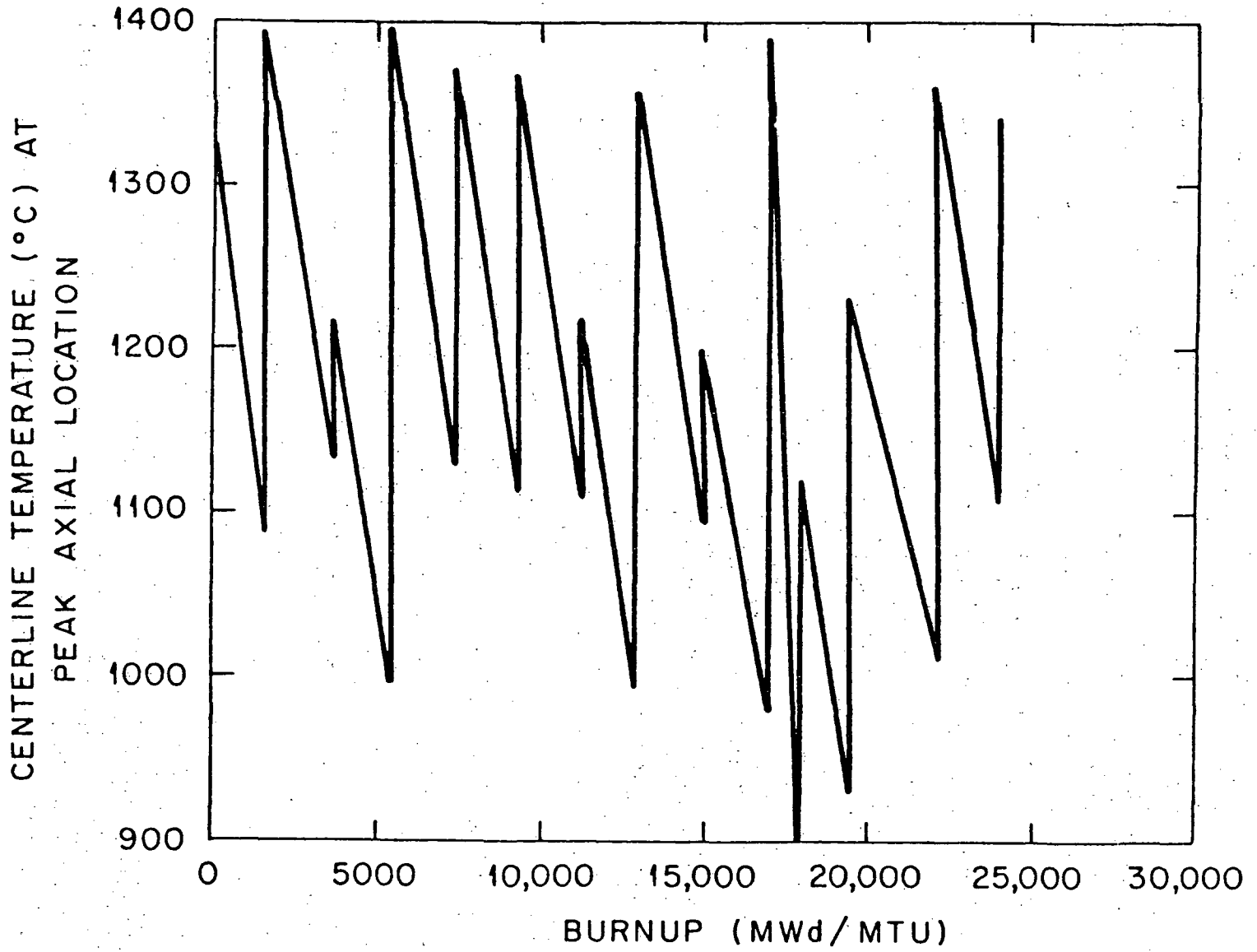


Fig. 1. Centerline temperatures calculated for rod BETT 79-163.

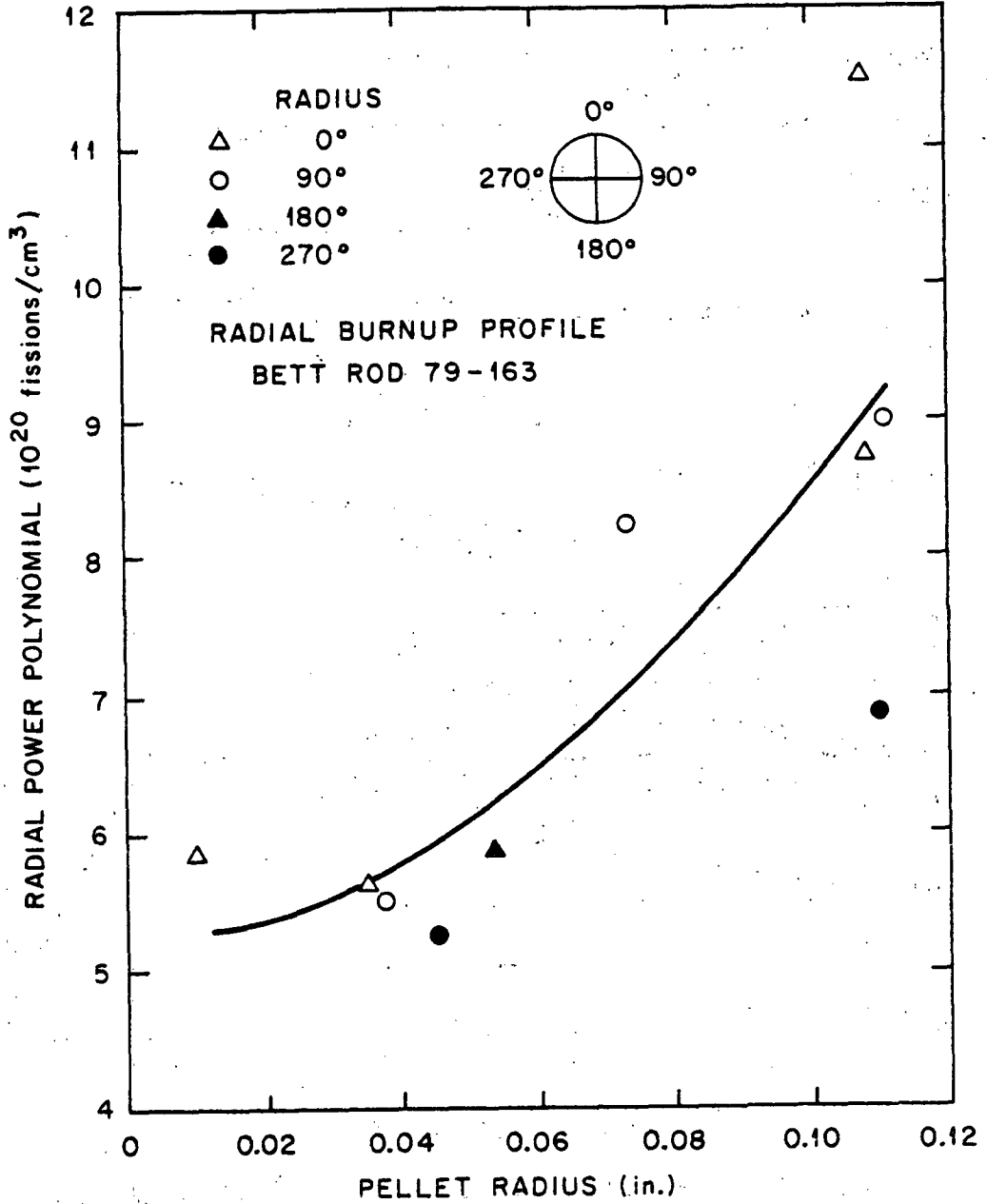


Fig. 2. Best polynomial fit to the radial burnup data.

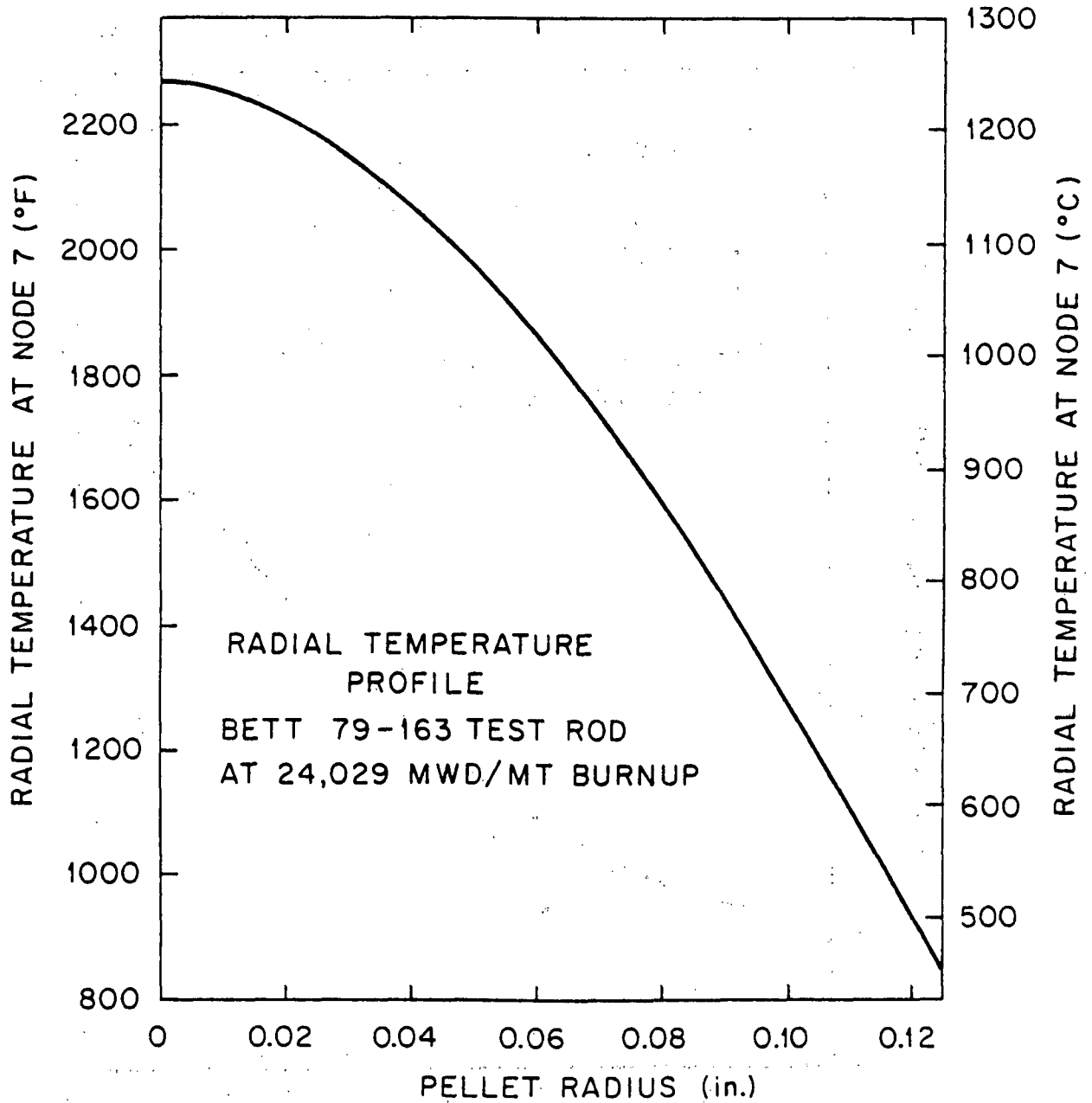


Fig. 3. Radial temperature profile at end of irradiation.

NRC FORM 335 (7-77)		U.S. NUCLEAR REGULATORY COMMISSION BIBLIOGRAPHIC DATA SHEET		1. REPORT NUMBER (Assigned by DDC) NUREG/CR-2507	
4. TITLE AND SUBTITLE (Add Volume No., if appropriate) Background and Derivation of ANS-5.4 Standard Fission Product Release Model				2. (Leave blank)	
7. AUTHOR(S) ANS-Working Group 5.4				5. DATE REPORT COMPLETED MONTH July YEAR 1981	
9. PERFORMING ORGANIZATION NAME AND MAILING ADDRESS (Include Zip Code) Dr. S. E. Turner, Chairman ANS-Working Group 5.4 Southern Science Applications, Inc. P.O. Box 10, Dunedin, Florida 33528				DATE REPORT ISSUED MONTH January YEAR 1982	
12. SPONSORING ORGANIZATION NAME AND MAILING ADDRESS (Include Zip Code) Division of Systems Integration Office of Nuclear Reactor Regulation U.S. Nuclear Regulatory Commission Washington, DC 20555				6. (Leave blank)	
13. TYPE OF REPORT Formal Technical Report				PERIOD COVERED (Inclusive dates)	
15. SUPPLEMENTARY NOTES				10. PROJECT/TASK/WORK UNIT NO.	
16. ABSTRACT (200 words or less) <p>This report summarizes work performed by the ANS-5.4 Working Group on Fuel-Plenum Fission Gas Inventory and is a compilation of individual contributions by members of the Working Group. The report was compiled to document the basis for the ANSI/ANS Standard on "Method for Calculating the Fractional Release of Volatile Fission Products from Oxide Fuels," ANSI/ANS 5.4-1981. The information contained in this report is important to an understanding of the Standard, and has been reviewed and approved by the Working Group.</p>				11. CONTRACT NO.	
17. KEY WORDS AND DOCUMENT ANALYSIS				14. (Leave blank)	
17a. DESCRIPTORS				17b. IDENTIFIERS/OPEN-ENDED TERMS	
18. AVAILABILITY STATEMENT UNLIMITED		19. SECURITY CLASS (This report) UNCLASSIFIED		21. NO. OF PAGES	
20. SECURITY CLASS (This page) UNCLASSIFIED		22. PRICE S			

UNITED STATES
NUCLEAR REGULATORY COMMISSION
WASHINGTON, D. C. 20555

OFFICIAL BUSINESS
PENALTY FOR PRIVATE USE, \$300

POSTAGE AND FEES PAID
U.S. NUCLEAR REGULATORY
COMMISSION



120555056775 1 ANR3
US NRC
NRR-DIV SYSTEMS INTEGRATION
SECTION LEADER/FUELS
CORE PERFORMANCE BRANCH
P-924C
WASHINGTON DC 20555